ANG II-INDUCED CARDIAC REMODELING: ROLE OF PI3-KINASE-DEPENDENT AUTOPHAGY

A Dissertation
Submitted to the Graduate Faculty
of the
North Dakota State University
of Agriculture and Applied Science

By

Tiecheng Zhong

In Partial Fulfillment of the Requirements
for the Degree of
DOCTOR OF PHILOSOPHY

Major Department:
Pharmaceutical Sciences

August 2018

Fargo, North Dakota

North Dakota State University
Graduate School

Title

ANG II-INDUCED CARDIAC REMODELING: ROLE OF PI3-KINASE-DEPENDENT AUTOPHAGY

By

Tiecheng Zhong

The Supervisory Committee certifies that this ***disquisition*** complies with North Dakota State University's regulations and meets the accepted standards for the degree of

DOCTOR OF PHILOSOPHY

SUPERVISORY COMMITTEE:

Dr. Chengwen Sun
Chair

Dr. Stephen T. O'Rourke

Dr. Sathish Venkatachalem

Dr. Pinjing Zhao

Approved:

09/05/2018
Date

Dr. Jagdish Singh
Department Chair

ABSTRACT

Heart failure (HF) is a pathological state indicating insufficient blood supply to the peripheral tissues from the heart. The pathophysiology of HF is multifactorial like cardiac remodeling including cardiac hypertrophy, perivascular fibrosis and apoptosis to compensate for the heart's inability to pump enough blood. Cardiac hypertrophy is initially adaptive to hemodynamic overload; however, it chronically contributes to heart failure and sudden cardiac death. The extracellular regulatory factors and intracellular signaling pathways involved in the cardiac remodeling are not yet fully clear.

PI3-kinase is an important intracellular kinase in organ size control. Cardiac overexpression of Class I PI3-kinase caused heart enlargement in transgenic mice. Autophagy as a dynamic process involving the degradation of damaged mitochondria prevents ROS overproduction which leads to the cardiac remodeling. Therefore, our aim was to study the relationship between PI3-kinases and Ang II-induced cardiac remodeling via an autophagy-dependent mechanism.

Ang II significantly increased autophagy with two distinctive phases: an increasing phase at low doses and a decreasing phase at high doses in cardiomyocytes. The Ang II-induced autophagic depression was attenuated by a Class I PI3-kinase inhibitor and potentiated by Class III PI3-kinase inhibitor. Besides, Ang II-induced cardiac hypertrophy and mitochondria ROS generation were attenuated via blockade of Class I PI3-kinase or mTOR.

To further validate our *in* vitro data, we studied the role of Class I PI3-kinase in Ang II-induced cardiac remodeling *in vivo*. We successfully transferred Lv-DNp85 (Class I PI3-kinase blockade) and Lv-GFP (control) into adult rat hearts and found that cardiac transfer of Lv-DNp85 did not alter Ang II-induced pressor effect, but attenuated Ang II-induced cardiac hypertrophy,

perivascular fibrosis and cardiac dysfunction. Ang II-induced cardiac remodeling was associated with impaired autophagy and mitochondrial ROS overproduction, which were significantly attenuated by Lv-DNp85-induced blockade of Class I PI3-kinase.

Taken together, these data suggest that Class I PI3-kinase is involved in Ang II-induced impairment of autophagy via Akt/mTOR pathway, leading to mitochondrial ROS overproduction and cardiac remodeling. These results are not only highly significant from a pathophysiological perspective, but also have important pharmacological implications in the control of cardiac hypertrophy to prevent decompensation and failure in cardiac function.

ACKNOWLEDGEMENTS

There are so many people to whom that I owe a large debt of heartfelt appreciations. This dissertation would not have been possible without the kind and generous support of the people I am about to acknowledge. As a foreign student, I appreciate all the faculty, staff and students from the Department of Pharmaceutical Sciences at North Dakota State University. The atmosphere in the department made my happy and wonderful stay.

I am extremely thankful to many people for their support throughout the adventure of my Ph.D. I would like to first thank my major advisor, Dr. Chengwen Sun, for giving me the opportunity to obtain my degree in his lab. I am grateful for his mentorship and the time and energy that he devoted to me, without which I may not be successful. I greatly admire his enthusiasm, discipline, and attitude for research and hope I can emulate these traits in my future career.

I am grateful to my dissertation advisory committee members, Dr. Stephen T. O'Rourke, Dr. Sathish Venkatachalem, and Dr. Pinjing Zhao for their guidance and generous support without which it would have been impossible to complete my graduate studies. Their pioneering suggestions were really helpful for me to prepare for my future career. Especially I would also like to express my deeply heartfelt appreciation to Dr. Jagdish Singh for letting me to join such wonderful Department of Pharmaceutical Sciences, and for supporting me in various scholarship applications.

I was fortunate to participate in numerous collaborative efforts throughout my thesis work and am grateful for the interactions I shared with other researchers. I am indebted to my previous lab mates Dr. Chengluan Xuan and Dr. Neha Singh, for training me on various in vivo techniques on living rats as well as cellular & molecular biology techniques. I also thank Dr. Lirong Guo, Dr.

Wen Yan, Dr. Amit Modgil, Dr. Shuang Hao, Dr. Shan Jiang, Dr. Kai Cui and Dr. Jiang Tan for helping me with experiments. They always created a friendly environment in the lab.

Words fail to express my sentiments for my parents for sowing in me the strength, the determination and the will to adapt to every situation in my life. Sincerely, I would like to thank Janet Krom, Jean Trautmann, and Diana Kowalski because they were there for me in so many ways. Not only for their kind greetings mixed with advice, but also for their constantly providing with necessary assistance in various applications and equipment reservations.

I need to acknowledge all the faculty, graduate students and the whole department of pharmaceutical sciences. Though, I have not named everyone, whose kind help aided in the compilation of this work, gratitude towards them is heart-felt.

Last but not the least, typesetting and formatting this document would not have been accomplished without the guidance provided by graduate school staff through relevant workshops.

TABLE OF CONTENTS

ABSTRACT iii

ACKNOWLEDGEMENTS v

LIST OF FIGURES xi

LIST OF ABBREVIATIONS xiv

CHAPTER I. INTRODUCTION 1

1.1. Etiology and pathophysiology of congestive heart failure 2

1.2. Symptoms, preventions and therapeutic treatments of congestive heart failure 5

1.3. Sympathetic nervous system (SNS) and renin angiotensin aldosterone heart system (RAAS) in heart failure 7

1.4. Cardiac remodeling in heart failure 9

1.5. ROS and cardiac hypertrophy 11

1.6. Autophagy in cardiac hypertrophy 13

1.7. PI3-kinases in cardiac hypertrophy 16

1.8. Overall hypothesis of the current study 18

CHAPTER II. THE ROLE OF CLASS I PI3-KINASE-DEPENDENT SIGNALING PATHWAYS IN ANG II-INDUCED AUTOPHAGY, ROS GENERATION, AND HYPERTROPHY IN PRIMARY CARDIOMYOCYTES 21

2.1. Introduction 21

2.2. Materials and methods 23

2.2.1. Preparation of cardiomyocyte cultures 23

2.2.2. Treatment protocol 24

2.2.3. Autophagy determination 25

2.2.4. ROS detection 26

2.2.5. Cardiac hypertrophy determination 27

2.2.6. Western blot analysis 28

2.2.7. Class I PI3-kinase activity assay 28

2.2.8. Data analysis 29

2.3. Results 30

2.3.1. Dose-dependent effect of Ang II on autophagy, Class I PI3-kinase activity and phosphorylation of Akt 30

2.3.2. The effect of LY-294002, a Class I PI3-kinase inhibitor on autophagy, ROS generation, cardiac hypertrophy and Class I PI3-kinase activity 34

2.3.3. The effect of blocking different types of Ang II receptors on Ang II-induced autophagy, ROS generation, cardiac hypertrophy and Class I PI3-kinase activity 39

2.3.4. The effect of rapamycin, an mTOR inhibitor and autophagic inducer on Ang II-induced ROS generation and cardiac hypertrophy 47

2.3.5. The effect of mito-TEMPO, a mitochondrial ROS scavenger on autophagy, ROS generation, and cardiac hypertrophy 49

2.4. Data summary and conclusion 52

CHAPTER III. THE ROLE OF CLASS III PI3-KINASE-DEPENDENT SIGNALING PATHWAYS IN ANG II-INDUCED AUTOPHAGY, ROS GENERATION, AND HYPERTROPHY IN PRIMARY CARDIOMYOCYTES 54

3.1. Introduction 54

3.2. Materials and methods 55

3.2.1. Preparation of cardiomyocyte cultures 55

3.2.2. Treatment protocol 56

3.2.3. Autophagy determination 57

3.2.4. ROS detection 58

3.2.5. Cardiac hypertrophy determination 58

3.2.6. Class III PI3-kinase activity assay 59

3.2.7. Data analysis 60

3.3. Results 60

3.3.1. Dose-dependent effect of Ang II on Class III PI3-kinase activity 60

3.3.2. The effect of 3-MA, a Class III PI3-kinase inhibitor on Ang II-induced autophagy, ROS generation, cardiac hypertrophy, and Class III PI3-kinase activity 61

3.3.3. The effect of blockade of different Ang II receptor types on Class III PI3-kinase activity 65

3.4. Data summary and conclusion 66

CHAPTER IV. VALIDATION OF THE ROLE OF CLASS I PI3-KINASE, AUTOPHAGY, AND ROS GENERATION IN ANG II-INDUCED CARDIAC HYPERTROPHY IN CHRONIC ANG II-PERFUSED VERSUS CONTROL RATS 69

4.1. Introduction 69

4.2. Materials and methods 71

4.2.1. Animals 71

4.2.2. Myocardial *in vivo* gene delivery 71

4.2.3. Ang II subcutaneous infusion and blood pressure (BP) recording 72

4.2.4. Measurement of cardiac hypertrophy 73

4.2.5. Assessment of perivascular fibrosis 73

4.2.6. Western blots analysis 74

4.2.7. Immunofluorescence staining of heart tissue 75

4.2.8. Class I PI3-kinase activity assay 76

4.2.9. Reactive Oxygen Species (ROS) generation assay in heart tissues 77

4.2.10. Data analysis 77

4.3. Results 77

4.3.1. Identification of Lv-GFP delivery into the cardiomyocytes in adult rat hearts 77

4.3.2. Effect of cardiac transfer of Lv-DNp85 into adult rat hearts on Ang II-induced Class I PI3-kinase activity 78

4.3.3. Effect of blockade of Class I PI3-kinase on Ang II-induced cardiac function changes in adult rats 79

4.3.4. Effect of blockade of Class I PI3-kinase on Ang II-induced cardiac hypertrophy 81

4.3.5. Effect of blockade of Class I PI3-kinase on Ang II-induced perivascular fibrosis 83

4.3.6. Effect of blockade of Class I PI3-kinase on Ang II-induced oxidant stress 84

4.3.7. Effect blockade of Class I PI3-kinase on Ang II-induced autophagic impairment 85

4.3.8. Effect of blockade of Class I PI3-kinase on Ang II-induced Akt and mTOR phosphorylation 87

4.4. Data summary and conclusion 89

CHAPTER V. OVERALL DISCUSSION 93

5.1. Intracellular mechanisms for the heart switching from compensation to decompensation 93

5.2. Role of Ang II in cardiac remodeling 98

5.3. Autophagic alterations in Ang II-induced cardiac remodeling 101

5.4. PI3-kinases-dependent autophagic alterations in Ang II-induced cardiac remodeling 104

CHAPTER VI. CONCLUSION AND FUTURE DIRECTIONS 110

6.1. Overall conclusions 110

6.1.1. *In vitro* studies on primary cardiomyocytes of neonatal SD rats 111

6.1.2. *In vivo* study on adult SD rat hearts 112

6.2. Future research directions 113

6.3. Clinical significance 114

REFERENCES 116

LIST OF FIGURES

Figure		Page
1:	Cardiac output determinants.	3
2:	Summary of the compensatory responses of SNS and RAS activation during congestive heart failure.	9
3:	Autophagy flux process.	14
4:	The structures and functions of PI3-kinases.	17
5:	Identification of autophagy in primary cardiomyocytes.	26
6:	Dose-dependent effect of Ang II on autophagy in cardiomyocytes.	31
7:	Dose-dependent effect of Ang II on the activity of Class I PI3-kinase in cardiomyocytes.	32
8:	Dose-dependent effect of Ang II on the phosphorylation of Akt in cardiomyocytes.	33
9:	Effect of blockade of Class I PI3-kinase on Ang II-induced autophagy in cardiomyocytes.	35
10:	Effect of blockade of Class I PI3-kinase on Ang II-induced mitochondrial ROS generation in cardiomyocytes.	36
11:	Effect of blockade of Class I PI3-kinase on Ang II-induced cardiac hypertrophy in cardiomyocytes.	38
12:	Effect of blockade of Class I PI3-kinase on Ang II-induced Class I PI3-kinase activity in cardiomyocytes.	39
13:	Effect of blockade of Ang II receptor type 1 or type 2 on Ang II-induced autophagy in cardiomyocytes.	41
14:	Effect of blockade of Ang II receptor type 1 or type 2 on Ang II-induced ROS generation in cardiomyocytes.	43
15:	Effect of blockade of Ang II receptor type 1 or type 2 on Ang II-induced cardiac hypertrophy in cardiomyocytes.	45
16:	Effect of blockade of Ang II Receptor Type 1 or Type 2 on Ang II-induced Class I PI3-kinase activity in cardiomyocytes.	46
17:	Effect of blockade of mTOR on Ang II induced-ROS generation in cardiomyocytes.	48

18: Effect of blockade of mTOR on Ang II induced-cardiac hypertrophy in cardiomyocytes. 49

19: Effect of scavenging mitochondrial ROS on Ang II-induced autophagy in cardiomyocytes. 50

20: Effect of scavenging mitochondrial ROS on Ang II-induced ROS generation in cardiomyocytes. 51

21: Effect of scavenging mitochondrial ROS on Ang II-induced cardiac hypertrophy in cardiomyocytes. 52

22: Dose-dependent effect of Ang II on the activities of Class III PI3-kinase in cardiomyocytes. 61

23: Effect of blockade of Class III PI3-kinase on Ang II-induced autophagy in cardiomyocytes. 62

24: Effect of blockade of Class III PI3-kinase on Ang II-induced mitochondrial ROS generation in cardiomyocytes. 63

25: Effect of blockade of Class III PI3-kinase on Ang II-induced cardiac hypertrophy in cardiomyocytes. 64

26: Effect of blockade of Class III PI3-kinase on Ang II-induced Class III PI3-kinase activity in cardiomyocytes. 65

27: Effect of blockade of Ang II Receptor Type 1 or Type 2 on Ang II-induced Class III PI3-kinase activity in cardiomyocytes. 66

28: Effect of cardiac transfer of Lv-GFP in adult rat hearts. 78

29: Effect of Ang II and cardiac transfer of Lv-DNp85 on Class I PI3-kinase activity in adult rat hearts. 79

30: Effect of Ang II and cardiac transfer of Lv-DNp85 on MAP, HR and dp/dt Max in adult rats. 81

31: Effect of Ang II and Lv-DNp85 on HW/BW ratio and cardiac morphology. 82

32: Effect of Ang II and Lv-DNp85 on cardiac histology. 83

33: Effect of Ang II and Lv-DNp85 on cardiac perivascular fibrosis. 84

34: Effect of Ang II and Lv-DNp85 on ROS generation in adult rat hearts. 85

35: Effect of Ang II and Lv-DNp85 on autophagy in adult rat hearts. 86

36: Effect of Ang II and Lv-DNp85 on Akt phosphorylation in adult rat hearts 88

37: Effect of Ang II and Lv-DNp85 on mTOR phosphorylation in adult rat hearts..... 88

38: Diagram summarizing proposed Ang II-induced PI3-kinase-dependent pathways activation in cardiomyocytes. 110

LIST OF ABBREVIATIONS

3-MA……..……..……..……...3-Methyladenine

µg/mL..……..……...Microgram per milliliter

µM…….…..…….Micro molar

µL……..…Micro liter

ACE…….Angiotensin converting enzyme

Ang……..Angiotensin

ANP…….Atrial natriuretic peptide

AT1R or AT2R……..…..Angiotensin receptor type I or II

BP…….……Blood pressure

bpm……...Beats per minute

Brdu…….…….Bromodeoxyuridine

BSA……..Bovine serum albumin

BW……..…..Body weight

CHF……...……Congestive heart failure

CO…….……Cardiac output

DAPI…….……Diamidino-phenyl-indole

DMEM……..Dulbecco's modified eagle medium

DN…….Dominant negative

DMSO……..….Dimethyl sulfoxide

DNA……..……Deoxyribonucleic acid

EDTA……Ethylene diamine tetra acetic acid

EF……..Ejection fraction

ELISA……...Enzyme linked immunosorbent assay

ETC……...Electron transportation chain

FBS……Fetal bovine serum

GAPDH…….……Glyceraldehyde 3-phosphate dehydrogenase

GFP……...……..…Green fluorescence protein

GPCR…….……G-protein coupled receptor

HBSS…….Hank's balanced salt solution

H & E…….Hematoxylin and Eosin

HF……..Heart Failure

HR……..Heart rate

HW……...……..Heart weight

LV……..Lenti-virus

LVEDP(V)……..……...Left ventricular end diastolic pressure (volume)

Lv dp/dt max…….……..…Left ventricular dp/dt max

MAP……...Mean atrial pressure

MAP-LC3……...Microtubule-associated proteins light chain 3

mM…….……Milli-mole

mRNA……Messenger ribonucleic acid

mTOR…….……Mammalian target of rapamycin

NOX……..…..... Nicotinamide adenine dinucleotide phosphate oxidase

nM……...…Nano molar

PBS…….Phosphate Buffered Saline

PBST……..……Phosphate Buffered Saline tween 20

PCR…….……...Polymerase Chain Reaction

PE……...Phosphatidylethanolamine

PI3-K……..…Phosphatidylinositol-3-kinase

PIP……...……...Phosphatidy inositol [1]-mono phosphate

PIP_3……Phosphatidy inositol (3,4,5)-trisphosphate

PKB/C……Protein kinase B/C

RAAS……..……...Renin angiotensin-aldosterone system

RAS……..……..Renin angiotensin system

RNA…….…..Ribonucleic Acid

ROS……....Reactive oxygen species

SD……..Sprague Dawly

SDS-PAGE……Sodium Dodecyl Sulfate-Poly Acrylamide Gel Electrophoresis

SDS……..……..…Sodium dodecyl sulfate

SNS……..……..…Sympathetic nervous system

SV…….……..Stroke volume

TBST…….….Tris buffered saline plus tween 20

TEMED…….….N, N, N, N- tetramethylethylenediamine

TPR…….....Total peripheral resistance

XOR…….……...Xanthine oxidoreductase

CHAPTER I. INTRODUCTION

The primary function of the heart is to pump the blood into various peripheral organs and tissues, providing them with nutrients & oxygen, and eliminating the waste produced in those places. Heart failure (HF) means the cardiac output is insufficient to meet the body's oxygen and nutrient demand. The consequences of heart failure are rather severe and sometimes even fatal including multiple organ dysfunctions such as dyspnea, edema and decreased exercise tolerance. The epidemiology of heart failure is quite harsh nowadays. So far, the most disappointing information is that there are more patients die of heart failure than all forms of cancer, and the nationwide number of new patients with heart failure reaches 550,000 annually based on the reports from American Heart Association [1, 2]. Heart failure immensely imposes a skyrocketing health and economic burden accompanied with the development of aging and industrialization process in the US and worldwide. In 2012, the published assessment of HF cost was $ 30.7 billion, taking up about 17.9 % of the World Bank GDP invested in health care, and it is estimated that this expense will reach $ 69.7 billion by 2030 [3, 4]. The growing incidence and prevalence of CHF globally in senior citizens over the age of 65 are the result of better clinical treatment of acute myocardial infarction along with the ageing population. Also, the advent of the pandemic of cardiovascular diseases in economically developing nations partially accounts for the incidence rise of CHF [5]. Therefore, heart failure, regarded as the disease of civilization, is the leading cause of mortality in developed countries and has a growing trend in developing countries, exerting major impacts on life expectancy. Since other cardiovascular diseases become more efficient to be dealt with, increasing numbers of patients are surviving long enough to develop heart failure, making this epidemic prevalent.

1.1. Etiology and pathophysiology of congestive heart failure

CHF is a morbid state when the heart is no longer able to pump adequate blood to meet the body need in the peripheral metabolizing organs and tissues with a gradual reduction in cardiac performance. Factors such as anomalous cardiac structure, function, conduction or contractility contribute to the emergence and progression of congestive heart failure [6]. It is often reported that congestive heart failure (CHF) is the end stage of several cardiovascular diseases such as ischemic heart disease, hypertension, myocardial infarction, obesity, viral infection, and cardiomyopathy [7]. All of those diseases exert influences on cardiac output (CO). Cardiac output refers to the product of heart rate (HR) and stroke volume (typically 4~8L/min) and it is the combined outcome of interactions among physiological factors. Stroke volume is determined by mutual interactions of preload, afterload, and contractility with the value of 1mL/kg or roughly 60~100 mL in normal individuals [8]. Furthermore, heart rate is an intrinsic factor which could be influenced by autonomic, humoral, and local circumstances. The relationship of those factors is shown in Figure 1. Disturbance of any above-mentioned physiological factor(s) may cause an imbalance in the circulation system and eventually lead to heart failure with diminished ejection fraction (EF) or impaired heart contractility.

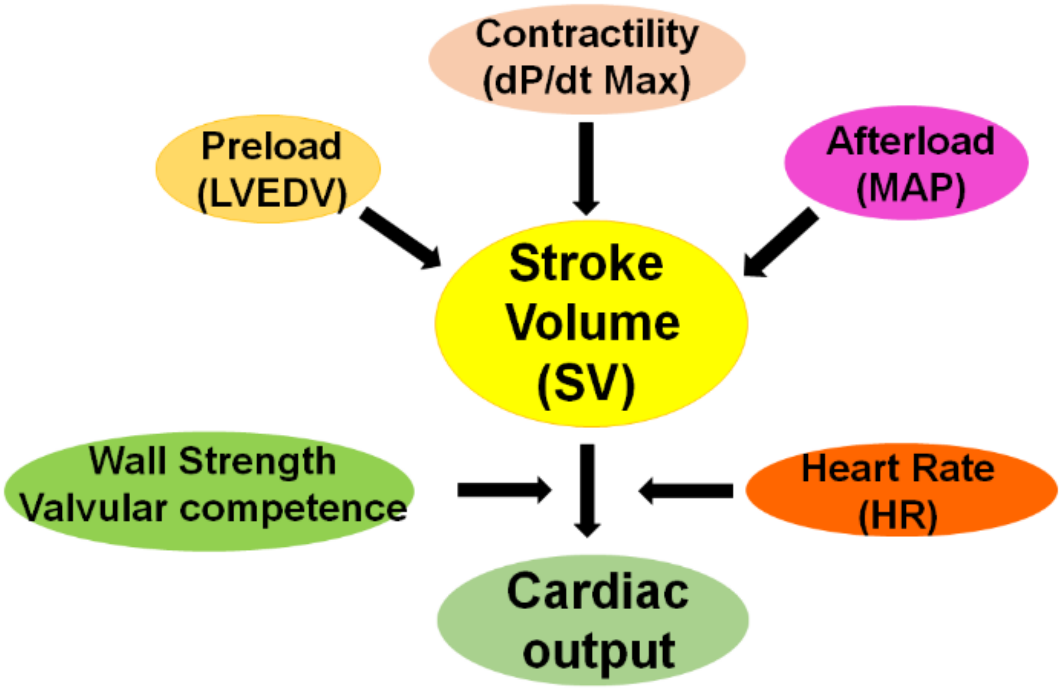

Figure 1: Cardiac output determinants. Cardiac output refers to the amount of left ventricle-ejected blood within one minute. Stroke volume predominately determines the cardiac output. Heart rate is an inherent component involving autonomic, humoral, and local circumstances. Stroke volume is principally determined by preload, afterload and contractility [9].

Preload is the maximum degree of myocardial fiber stretching at the end of diastolic stage just prior to contraction. End diastolic pressure/volume in left ventricle (LVEDP/V) is an indirect index of preload since it is impossible to precisely determine the length of a single myocardial sarcomere in the intact heart of living animals. According to the Frank-Starling mechanism, the contractility and stroke volume are proportional to the initial length of cardiomyocyte fiber within a certain range. In normal hearts, the LVEDP rises along with the LVEDV elevation, making the myocardium stretch as the response of cardiac output (CO) escalation. However, elevation of CO has a limitation as the continuous rise of preload, once higher than the upper limit, the increasing trend of CO is lessened due to the overstretching of cardiomyocyte fibers and the SV-LVEDP curve flattens out [8].

Afterload is defined as the resistance to be overcome in the peripheral vascular system to prevent the blood ejection, and the index of afterload is the mean arterial pressure (MAP). The equation of $\sigma = P \cdot r/h$ is used to define afterload, where P refers to ventricular pressure, r refers to the ventricular radius, and h refers to the ventricular wall thickness. When a downfall of cardiac output occurs, there is a reflex increase in systemic vascular system which is mediated through SNS outflow, catecholamine in the circulation system, and RAS. The potent vasoconstrictor peptide of endothelin also participates this process. Afterload is enhanced by elevating aortic pressure and/or systemic vascular resistance, resulting in rising end systolic volume and reduction of stroke volume which would reduce arteriolar tone in heart failure [8].

Contractility/inotropy indicates the competence of heart muscle fiber to contract into a certain fiber length. Inotropy alterations adjust the degree of contracting force and ventricular pressure development. Inotropy, regarded as a heart failure condition index, is positively proportional to ejection fraction [8].

The normal cardiac output is about 4~8 L/min; once there is a downfall of cardiac output, several neurohormonal systems such as renin angiotensin system [10] and sympathetic nervous system (SNS) are activated to keep normal heart function, leading to eventual heart structural abnormality if improperly treated. Those physiological alterations facilitate renal retention of Na+ & water as well as vasoconstriction in the peripheral vascular system, promoting the contraction of heart muscle. Those compensatory responses are beneficial to sustain the cardiac output and blood supply required in the peripheral system, whereas long-term activation of RAS and SNS is harmful to the cardiovascular system, resulting in pathological effects. Under such stress, the myocardium suffers decompensation, and a series of cardiac complications occur with harmful outcomes jeopardizing organs besides heart, such as kidneys, lungs, muscles and blood vessels, bringing about classic CHF clinical symptoms [11].

Long-term cardiac hemodynamic load alters myocardial size, shape, structure, and function referred to as cardiac remodeling including alterations of myocardial mass, composition, volume and geometric dimensions from elliptical to spherical. At first, the failing heart thrives to expand ventricular volume, sustain greater SV and heighten CO although there is an EF reduction. Simultaneously, ventricular wall thickness and mass are also elevated, giving rise to enhanced contractility. However, as the ventricle goes on expanding with myocardium hypertrophy, ischemic changes happen with diastolic filling impairment, leading to the wall tension and fibrosis would undermine cardiac contractility ultimately. Myocardial apoptosis is the eventual consequence of the long-standing process of cardiac remodeling and the ventricle would lose the ability to contract synchronically, leading to less efficiency to eject the blood into the peripheral organs and tissues [9].

Hence, the etiology and pathophysiology of congestive heart failure are complicated and multifactorial, and stem from the combined interactions with a series of genetic and environmental factors. Knowing some basic knowledge of the underlying mechanisms behind the emergence and adaptive response of HF is beneficial for us to adopt pharmacological and surgical approaches to improve HF patients' survival rate.

1.2. Symptoms, preventions and therapeutic treatments of congestive heart failure

Insufficient cardiac output and shortage of enough venous return cause the loss of competence for the heart to pump adequate blood and result in the heart failure symptoms with distinctive signs such as fluid build-up development and salt retention. Pulmonary edema, cough, and dyspnea in the respiratory system is the consequence of fluid accumulation. Confusion, anxiety and amnesia happen due to diminished oxygen supply to the central nervous system. The inability of the right ventricle to hold systemic venous return incurs lower extremity edema along with ascites. Appetite loss and nausea occur because of the switch of blood into essential organs,

diminishing the supply of gastrointestinal (GI) tract. The downfall of cardiac output and emergence of sodium & water retention also cause fatigue and limb weakness as the initial symbols of HF. The final stage of HF presents cardiac cachexia (malnutrition) and cyanosis (bluish skin) since excessive hemoglobin is denatured for oxygen deprivation [9, 11]. Proper diagnoses from above-mentioned symptoms plus physical examination, lab tests, X-ray, and echocardiography methods help us to find out the etiology of HF.

Preventive approaches for CHF mainly include lifestyle modification. For obese patients, they are required to lose excess weight. For those using tobacco and alcohol, it is wise to quit these hazardous materials. Appropriate exercise helps promote physical condition. Suitable medical therapies on the preceding diseases such as hypertension, hyperlipidemia, diabetes, and arrhythmias with strict restriction of water and sodium also slow the progress of HF.

Once congestive heart failure is diagnosed and those preventive practices prove futile, two major approaches of treatment to combat this fatal disease will be adopted: 1). Decelerating the process as much as possible and alleviating the symptoms when in a relatively stable morbid state, 2). Proper treatment in acute decompensatory heart failure to promote the life quality. For pharmacological treatment of acute heart failure, traditional positive inotropic agents of cardiac glycosides like digoxin are extensively used for over two centuries in order to enhance ventricular contracting force via promotion of myocardial function and strength, and reduction of SNS and RAAS activation. Nevertheless, wide usage of non-cardiac targeting reagents is more beneficial than the solely treatment of reinforcing heart inotropy. There are several approaches: 1). Diuretics: they facilitate the edema fluid and sodium excretion and ameliorate the cardiac output in failing heart; 2). Angiotensin-converting enzyme inhibitors (ACEI): prevention of conversion of Ang I to Ang II attenuates provocation of RAAS; 3). Angiotensin receptor blockers (ARBs): this kind of reagents successfully evades that side effects brought about by ACEI such as bradykinin-induced

dry cough, and act directly on the angiotensin receptors as the final downstream target of RAAS pathway; 4). β-receptor blockers: the heart and vasculature are protected from deleterious effects of SNS over-activation, and the heart rate also falls for more efficient contraction; 5). Aldosterone receptor antagonists: direct inhibition of RAAS; and 6. Bipyridines: Compounds of this kind inhibit phosphodiesterase and facilitate longer existence of cAMP which helps to strengthen the inotropic effect [12].

Besides the above-mentioned non-invasive pharmacological treatment, invasive surgical treatments are widely used to improve the cardiac function promptly. The surgeries consist of cardiac resynchronization therapy (CRT, restoration of ventricular efficiency by pacing both ventricles concurrently), surgical ventricular remodeling (SVR), coronary revascularization, ventricular assist device (VAD) implantation, and heart transplantation ultimately [9].

1.3. Sympathetic nervous system (SNS) and renin angiotensin aldosterone heart system (RAAS) in heart failure

Sympathetic nervous system (SNS) and renin angiotensin aldosterone system (RAAS) are two major compensatory mechanisms activated at the initial stage of heart failure due to the downfall of cardiac output. Those two factors plus pro-inflammatory activation contribute to the cardiac remodeling process and signal transduction in maladaptive hearts [13]. From the equation of MAP=CO×TPR, we know that TPR is increased to maintain MAP once there is a decrease of CO as the negative feedback. Meanwhile, a lot of neurohormones facilitates the retention of sodium and water in order to magnify stroke volume through the Frank-Starling mechanism.

The sympathetic nervous system is an essential component of the autonomic nervous system to mobilize energy whenever it is needed. The SNS acts on cardiovascular systems extensively, provokes heart rate increase and contractility, constricts resistance vessels and turns down venous capacitance [14]. The MAP decrease in HF patients stimulates sympathetic nervous

system (SNS) and facilitates the secretion of catecholamines (epinephrine and norepinephrine) which directly elevates heart rate and cardiac contractility, while the vasoconstrictive effect of catecholamines in the peripheral vasculature raises SV and TPR to enhance MAP. Short-term activation of SNS temporarily improves cardiac output, whereas long-term dependence on SNS exerts destructive and detrimental consequences to heart function known as catecholamine toxicity as interstitial fibrosis, dysfunctional pumping, and eventually apoptosis or even necrosis [15]. Long-term exposure to norepinephrine causes significant apoptosis in cardiomyocytes because of the oxidative stress generation via reactive intermediates and free radicals generated through auto-oxidation of catecholamines [16]. Three kinds of receptors of β1, β2, and α1 mainly mediate sympathetic nervous system leading to myocardial toxicity with lowered EF, arrhythmias, and tachycardia. Activation of β_1 and α_1 in peripheral vasculature prompt renin-angiotensin-aldosterone system (RAAS), leading to vasoconstriction, sodium retention thirst which makes MAP augmentation [17].

For renin angiotensin system [10], it is activated due to both increased sympathetic activation and reduced renal blood flow, causing the release of renin. After the entry of renin into circulation system, renin converts angiotensinogen to angiotensin I (Ang I) in the liver. When circulating Ang I encounters pulmonary-located angiotensin converting enzyme [18], it is converted into angiotensin II (Ang II). It is well established that the effect of Ang II is to constrict the peripheral vasculature, enhance contractility, and promote the secretion of aldosterone. The final consequences of RAAS activation are to speed up norepinephrine release, enhance water and sodium reabsorption, improve contractility, and trigger vasopressin discharge [9]. Those effects of regulatory pathways are shown in Figure 2.

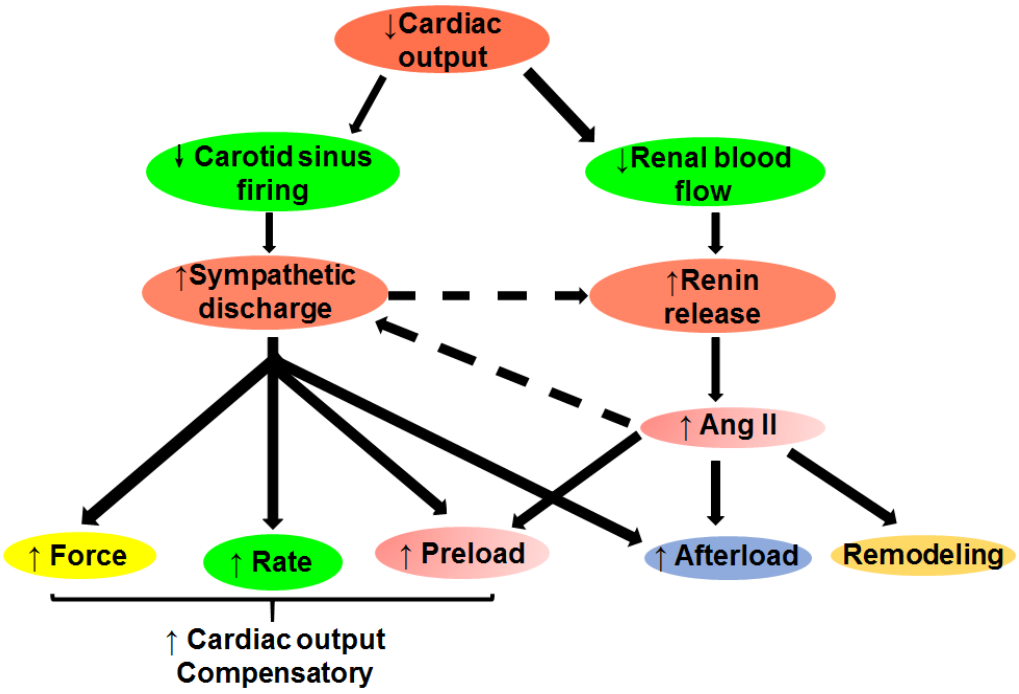

Figure 2: Summary of the compensatory responses of SNS and RAS activation during congestive heart failure. The diagram shows the reset of baroreceptor reflex with a lower sensitivity to arterial pressure in HF patients. Besides the displayed effect, sympathetic discharge augmentation causes renin secretion producing more Ang II. Reversely, Ang II increases NE release by acting on sympathetic nerve endings [19].

1.4. Cardiac remodeling in heart failure

The most essential inherent compensatory mechanism in heart failure is myocardial hypertrophy which refers to the increase of muscle mass with several key features such as cardiomyocyte size enlargement, heart expansion, gene expression alteration, enhanced synthesis of protein and contractile machinery reorganization [20].

Physiological hypertrophy is a reversible process with normal cardiac structure. Meanwhile, it is beneficial to adapt to the increased hemodynamic workload in healthy individuals during normal postnatal growth, exercise and pregnancy, and this enlargement of cardiomyocytes helps keep the heart function without the linkage to cardiac damage. The enhanced cardiac function enables the oxidation of fatty acid and glucose utilization [21].

For pathological hypertrophy, state-related stress like hypertension, obesity and myocardial infarction elicits maladaptive cardiac hypertrophy in which unusual cardiac metabolisms, structures, and abnormal cardiac functions emerge. Normal cardiomyocytes are lost and replaced by fibrosis, leading to cardiac dysfunction and risk of heart failure or even sudden death. There are distinct structural, functional, metabolic, biochemical and molecular variations between physiological and pathological hypertrophy in cardiomyocytes [21]. For instance, elevated ANP, BNP, and β-MHC levels were observed in mice with aortic banding-induced pathological hypertrophy when compared with their physiological hypertrophy counterparts via swimming training. Meanwhile, M-mode echocardiography and interstitial fibrosis studies demonstrated this aortic banding-induced pathological hypertrophy severely undermined cardiac function which was not present in swimming training-induced physiological hypertrophy [22].

Hypertrophy is an inevitable stage of hypertension-induced heart failure with both compensatory and decompensatory manners to sustain cardiac performance. Hypertension, at the initial stage, causes concentric hypertrophy to compensate for the increasing hemodynamic or blood pressure overload with an adaptive manner. However, as this process goes on, cardiac hypertrophy gradually steps into eccentric type not only due to strengthened mechanical stress but also because of neuro-hormone secretion alteration, and this type of hypertrophy progresses into heart failure and ultimately cardiomyocytes death with ventricular dilation and a downfall of contractility [23]. Sarcastically, identical neurohormones in SNS and RAAS are attributed to cardiomyocytes death even though they stimulate the compensatory hypertrophy to counteract the initial hemodynamic stress. The exact pathways such as necrosis/oncosis, apoptosis, and autophagy-induced cardiomyocyte death are dependent on certain physiological circumstances [24].

1.5. ROS and cardiac hypertrophy

Since the heart is beating continuously, there is an indispensable need for oxygen supply to maintain heart function. Be that as it may, the consumption of oxygen is essential to the generation of ROS as byproducts. It is known that almost 5% of the oxygen is converted into ROS in normal tissues which attributes to the pathophysiology of heart failure [25]. ROS is the abbreviation of reactive oxygen species, and the major ROS are small molecules derived from oxygen, including oxygen radicals such as superoxide anion ($O_2^{-\bullet}$), hydroxyl ($^{\bullet}OH$), peroxyl ($RO_2^{\bullet}$), peroxynitrites ($ONOO^{-\bullet}$), and alkoxyl ($RO^{\bullet}$), as well as certain nonradicals that are either oxidizing agents and/or are easily converted into radicals such as hydrogen peroxide (H_2O_2), hypochlorous acid (HClO), and ozone (O_3) [26]. Also, nitrogen-containing oxidants are defined as reactive nitrogen species [27]. The most distinctive feature of ROS is that there are unpaired electrons within the outer orbit. Most ROS exist transiently: for example, the half-life ($t_{1/2}$) of superoxide anion ($O_2^{-\bullet}$) is only a few seconds. Superoxide anion ($O_2^{-\bullet}$) has a very low diffusion capacity due to its limited cellular membrane permeability. Therefore, the main place of its action is strictly confined in intracellular components [28]. However, H_2O_2 has a stronger cellular membrane permeability and survives longer than $O_2^{-\bullet}$, and hydroxyl ($^{\bullet}OH$) is the most reactive ROS formed by H_2O_2 via Fenton reactions, and its amount is negligible in normal conditions while accumulated in pathological circumstance to exert oxidative stress-associated cellular damage [25].

Both favorable and hazardous outcomes of ROS generation are reported in living organisms: On the one hand, ROS functions as the 2nd messengers to adjust the downstream regulatory ligands like Ang II, ET, PDGF, FGF-2, TNF-α, TGF-β1, and many others, and this process is defined as redox-signaling [25]. Then numerous downstream redox-sensitive protein kinases and transcription factors like activator protein 1 (AP-1), nuclear factor-κB (NF-κB), and hypoxia-inducible factor-1 (HIF-1) are activated to induce genotype and phenotype expression,

while the action of protein tyrosine phosphatases might get arrested. Those cascade activations stimulate normal cellular growth and proliferation, facilitating the survival of cells [29]. While on the other hand, when ROS levels are overwhelmingly exceeding the threshold that the cellular antioxidant defense system could cope with, the cellular membrane lipids, proteins, and nucleic acids are vulnerable to be directly attacked, leading to cellular dysfunction or even death. The reason behind is that one ROS radical production could generate several other ROS molecules through radical chain reactions since radicals attack their adjacent counterparts, creating multiple radicals that mainly consisted of lipid radicals. Those lipid radicals accumulate in the cellular membrane in this chain reaction, causing plasma leakage and membrane-bound receptors dysfunction. Furthermore, ROS may straightly cause DNA mutagenesis such as strand breaks, purine oxidation, and protein-DNA cross-linking, disturbing normal gene expression and denaturing protein functions [29].

To keep health, redundant ROS should be efficiently eliminated by both intrinsic enzymatic and non-enzymatic antioxidant defense systems such as superoxide dismutase (SOD), catalase (CAT), and glutathione (GSH) peroxidase enzymes. $O_2^{-\cdot}$ is rapidly converted to H_2O_2 *in vivo* under SOD with many isoforms like Cu/Zn SOD (SOD_1) in cytosol, concentrated Mn SOD (SOD_2) in mitochondria, and extracellular SOD (SOD_3) within the plasma membrane or extracellularly-compartments [30]. H_2O_2 level is strictly monitored by catalase and glutathione peroxidase, and H_2O_2 is scavenged with the final product of water and oxygen [31]. A series of antioxidants such as ubiquinone (Q_{10}), lipoic acid, and ascorbic acid are catalyzed by thioredoxin reductase to fight against ROS. Glutathione is the reducing substrate for glutathione peroxidase in the enzymatic reaction. The major non-enzymatic anti-ROS mechanisms involve utilization of vitamins C & E, β-carotene (vitamin A precursor), and urate [29].

As for the relationship between ROS generation and cardiac hypertrophy, excessive ROS provoke a series of downstream signaling pathways such as protein kinases C (PKCs), protein kinase B (PKB or Akt), mitogen activated protein kinases (MAPKs), and the transcription factors of NFAT, GATA4, SRF, NF-κB, and AP-1 [29]. ROS impact cardiac hypertrophy relies on the fact that endogenously generated ROS directly or indirectly modulate various hypertrophy signaling kinases and transcription factors via intertwined intracellular signaling pathways regarding the redox status [26]. For direct modulation, cysteine and methionine thiols in macromolecules are the most susceptible targets. For indirect modulation, several mechanisms are involved: reactions between NO and ROS impair not only topical NO availability, but also the formation of cysteine oxidation with disulfide, nitrosylation and/or glutathiolation [25].

1.6. Autophagy in cardiac hypertrophy

Autophagy is evolved from the Greek words auto (self) and phagy (eating) from the etymological aspect, indicating the lysosomal degradation of intracellular materials rather than the extracellular material degradation (heterophagy) [32]. Autophagy was initially identified in the 1950s from studies on ultrastructural organelles as a self-degradative process in the lysosome/vacuole by electron microscopy of original single- and double- membrane vesicles with organelles and components at different degradation stages, and autophagy is a vital process for cells to fight against various types of harmful stress such as hypoxia, oxidative stress, pathogen infection, and most remarkably nutrient starvation [33]. This process is involved in the removal and recycling of pathogens, long-lived, redundant or damaged proteins, lipids, and dysfunctional cellular organelles, maintaining intracellular homeostasis, anti-oxidant defense, and cellular survival under various hazardous stimuli. Meanwhile, when it goes too far, superfluous autophagy without appropriate controlling mechanisms would cause vital cellular molecules and organelles exhaustion, leading to autophagic-induced cellular death as a two-bladed sword [34]. Besides,

autophagy may also occur in cellular organelle-specific manners within diversified intracellular places besides cytoplasm, e.g., selectively targeting at nucleus (nucleophagy), mitochondria (mitophagy), lipid droplets (lipophagy), ribosomes (ribophagy), peroxisomes (pexophagy), endoplasmic reticulum (reticulophagy), and microorganisms (xenophagy) [35].

The major course of autophagy consists of the following four steps: 1) Induction & Nucleation: A bilayer isolation membrane defined as phagepore is formed under various hazardous or pathological stimuli. When the phagepore is established, it directly targets to and then engulfs the cytosolic components including molecules and/or components to be degraded [36]. 2) Elongation & Expansion: the phagepore encompasses the cytosolic components to be degraded and creates an autophagosome. 3) Fusion: an autophagosome gets fused with a lysosome to establish an autolysosome in which lysosomal hydrolyases are present so as to digest those unwanted cellular organelles and macromolecules [37]. 4) Degradation: After the completion of digestion, the degraded components are transported back into the cytoplasm for further usage by intracellular recycling [38]. The processes of autophagy are shown in Figure 3.

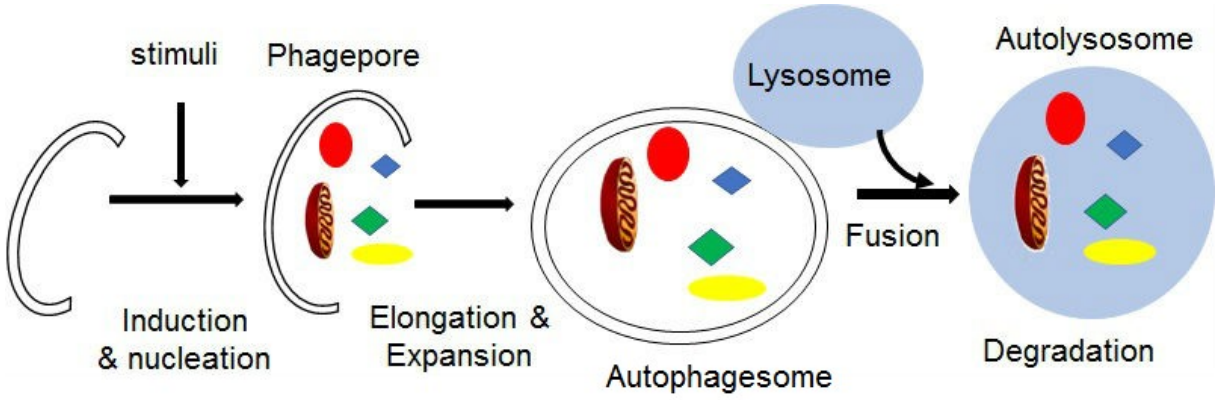

Figure 3: Autophagy flux process. Macroautophagy contains four steps as 1. Induction & nucleation, 2. Elongation & expansion, 3. Fusion, and 4. Degradation. A few autophagy-related (Atg) proteins are recruited to modify autophagy initiation and procedure within different steps [39].

Over 30 intracellular regulatory components are reported to be involved in the supervision and arrangement of autophagy [40]. Some of those most essential regulators are: 1) Mammalian target of rapamycin (mTOR): this important autophagic regulator is influenced by the single or multiple combined hazardous factors such as shortage of amino acid or ATP supply, loss of growth factors, hypoxia [41, 42], etc. Those unfavorable conditions including accumulation of ROS make mTOR dissociate from lysosomes, activate autophagic-friendly components such as AMPK [43] or TSC1/2 [44], and inhibit autophagic-unfriendly components like Akt and Rheb [44], facilitating autophagy. It's reported that mTOR is essential for animal survival as its gene knockout causes prenatal death during the embryonic stage in mice [45]. 2) Beclin-vacuolar protein sorting 34 (Bcl-Vps34) complex: this is one of the downstream components of mTOR and monitored by nuclei transcripts such as NF-κB and E2F. Association of Belcin-1 with Class III PI3-kinase aids autophagosome nucleation via Vps34 phosphorylation. Alternative factors such as Rubicon, HMGB1, and NRBF2 also govern the binding between Beclin-1 and VPS34, assisting with subsequent autophagy [46, 47]. Activation of Beclin-1/Vps34 complex facilitates PIP production which is perceived by the downstream WIPIs with subsequent control by ATG9, promoting autophagy [48]. 3-methyladenine (3-MA) is an autophagic inhibitor by downregulation of Beclin/Vps34 activity [49]. 3) MAP-LC3 homologs: MAP refers to microtubule-associated proteins which have 4 groups to maintain cellular configuration, and LC means light chain. There are three light chains and one heavy chain within MAP1 family and LC3 is the tiniest among those three light chains [50]. After disposition by several regulatory proteins such as Atg 3 and Atg 4, those MAP-LC proteins are lipidated by phosphatidylethanolamine (PE) and enter autophagosomes to assist autophagy. The formation of MAP-LC3 II from MAP-LC3 I is the marker of autophagy initiation, and the larger LC3 II/LC3 I ratio indicates stronger autophagy [51, 52].

Autophagy is intricate but fundamental to keep the homeostasis of the cardiovascular system [53]. Convincing evidence shows that ROS generation, predominantly O_2^-, is one of those initiating inducers that provoke autophagy in nutrient starvation by deprivation of nourishing materials such as glucose, glutamine, serum and/or pyruvate [54]. Thus, ROS may serve as an essential part of autophagic induction, and electrophilic antioxidants are useful to incompletely or thoroughly reverse this autophagic process [55].

Altogether, two most prominent roles of autophagy are: 1) as an alternative energy resource to supply with vital materials such as amino acids for intracellular protein synthesis and free fatty acids during organism exploitation; 2) as a vital part of the cellular means for quality control, assured by removal of abnormal proteins and organelles [56].

1.7. PI3-kinases in cardiac hypertrophy

The family of lipid kinases termed as phosphoinositide 3-kinases (PI3Ks) was initially discovered in the 1980s. The main function of this type of kinases is to catalyze the formation of PIP3 which is an essential intracellular secondary messenger. This PI3-kinase pathway is highly conserved during the evolutionary process from yeast to mammalians as the downstream effector of receptor tyrosine kinases (RTKs) and G protein coupled receptors (GPCRs) [57]. An awful lot of cellular mechanisms such as metabolism, survival, proliferation, differentiation, migration, and apoptosis are under the regulation of PI3-kinase family in a context-dependent manner [57]. Three types of PI3-kinases have been identified as Class I (formation of $PI(3,4,5)P_3$ from $PI(4,5)P_2$), Class II (formation of $PI(3,4)P_2$ from PI(4)P), and Class III (formation of PI(3)P from PIP) PI3-kinases according to their varied functions, substrate specificity, and molecular structures [58]. Of note, the tumor suppressor kinase of PTEN (phosphatase and tensin homolog deleted from chromosome 10) is the most prominent negative regulator of the PI3-kinases signaling pathways since this kinase is able to reverse the process of PIP products formation with the opposing activity

of PI3-kinases. It is often observed that PTEN is mutated or even deleted in tumors [59]. The structures and functions of various PI3-kinases are shown in Figure 4.

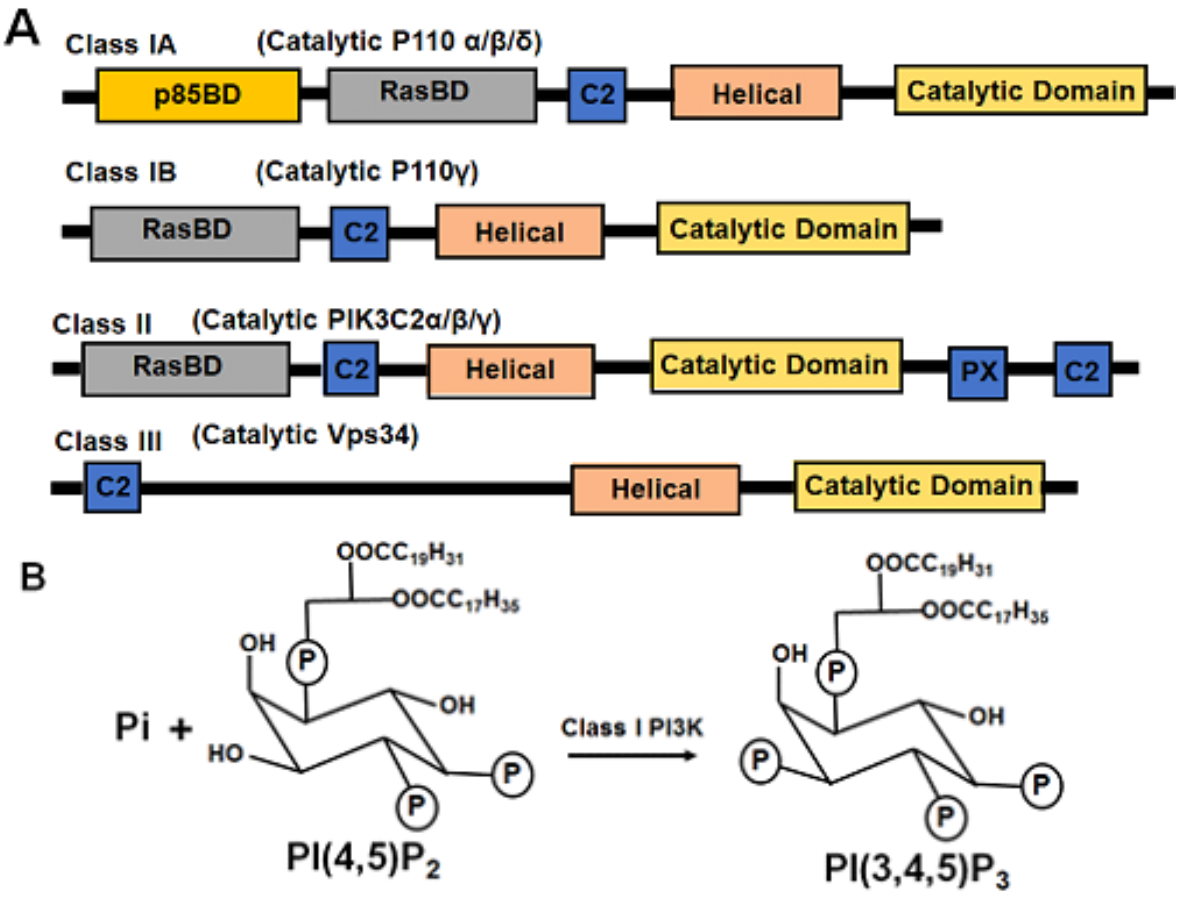

Figure 4: The structures and functions of PI3-kinases. A: Phosphoinositide 3-kinase (PI3K) family members are divided into Class IA (p110 catalytic subunit and p85 regulatory subunit, activated by RTKs), Class IB (heterodimer with a catalytic p110γ subunit and a p101 regulatory subunit exclusively activated by GPCRs), Class II (Begin with Ras binding domain (RasBD) from N-terminal, C2 domain, helical domain, and catalytic domain with PX and C2 domains at the C-terminal), and Class III (single catalytic subunit Vps34) due to the structural characteristics and substrate specificity. **B:** The intracellular PIP_3 level is modulated by Class I PI3-kinase [58].

PI3-kinases play fundamental roles in organ size control. In the cardiovascular system, abundant evidence suggests that only Class I and Class III PI3-kinase are expressed in the heart [60]. Class I PI3K/Akt signaling pathway is one of those well-studied signal transduction pathways that control cardiomyocyte survival and normal functions. Targeted overexpression of constitutively activate class I PI3-kinase in the heart results in increased organ size, which is

associated with a similar increase in cardiomyocyte size. While overexpression of dominant negative Class I PI3-kinase in the heart leads to smaller heart in mice, while dominant negative [61] treatment-induced inactivation of certain essential signaling transduction components such as p110 subunit inside Class I PI3-kinase in the heart attenuated cardiac hypertrophy in transgenic mice [62]. Oxidative stress-induced Class I PI3-kinase activation causes p70S6K1 activation and makes cardiomyocyte size growth, and this activation is associated with one 85-kDa regulatory subunit by tyrosine (TYR) phosphorylation and this hypertrophy was alleviated by wortmannin and rapamycin targeting at Class I PI3-kinase and mTOR respectively [63]. Also, inactivation of Class III PI3-kinase via deletion of the cardiac and hepatic Vps34/Pik3c3 component in $Vps34^{f/f}$ gene knockout mice provoked severe cardiac hypertrophy with impaired heart contractility and hepatomegaly with enhanced steatosis [64]. Therefore, the information demonstrates the importance of PI3-kinases in the progress of heart diseases.

1.8. Overall hypothesis of the current study

Heart failure means that the heart cannot meet the body's metabolic demand since it is unable to pump enough blood to the peripheral organs and tissues, bringing about major health issues and threatening people's well-beings in developed countries. In spite of significant therapeutic technical progresses, there are no sufficient advanced treatments for HF with an effective manner. Therefore, it is our primary concern to explore innovative clinical treatments for patients.

The pathophysiology of CHF is complicated and multifactorial to compensate for the weakened cardiac contractility and pump enough blood. The most essential point is that this compensatory mechanism leads to increased Ang II secretion by activating renin angiotensin system [10]. Ang II exposure to heart tissue may activate intracellular ROS generation in cardiomyocytes, trigger several kinases and transcription factors, and lead to subsequent cardiac

remodeling like hypertrophy, perivascular fibrosis, and apoptosis, resulting in cardiac dysfunction and aggravated symptoms of CHF. Furthermore, overexcitation of RAS plays a pivotal role in the pathogenesis of heart failure. It seems that chronic exposure to high dosage of Ang II may also impair autophagy in cardiomyocytes, resulting in damaged mitochondria accumulation. It is well known that autophagy is a very important intracellular mechanism to protect cells from hazardous material accumulation by scavenging damaged mitochondria or proteins that produce reactive oxygen species (ROS). Accumulating evidence indicates the possible involvement of autophagy in the pathophysiology of Ang II-induced cardiac hypertrophy. However, the intracellular mechanisms involved in the accumulation of damaged mitochondria-derived ROS generation and how impaired autophagy contributes in Ang II-induced cardiac hypertrophy are still unclear.

Recently, increasing evidence indicates the possible involvement of activated PI3-kinases in Ang II-induced heart failure. Besides previous literature reports, our preliminary data has also shown that the degree of autophagy was initially increased under lower dose of Ang II exposure and reached its peak at the Ang II concentration of 10^{-7} M, while autophagy became impaired as the dose of Ang II continued to rise. In addition, our preliminary data also indicated that under higher dosage of Ang II, pretreatment of Class I PI3-kinase inhibitor LY-294002 elevated autophagy, and attenuated ROS generation and hypertrophy, while pretreatment of Class III PI3-kinase inhibitor 3-MA diminished autophagy, and potentiated ROS generation and hypertrophy. The preliminary data suggest the possible involvement of both PI3-kinases in Ang II-induced cardiac remodeling via autophagic alteration. All the background information and our preliminary data lead us to hypothesize that **activation of Class I and Class III PI3-kinases in the heart is involved in Ang II-induced cardiac hypertrophy by ROS accumulation via an autophagic-dependent mechanism.** However, the role of the PI3-kinases in Ang II-induced cardiac

hypertrophy and the underlying intracellular mechanisms are still not fully clear. Thus, the current study was designed to test this hypothesis via the following specific aims:

Aim 1. To determine the role of Class I PI3-kinase-dependent signaling pathways in Ang II-induced autophagy, ROS generation, and hypertrophy in primary cardiomyocytes.

Aim 2. To examine the role of Class III PI3-kinase-dependent signaling pathways in Ang II-induced autophagy, ROS generation, and hypertrophy in primary cardiomyocytes.

Aim 3. To validate the role of Class I PI3-kinase in autophagy, ROS generation, cardiac hypertrophy and perivascular fibrosis in chronic Ang II-perfused rats.

Therefore, our major purpose of this current project was to provide evidences to evaluate the above-mentioned hypothesis. Furthermore, the main goal of this dissertation was to investigate the novel intracellular molecular mechanisms between the relationships of Ang II-induced cardiac hypertrophy and PI3-kinase activation-induced autophagic alteration. The combinations of *in vitro* and *in vivo* techniques with cellular, molecular and physiological approaches were used to realize this purpose. After the completion of those proposed aims, we believe a novel PI3-kinase-dependent autophagic pathway will be identified in the development of Ang II-induced cardiac hypertrophy. It would be the first signaling pathway identified switching the heart function from compensation to decompensation by distinguishing two stages of hypertrophy. Thus, the data generated from this project would facilitate novel therapeutic approaches by specific targeting of PI3-kinase signaling pathway.

CHAPTER II. THE ROLE OF CLASS I PI3-KINASE-DEPENDENT SIGNALING PATHWAYS IN ANG II-INDUCED AUTOPHAGY, ROS GENERATION, AND HYPERTROPHY IN PRIMARY CARDIOMYOCYTES

2.1. Introduction

Among the physiological and pathological factors that cause cardiac hypertrophy, angiotensin II (Ang II) stimulation plays an essential role [65, 66]. It is universally recognized that Ang II, acting as a vasoconstrictor, mainly stimulates cardiomyocytes via triggering angiotensin receptors type 1 (AT1R) on the cellular surface membrane [67, 68]. It is well established that Ang II is involved in the initial physiological compensatory mechanism to keep the cardiac output by inducing cardiac hypertrophy. Elevated circulating Ang II levels are due to sympathetic activation-induced renin release and reduced renal blood flow. At the initial stage, Ang II increases the preload and afterload to maintain normal cardiac function via compensatory mechanisms. In addition, long-term exposure and high level of Ang II contributes to the damaging effects on the heart and causes cardiac remodeling [69]. Accelerated protein synthesis takes place in cardiomyocytes and the molecular basis of myocardial fibers are restructured. As a result, cardiac hypertrophy shifts from compensatory to decompensatory, and cardiac output cannot meet the body metabolism in this stage, causing congestive heart failure [70].

Increasing information indicates that elevated ROS generation is involved in Ang II-induced cardiac hypertrophy. ROS generation is induced by stimulating intracellular ROS-producing enzymes such as NADPH oxidase (NOX, the main enzyme for ROS generation), xanthine oxidase (XO), uncoupled NO synthase (NOS), monoamine oxidase (MAO) and Cytochrome P450 oxidase. There might be a positive feedback relationship between Ang II receptor (ATR) and ROS generation, which means that Ang II-induced ROS generation would in turn, at least partially enhance the sensitivity of ATR, leading to elevated oxidative stress as a

vicious cycle [71]. ROS generation activates several cytosolic protein-synthesizing kinases like MAPK or Akt and intranuclear transcription factors like NFAT, GATA4 or NF-κB, and promote protein synthesis and subsequent hypertrophy [13, 26]. However, as is reported in recent literatures, genetic modification induced-inactivation of gp91phox subunit (a vital component of NADPH oxidase) in transgenic mice didn't show significant beneficial effects to alleviate Ang II-induced hypertension or cardiac hypertrophy, suggesting there might be an alternative intracellular pathway to generate ROS in cardiomyocytes in prolonged period of Ang II administration [72]. Abundant evidence indicates that Ang II-triggered mitochondrial dysfunction in cardiomyocytes generates redundant ROS and such excessive oxidative stresses own a positive effect on hypertrophy and subsequent heart failure [73]. Thus, clarifying the origin of ROS generation is essential for us to seek appropriate approaches to combat Ang II-induced cardiac hypertrophy.

Accumulation of ROS generation is a direct consequence of impaired autophagy. Autophagy, as a self-degradative process which removes and recycles damaged cellular organelles and proteins, keeps a homeostatic intracellular environment and the survival of cells [74]. For cardiomyocytes, though remarkably long-lived, they own a limited capacity of regeneration in adult hearts with a life-long activity of contractile action. Therefore, a constant procedure of cellular repair including elimination and substitution of impaired intracellular structures should be engaged [53]. Impaired autophagy in the heart could lead to the accumulation of defective mitochondria and proteins in cardiomyocytes, which may further lead to ROS generation [75]. Damaged mitochondria may continue generating greater levels of ROS that could stimulate stress-related signaling pathway, cardiac hypertrophy, and cardiac damage if they are not instantly got rid of due to impaired autophagy (mitophagy) [71]. Besides, DNA within mitochondria (mtDNA) has proinflammatory unmethylated CpG motifs, and mtDNA gathering could induce a toll-like receptor (TLR) inflammatory response, leading to cardiac hypertrophy and heart failure [18].

Class I PI3-kinase is one of those downstream signaling transduction kinases of Ang II receptor (AT) in cardiomyocytes with its downstream cascade components of Protein kinase B (Akt) and mammalian target of rapamycin (mTOR). Previous reports demonstrated that Class IA PI3-Kinass strongly provoke heart growth and cardiac hypertrophy, while nullification of this kinase by knocking out p85β subunit diminished heart size and alleviated cardiac hypertrophy [76] since Class I PI3-kinase negatively regulates autophagy via the Akt/mTOR-dependent mechanism. However, the role of Class I PI3-kinase in the progress Ang II-induced cardiac hypertrophy has not been fully investigated yet. Therefore, it is crucial to detect whether this kinase is involved in Ang II-induced cardiac hypertrophy.

In this chapter, we have investigated the intracellular signaling pathway mediated by Class I PI3-kinase and the relevant participating components in primary cardiomyocytes from SD rats under Ang II exposure to verify our hypothesis that activation of Class I PI3-kinase is essential for Ang II-induced cardiac hypertrophy via autophagic impairment. More specifically, the role of Class I PI3-kinase was studied in the action of Ang II on autophagy, ROS generation, cardiac hypertrophy, and expression of relevant phosphorylated kinases in cardiomyocytes using various biochemical and pharmacological tools.

2.2. Materials and methods

2.2.1. Preparation of cardiomyocyte cultures

Twelve-week-old male and female SD rats were obtained from Charles River Farms (Charles River Laboratories International, Wilmington, MA). Rats were housed at 25 ± 2°C on a 12:12-h light-dark cycle and provided with food and water ad libitum. All animal protocols were approved by the North Dakota State University Institutional Animal Care and Use Committee. Primary cardiomyocytes were randomly divided into each group. Generally, dissociated neonatal rat primary cardiomyocytes were cultured for 5 days, and culture media was changed every other

day. Then cardiomyocytes were treated with relevant reagents: 10^{-9} M~10^{-5} M Angiotensin II (Ang II, Alfa Aesar, J60866, Reston, VA), 1 μM LY-294002 (LY, Sigma Aldrich, L9908, St. Louis, MO), 100 nM rapamycin (Rapa, Alfa Aesar, J62473, Reston, VA), 1 μM Losartan (Los, Sigma Aldrich, 61188, St. Louis, MO), 1 μM PD-123319 (PD, Sigma Aldrich, P186, St. Louis, MO), 1 μM Mito-TEMPO (Mito, Santa Cruz Biotechnology, sc-221945, Santa Cruz, CA). All those reagents were administrated 30 minutes before Ang II stimulation in all experiments except dosage dependent-autophagy effect test of Ang II. After dosage-dependent effect test of Ang II, only 10^{-6} M Ang II was administrated after the pretreatment of relevant reagents. HBSS was used as negative control in Ang II dosage-autophagy effect test while 0.1% DMSO vehicle control was used as negative control for other subsequent experiments. The total exposure duration of Ang II and other reagents was 24 hours for autophagy and hypertrophy determination. While for ROS generation determination, intracellular ROS levels were measured immediately after addition of Ang II or HBSS control by incubation with MitoSOX since superoxide is unstable and gradually neutralized by intracellular superoxide dismutase (SOD) as time elapses.

2.2.2. Treatment protocol

1~3 days old neonatal SD rats were anesthetized by sodium pentobarbital (200 mg/kg, *i.p.*, Sigma, St. Louis, MO). Ventricle parts of the heart were quickly excised, minced into small pieces in cold HBSS and washed for several additional times. The minced tissue was digested with 0.1% trypsin in a 37ºC water bath with shaking for 5-min rounds of tissue digestion (10-12 times). After each incubation, the supernatant was added to an equal volume of DMEM containing 10% FBS. Then, isolated cells were filtrated with 70 μm cellular sieve, centrifuged at 1,000 rpm for 10 min. Supernatants were discarded after centrifuge; and cellular pellets were suspended in DMEM composed of 10% FBS and 1% penicillin-streptomycin at 37℃ for 1.5 hr in a humidified atmosphere with 95% O_2 and 5% CO_2 to allow the most of non-myocyte cells, such as fibroblasts,

to attach on the plate bottom. Suspended cellular solution (final cellular density 5×10^5 cells/cm^2) was transduction to a 24-well plate for morphological studies and to a 96-well plate for measurement of ROS levels. In the first three days, Brdu (100 μM) was added to suppress fibroblast growth. All of the manipulations were performed in culture hood to ensure an aseptic environment. After the primary cardiomyocyte cultures reached confluence (5 days on average) in an incubator filled with a humidified atmosphere of 5% CO_2 at 37 °C, cardiomyocytes were used for *in vitro* experiments.

2.2.3. Autophagy determination

Cultured cardiomyocytes were treated with relevant reagents for 24 h. Each treatment was performed in triplicate wells. In brief, after treatment, cells were fixed in 4% PFA at 4℃ for 30 min, and washed with fresh washing solution (0.1% Triton X-100 in PBS) three times. After pre-incubation with 3% of bovine serum albumin (BSA) for 20 minutes, the cells were incubated with primary antibody of MAP-LC3 (Santa Cruz Biotechnology, sc-134226, Santa Cruz, CA), which was diluted to 1:100 with PBS containing 3% BSA, for overnight at 4℃. After three washings with the PBS solution, the cells were incubated with fluorescence-conjugated Alexa Fluor 488 fluorescence-conjugated goat anti-rabbit IgG antibody (Molecular probes, A-11034, Waltham, MA) (1:1000 diluted in PBS) for 2 h at room temperature in dark. Photographic images of cardiomyocytes were taken with a fluorescence microscope (Olympus Microsystems, Waltham, MA). The MAP-LC3 antibody immunostaining positive images were analyzed, the puncta inside cardiomyocytes were counted and the average puncta number in each cell was calculated with at least 10 area of cells in each sample [77, 78]. The more average puncta in each cell indicates the larger degree of autophagy occurrence. HBSS negative control group was set as “1” and the results of each sample were expressed as “Fold *vs* Control”.

Immunostaining fluorescence was performed to evaluate the presence of LC3 II formation using anti-MAP-LC3 antibody which is one of the markers of autophagy. To further verify the cellular type in which LC3 II particles are present, we have co-stained primary cardiomyocyte cultures with an anti-α-actin antibody, a cardiomyocyte marker. Figure 5 shows that the LC3 II are abundantly expressed in primary cardiomyocytes.

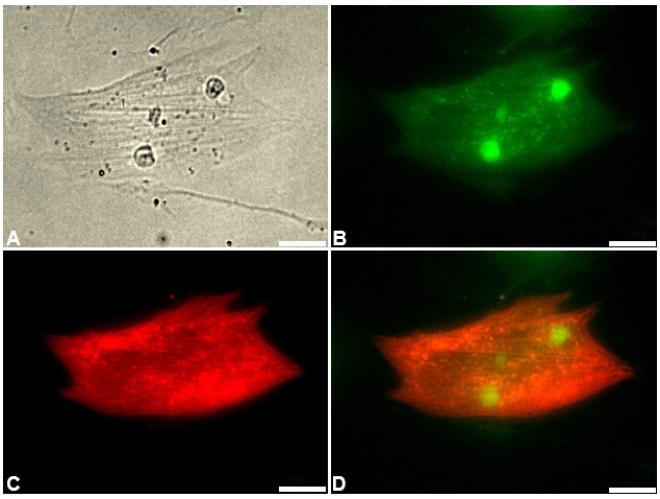

Figure 5: Identification of autophagy in primary cardiomyocytes. Immunofluorescence images showing autophagesomes marked with anti-MAP-LC3 antibody and cardiomyocyte-marker alpha-actin antibody (red). MAP-LC3 localization on cultured primary cardiomyocytes. A, Microscopic image taken from primary cardiomyocytes in optical phase. B, Fluorescence image demonstrating localization of autophagesomes. C, same field of cells as in A, immunostained with an anti-α-actin antibody. D, overlap of B and C, indicating that autophagesomes are localized within primary cardiomyocytes.

2.2.4. ROS detection

Mitochondrial ROS generation was determined using a superoxide-sensitive (O2·-) fluorogenic probe of MitoSox (Thermo Fisher, M-36008, Rockford, IL). MitoSOX has a dihydroethidium (DHE) part linked to triphenylphosphoninum (TPP) component and yields red fluorescence when oxidized (excitation/emission wavelength: 510/580 nm). This compound is more concentrated in the mitochondria than in the cytosol since the former has more positively charged TPP [79] . Cultured cardiomyocytes were pretreated with relevant reagents except Ang II

for 30 minutes. Then the cardiomyocytes were treated with Ang II (10^{-6} M) or HBSS control. Intracellular mitochondrial ROS levels were measured immediately after the addition of Ang II or HBSS control by incubation with MitoSOX (5×10^{-6} M, 15 minutes). The intracellular ROS levels were measured using a fluorometric imaging plate reader (Spectra Max Gemini EM, Molecular Devices) to detect changes in fluorescence resulting from intracellular probe oxidation. The vehicle (DMSO, 0.1%) control group was set as 100% MitoSOX fluorescence. Fluorescent images were also acquired using a fluorescence microscope (Olympus) to visualize the strength of MitoSOX fluorescence in primary cardiomyocytes.

2.2.5. Cardiac hypertrophy determination

Cultured cardiomyocytes were treated with relevant reagents and Ang II for 24 h. Each treatment was performed in triplicate wells. Anti-α-actin antibody was used for cardiac hypertrophy via immunofluorescence staining. In brief, cells were fixed in 4% PFA at 4℃ for 30 minutes, and washed with fresh washing solution (0.1% Triton X-100 in PBS) for three times. After pre-incubation with 3% of bovine serum albumin (BSA) for 20 minutes, the cells were incubated with primary antibody of sarcomeric α-actin (Santa Cruz Biotechnology, sc-53142, Santa Cruz, CA), which was diluted to 1:100 with PBS containing 3% BSA, overnight at 4℃. After three washings with the PBS solution, the cells were incubated with fluorescence-conjugated Alexa Fluor 594 goat anti-mouse IgG (Molecular probes, A-11032, Waltham, MA) (1:1000 diluted in PBS) for 2 h at room temperature in dark. Photographic images of cardiomyocytes were taken with a fluorescence microscope (Olympus Microsystems, Waltham, MA). The cellular surface area of positive image for α-actin staining cardiomyocytes was measured by the image analysis software (NIH Image J) [80]. Variations of cellular size were expressed as relative cellular surface area versus the control. The 0.1% DMSO negative control group was set as 100%.

2.2.6. Western blot analysis

Akt and p-Akt protein levels in primary cardiomyocyte cultures were assessed by western blot analysis to determine the phosphorylation degree of those downstream components of Class I PI3-kinase. Briefly, after drug treatment for 24 hours, primary cardiomyocyte cultures were washed with ice-cold PBS and scraped into a lysis buffer containing 20 mM Tris HCl (pH 6.8), 150 mM NaCl, 10% glycerol, 1% NP-40, and 8 µL/mL inhibitor cocktail (125 mM PMSF, 2.5 mg/mL aprotinin, 2.5 mg/mL leupeptin, 2.5 mg/mL antipain, and 2.5 mg/mL chymostatin). The samples were sonicated twice for 5 s each and were centrifuged at 12,000 rpm for 10 min at 4°C. Supernatants were transferred into new tubes and stored in a -80°C freezer. The protein concentration was determined with a protein assay kit (Bio-Rad Laboratories, Hercules, CA). An aliquot of 30 µg of protein from each sample was separated on a 10% SDS-PAGE gel and was transferred onto nitrocellulose membranes for 2 h at 120 V. After a 10-min wash in TBST, membranes were blocked in PBST containing 10% milk for 1 h, followed by an overnight incubation in rabbit anti-Akt (Santa Cruz Biotechnology, sc-8312, Santa Cruz, CA), and anti-p-Akt (Santa Cruz Biotechnology, sc-2448, Santa Cruz, CA) antibody (dilution 1:100) at 4 °C. After a 15-min wash in TBST, four 5-min washes in PBS-T will be carried out, and membranes will be then incubated for 2 h in an anti-rabbit peroxidase-conjugated antibody (dilution 1:15,000). Densitometry of p-Akt was normalized to total Akt, and immunoreactivity was detected by enhanced chemiluminescence autoradiography (ECL Western blotting detection kit, Amersham Pharmacia Biotechnology), and films were analyzed with Quantity One Software (Bio-Rad).

2.2.7. Class I PI3-kinase activity assay

After treatment of relevant reagents, primary cardiomyocytes from neonatal rats were rinsed with ice-cold PBS and Buffer A (20 mM Tris-HCl, pH 7.4, 137 mM NaCl, 1 mM $CaCl_2$, 1 mM $MgCl_2$, and 1 mM Na_3VO_4) three times each. Then Buffer A was removed and the cells were

immediately lysed in lysis buffer Lysis Buffer (Buffer A plus 1% NP-40 and 1 mM PMSF) at 4°C for 20 minutes by rocking. The cells were scraped from dishes, transferred to 1.5 mL microcentrifuge tubes and centrifuged for 10 minutes to sediment insoluble material. Thereafter, supernatant was transferred to new tubes added with 5 μL of anti-PI3-Kinase antibody (Millipore Corp, 06-195, Billerica, MA) previously described [81] to each tube and incubated for one hour at 4°C with gentle rotation. 60 μL of 50 % slurry of Protein A-agarose beads in PBS was added into each tube with gentle rotation for overnight, and tubes were centrifuged for 5 seconds for collection of immunoprecipitated enzymes. Sediments were washed three times with Buffer A plus 1% NP-40, three times with 0.1 M pH 7.4 Tris-HCl with 5 mM LiCl and 1 mM Na_3VO_4, twice with TNE (10 mM Tris-HCl, pH 7.4, 150 mM NaCl, 5 mM EDTA) containing 1 mM Na_3VO_4 and twice with KBZ Reaction Buffer. The last wash was aspirated completely and 30 μL of KBZ Reaction Buffer was added to cover the beads. Then the Class I PI3-kinase reactions were carried out using competitive enzyme-linked immunosorbent assay kit (Echelon Biosciences, K-1000s, Salt Lake City, UT) by exactly following the instructions provided by the manufacturer. A PIP_3 standard curve (ranging from 4.4 nM to 1.08 μM) was simultaneously prepared and determined at 450 nm wavelength. Each assay was repeated at least 3 times.

2.2.8. Data analysis

All data are presented as means ± S.E.M. Statistical significance was evaluated by one- or two-way ANOVA, as appropriate, followed by either a Newman–Keuls or Bonferroni post hoc analysis when indicated. Differences will be considered significant at $P<0.05$, and individual probability values are noted in figures.

2.3. Results

2.3.1. Dose-dependent effect of Ang II on autophagy, Class I PI3-kinase activity and phosphorylation of Akt

Accumulating evidence indicates the possible involvement of autophagy in the pathophysiology of Ang II-induced cardiac hypertrophy [82]. Autophagy is an very important intracellular mechanism to protect cells from hazardous material accumulation by scavenging damaged mitochondria or proteins that produce reactive oxygen species (ROS). Intracellular ROS plays an important role in the pathogenesis of cardiac hypertrophy. Thus, we examined the effect of Ang II on autophagy in cardiomyocytes using immunofluorescence staining with antibodies against microtubule-associated protein light chain 3 (MAP-LC3), an autophagosome marker. The autophagesomes within cardiomyocytes are visualized as green fluorescent puncta, which are able to be counted under microscope. The results are presented in Figure 6, indicating that Ang II treatment produces a dose-dependent increases in autophagy with two phases; an increasing phase at lower dosages (autophagy degree 1.00 ± 0.05 in Ctrl vs. 3.81 ± 0.13 in 10^{-7} M Ang II, increased by 281% $P < 0.01$ vs. HBSS Ctrl) and a decreasing phase at high dosages (autophagy degree 3.81 ± 0.13 in 10^{-7} M Ang II vs. 1.75 ± 0.08 in 10^{-5} M Ang II, decreased by 54.1 %, $P < 0.05$ vs. HBSS Ctrl). Still, the degree of autophagy at the maximum concentration of 10^{-5} M Ang II was higher than the baseline of HBSS control, suggesting elevated autophagy under Ang II stimulation. Taken together, those results demonstrate that lower dosage Ang II exposure elevated while higher dosage Ang II impaired autophagy.

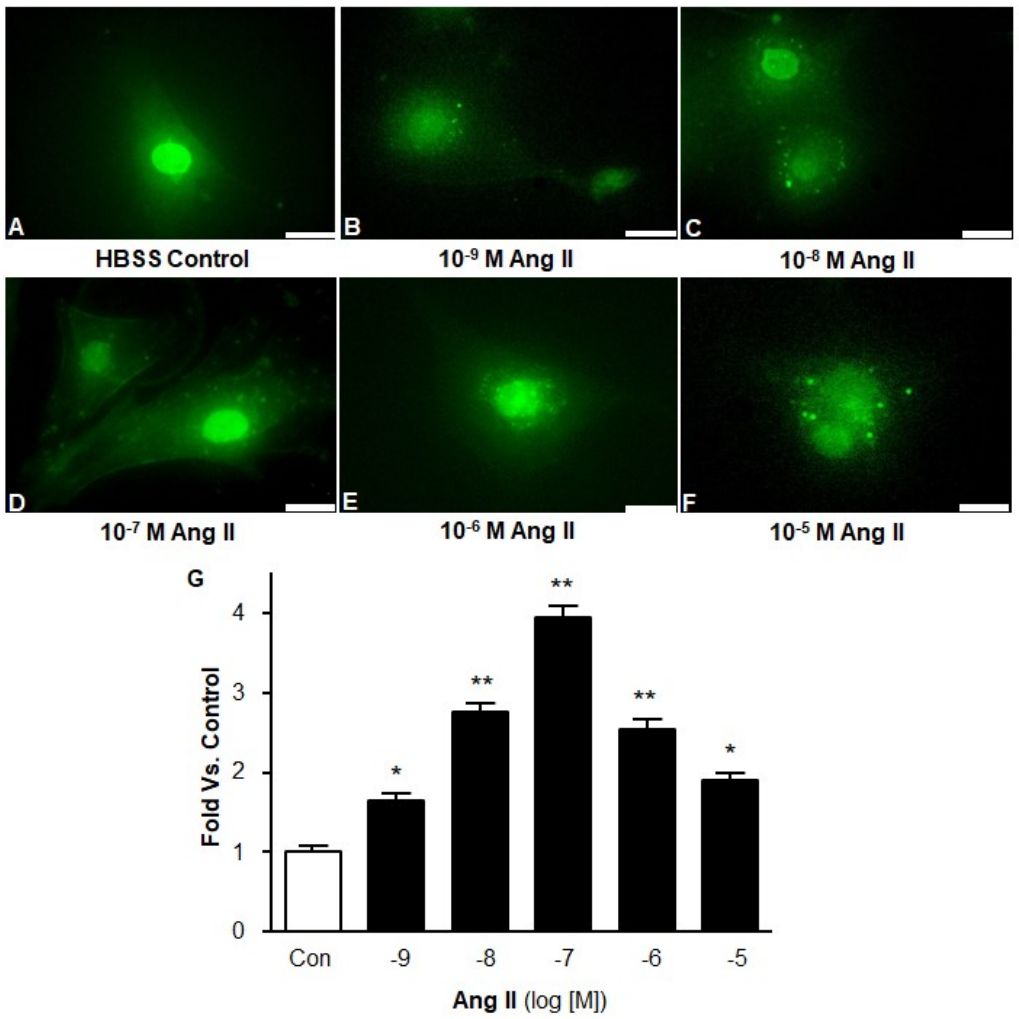

Figure 6: Dose-dependent effect of Ang II on autophagy in cardiomyocytes. Autophagy was examined in cardiomyocytes by immunostaining fluorescence with MAP-LC3 antibody 24 hours after treated with HBSS control or Ang II at dosages indicated in the figure. **A-F:** Representative fluorescence micrographs of cultured cardiomyocytes stained with MAP-LC3 antibody after the following treatments: HBSS control (A), 10^{-9} M Ang II (B), 10^{-8} M Ang II (C), 10^{-7} M Ang II (D), 10^{-6} M Ang II (E), or 10^{-5} M Ang II (F). **G:** Bar graphs summarizing quantitative analysis of autophagic alterations in cardiomyocytes treated with HBSS control or Ang II at different dosages (10^{-9} M - 10^{-5} M). The scale in the images is 25 μm. Data are presented as means ± SE and were derived from three experiments and at least triplicate wells in each experiment. $^{*}P < 0.05$ vs. HBSS control. $^{**}P < 0.01$ vs. HBSS control.

Class I PI3-kinase activity was measured since we assume this kinase is involved in the impairment of autophagy under pathological higher Ang II concentration. For this reason, a measurement of PIP_3 production is the indirect estimation of intracellular Class I PI3-kinase levels. PIP_3 levels were measured 24 hours after treatment of Ang II with different dosages or HBSS

control. After Ang II treatment, the cardiomyocytes were lysed for PIP_3 determination by the PIP_3 ELISA kit according to the manufacturer's protocol. Results are shown in Figure 7. The results indicate that the activity of Class I PI3-kinase is slightly elevated with lower dosages of Ang II by 80 % (PIP_3 production (in pmol/μg of protein) 1.45 ± 0.09 in Ctrl vs. 2.61 ± 0.12 in 10^{-7} M Ang II, P <0 .01 vs. HBSS Ctrl), while a sharp increase of Class I PI3-kinase activity is witnessed when the Ang II concentration exceeds 10^{-7} M (PIP_3 production (in pmol/μg of protein) 2.61 ± 0.12 in 10^{-7} M Ang II vs. 3.35 ± 0.13 in 10^{-5} M Ang II, P <0 .01 vs. HBSS Ctrl), suggesting Class I PI3-kinase is fully activated under higher dosage of Ang II exposure (exceeding 10^{-7} M Ang II). The dose-dependent stimulatory effect of Ang II on Class I PI3-kinase started at 10^{-8} M and reached to the peak at 10^{-6} M.

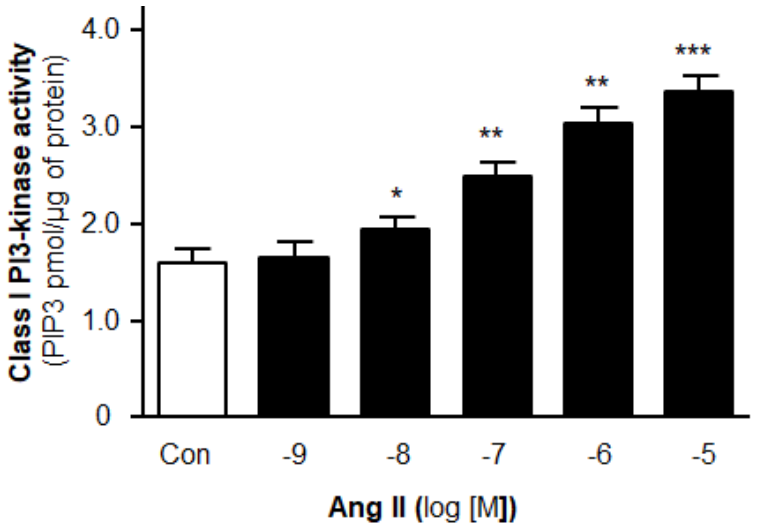

Figure 7: Dose-dependent effect of Ang II on the activity of Class I PI3-kinase in cardiomyocytes. Bar graphs summarizing the activities of Class I PI3-kinases measured using PIP_3 ELISA kits in cardiomyocytes as described in Methods. The Class I PI3-kinase activities are presented as the concentrations of PIP_3 in per microgram protein 24 hours after treated with HBSS control or Ang II with different dosages. Data are presented as means ± SE, which were derived from three experiments and at least triplicate wells in each experiment. $^{*}P < 0.05$, $^{**}P < 0.01$, $^{***}P < 0.001$ as compared with cardiomyocytes treated with HBSS control.

Akt is one of those direct downstream components of Class I PI3-kinase, and phosphorylation of Akt reflects the effect of Class I PI3-kinase. Thus, we measured the ratio of p-

Akt/Total Akt by western blot in cardiomyocytes treated by Ang II with different dosages. The results are shown in Figure 8, indicating that the activity of Akt is slightly elevated under lower dosage of Ang II (p-Akt/Total Akt from 0.072 ± 0.005 in Ctrl to 0.134 ± 0.007 in 10^{-7} M Ang II, P <0 .01 vs. HBSS Ctrl), while an intense increase of Akt phosphorylation is observed when the Ang II concentration exceeds 10^{-7} M (p-Akt/Total Akt 0.134 ± 0.007 in 10^{-7} M Ang II vs. 0.181 ± 0.013 in 10^{-5} M Ang II, P <0.001 vs. HBSS Ctrl), suggesting Akt is activated under higher dosage of Ang II exposure by phosphorylation and will activate its downstream components.

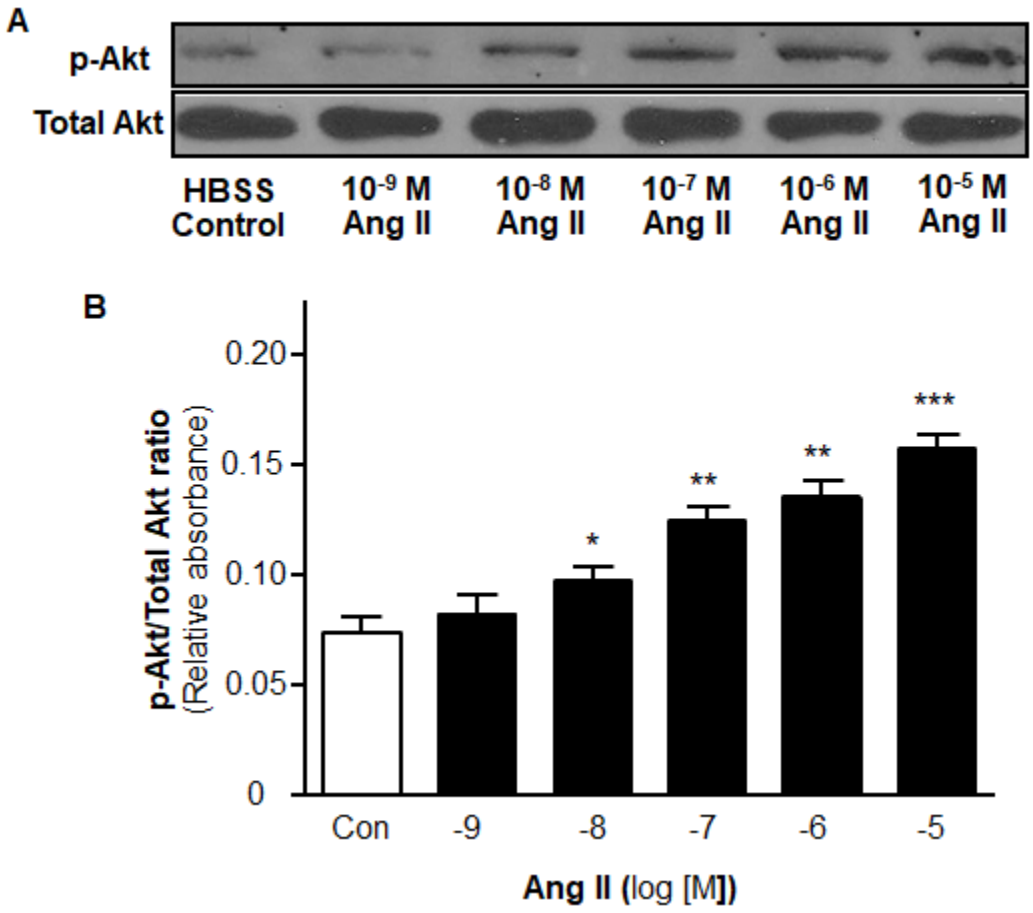

Figure 8: Dose-dependent effect of Ang II on the phosphorylation of Akt in cardiomyocytes. **A:** Representative western blots of cardiomyocytes lysate probed for phosphorylated Akt (p-Akt) and total Akt in each group of Ang II dosages (from 10^{-9} M to 10^{-5} M) respectively for 24 h. **B:** Bar graphs summarizing the ratio of phosphorylated Akt vs. total Akt. Data are means ± SE of the ratio of p-Akt/Total Akt. Data are presented as means ± SE, which were derived from three experiments and at least triplicate wells in each experiment. $^{*}P < 0.05$, $^{**}P < 0.01$, $^{***}P < 0.001$ as compared with cardiomyocytes treated with HBSS control.

2.3.2. The effect of LY-294002, a Class I PI3-kinase inhibitor on autophagy, ROS generation, cardiac hypertrophy and Class I PI3-kinase activity

To identify the intracellular mechanisms underlying Ang II-induced autophagy, the effect of high dose of Ang II on autophagy in cardiomyocytes was examined with and without presence of LY-294002 (LY, an inhibitor of Class I PI3-kinase). The results are presented in Figure 9 and demonstrated that Ang II (10^{-6} M) significantly induced an significant elevation in autophagy at the presence of vehicle by 161.0 % (DMSO, 0.1%, 1.00 ± 0.05 in control vs. 2.61 ± 0.12 in Ang II treatment, n=3 experiments, $P < 0.01$ vs. Vehicle Control). Preincubation of cardiomyocytes with LY-294002 (1 μM, 30 min) significantly potentiated Ang II-induced autophagy by 46.4% (1.06 ± 0.07 in LY-294002 alone vs. 3.82 ± 0.13 in LY-294002 plus Ang II, n=3 experiments, $P < 0.05$ vs. Ang II). In addition, treatment with LY-294002 alone did not alter the basal autophagy in cardiomyocytes. Taken together, Class I PI3-kinase contributes to Ang II-induced impairment in autophagy via a Class I PI3-kinase-mediated inhibitory mechanism.

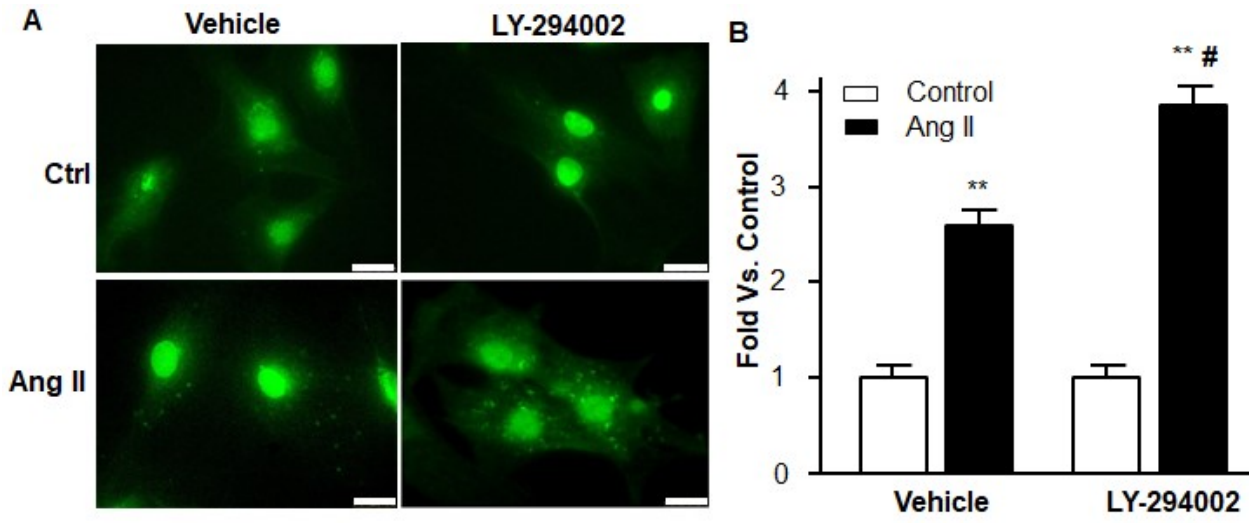

Figure 9: Effect of blockade of Class I PI3-kinase on Ang II-induced autophagy in cardiomyocytes. Autophagy was examined in cardiomyocytes by immunostaining fluorescence with MAP-LC3 antibody 24 hours after treated with Ang II (10^{-6} M) with or without the Class I PI3-kinase inhibitor, LY-294002 (LY, 1 μM, an inhibitor of Class I PI3-kinase). **A:** Representative fluorescence micrographs of cultured cardiomyocytes stained with MAP-LC3 antibody after the following treatments: Vehicle control, 1 μM LY-294002, an inhibitor of Class I PI3-kinase, 10^{-6} M Ang II, or LY-294002 + Ang II. MAP-LC3 immunofluorescence staining shows LY-294002 pretreatment elevates autophagy under 10^{-6} M Ang II exposure. **B:** Bar graphs demonstrating the effect of autophagy with the addition of LY-294002 under 10^{-6} M Ang II exposure. The scale in the images is 25 μm. Data are means ± SE and were derived from three experiments and at least triplicate wells in each experiment. $^{**}P < 0.01$ vs. cardiomyocytes that treated with vehicle control. $^{\#}P < 0.05$ vs. cardiomyocytes that treated with Ang II.

Accumulated evidence indicates that intracellular mitochondrial-ROS plays an important role in Ang II-induced cardiac hypertrophy [83] and that mitochondrial ROS is scavenged by autophagy [79]. Thus, we examined the role of Class I PI3-kinase in Ang II-induced mitochondrial ROS generation. The mitochondrial ROS generation was measured using the MitoSox fluorescence approach in cardiomyocytes treated by control or Ang II (10^{-6} M) with or without pretreatment with the Class I PI3-kinase inhibitor, LY-294002 (1 μM, 30 min). The results are presented in Figure 10, demonstrating that treatment of cardiomyocytes with Ang II significantly increased mitochondrial ROS generation at the presence of vehicle (DMSO, 0.1%) by 69.3 % as expected (100 ± 2.35 % in control vs 169.30 ± 3.60 % in Ang II, n=3 experiments, $P < 0.01$ vs. Vehicle Control). More interestingly, treatment with LY-294002 dramatically attenuated Ang II-

induced increases in mitochondrial ROS accumulation by 31.7 % in cardiomyocytes (95.30 ± 2.20 % in LY-294002 alone vs. 115.60 ± 3.02 % in LY-294002 plus Ang II, n=3 experiments, $P < 0.05$ vs. Ang II). In addition, treatment with LY-294002 alone did not alter the basal mitochondrial ROS generation. Those data suggest that Class I PI3-kinase is involved in Ang II-induced mitochondrial ROS accumulation in cardiomyocytes through a Class I PI3-kinase-dependent stimulatory mechanism.

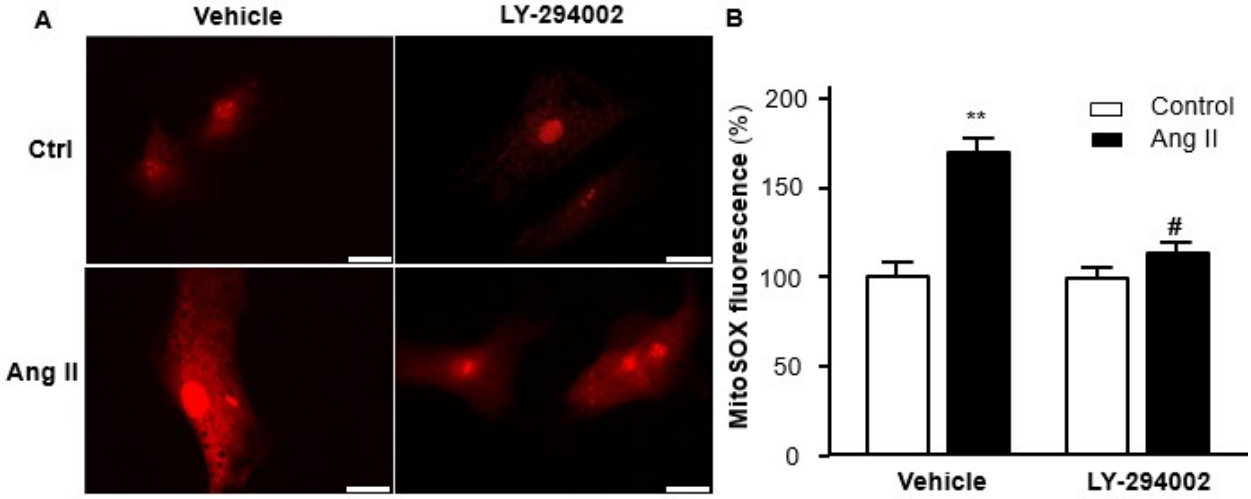

Figure 10: Effect of blockade of Class I PI3-kinase on Ang II-induced mitochondrial ROS generation in cardiomyocytes. Mitochondrial ROS levels were determined using the oxidant-sensitive fluorogenic probe MitoSOX in neonatal rat primary cardiomyocytes. Mitochondrial ROS levels were determined using the oxidant-sensitive fluorogenic probe MitoSOX in cardiomyocytes after treated with Ang II (10^{-6} M) with or without the Class I PI3-kinase inhibitor, LY-294002 (LY, 1 μM, an inhibitor of Class I PI3-kinase) for 24 hours. **A:** Representative fluorescence micrographs of cultured cardiomyocytes loaded with MitoSOX after the following treatments: Vehicle control, LY-294002 (LY, 1 μM), 10^{-6} M Ang II, or Ang II + LY. **B:** Bar graphs summarizing the effect on mitochondrial ROS production in cardiomyocytes treated with the conditions described in the above. The scale in the images is 25 μm. Data are presented as means ± SE, which were derived from three experiments and at least triplicate wells in each experiment. $^{**}P < 0.01$ vs. cardiomyocytes treated with vehicle control. $^{\#}P < 0.05$ vs. cardiomyocytes treated with Ang II.

After we measured the effect of blockade of Class I PI3-kinase on Ang II-induced ROS generation, we examined the role of Class I PI3-kinase in Ang II-induced cardiac hypertrophy. The cardiac hypertrophy in cardiomyocytes was measured using the α-actin immunofluorescence in cardiomyocytes treated by Vehicle control or Ang II (10^{-6} M) with or without pretreatment with

the Class I PI3-kinase inhibitor, LY-294002 (1 μM, 30 min). The results are presented in Figure 11, demonstrating that treatment of cardiomyocytes with Ang II significantly increased cardiac hypertrophy at the presence of vehicle (DMSO, 0.1%) by 104.6 % as expected (Relative cellular surface area 100 ± 4.7 % in control vs. 204.6 ± 8.5 % in Ang II, n=3 experiments, $P < 0.01$ vs. Vehicle Control). More interestingly, treatment with LY-294002 significantly attenuated Ang II-induced increases in cardiac hypertrophy by 38.7 % in cardiomyocytes (95.3 ± 2.2 % in LY-294002 alone vs. 125.2 ± 6.20 % in LY-294002 plus Ang II, n=3 experiments, $P < 0.05$ vs. Ang II). In addition, treatment with LY-294002 alone did not alter the basal hypertrophic state of cardiomyocytes. In summary, those data demonstrate that Class I PI3-kinases is involved in Ang II-induced cardiac hypertrophy in cardiomyocytes through a Class I PI3-kinase-dependent stimulatory mechanism.

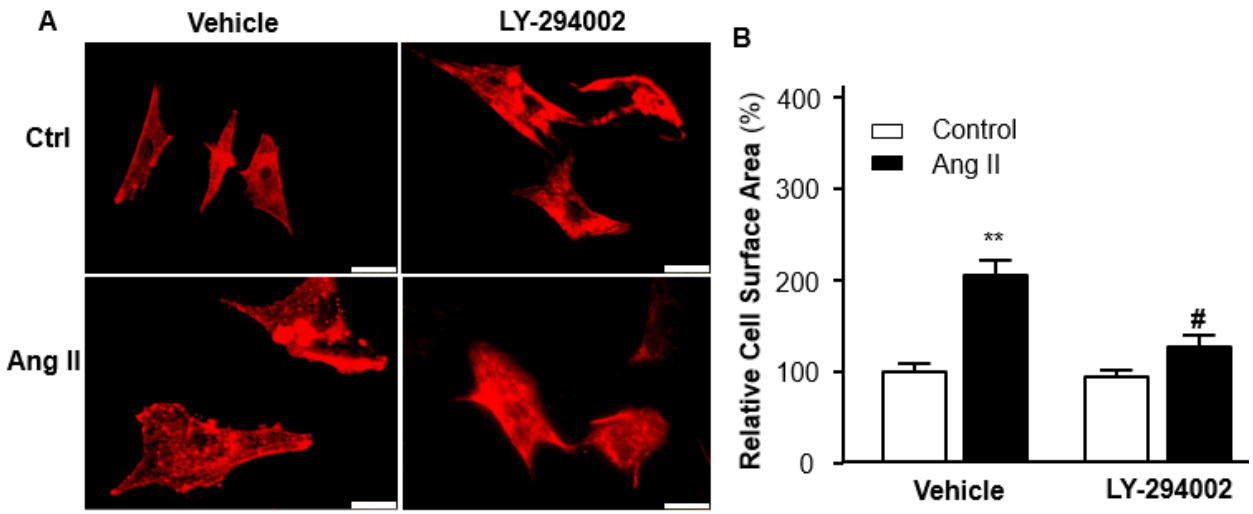

Figure 11: Effect of blockade of Class I PI3-kinase on Ang II-induced cardiac hypertrophy in cardiomyocytes. Cardiac hypertrophy in cardiomyocytes was determined using immunofluorescent staining with α-sarcomeric actin antibody after treated with Ang II (10^{-6} M) with or without the Class I PI3-kinase inhibitor, LY-294002 (LY, 1 μM, an inhibitor of Class I PI3-kinase) for 24 hours. **A:** Representative fluorescence micrographs of cultured cardiomyocytes loaded with α-sarcomeric actin antibody after the following treatments: Vehicle control, LY-294002 (1 μM, an inhibitor of Class I PI3-kinase), 10^{-6} M Ang II, or Ang II + LY. **B:** Bar graphs summarizing the effect on cardiac hypertrophy in cardiomyocytes treated with the conditions described in the above. The scale in the images is 25 μm. Data are presented as means ± SE, which were derived from three experiments and at least triplicate wells in each experiment. $^{**}P < 0.01$ vs. cardiomyocytes treated with vehicle control. $^{\#}P < 0.05$ vs. cardiomyocytes treated with Ang II.

Next, we measured the effect of blockade of Class I PI3-kinase on Ang II-induced Class I PI3-kinase activity. The Class I PI3-kinase activity was measured using the ELISA kit in cardiomyocytes treated by control or Ang II (10^{-6} M) with or without treatment with the Class I PI3-kinase inhibitor, LY-294002 (1 μM, 30 min). The results are presented in Figure 12, demonstrating that treatment of cardiomyocytes with Ang II significantly increased Class I PI3-kinase activity at the presence of vehicle (DMSO, 0.1%) by 108.3 % as expected (PIP_3 production (pmol/μg of protein) 1.45 ± 0.09 in control vs. 3.02 ± 0.08 in Ang II, n=3 experiments, $P < 0.01$ vs. Vehicle Control). More surprisingly, treatment with LY-294002 dramatically attenuated Ang II-induced increases in Class I PI3-kinase activity by 36.8% (PIP_3 production (pmol/μg of protein) 3.02 ± 0.08 in Ang II vs. 1.91 ± 0.12 in LY-294002 plus Ang II, n=3 experiments, $P < 0.05$ vs. Ang

II). Besides, the addition of 1 μM LY-294002 alone did not affect the basal activity of Class I PI3-kinase.

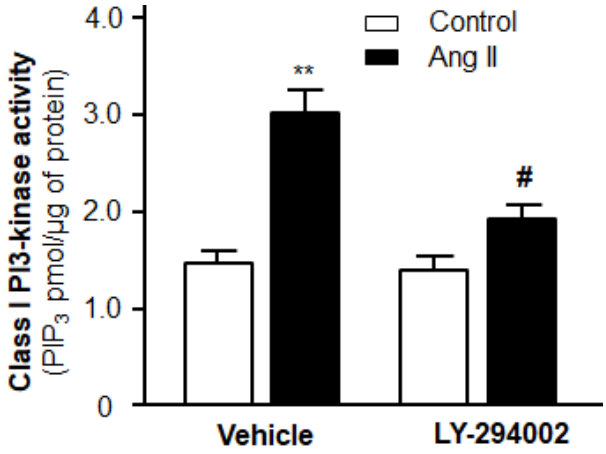

Figure 12: Effect of blockade of Class I PI3-kinase on Ang II-induced Class I PI3-kinase activity in cardiomyocytes. Class I PI3-kinase activity in cardiomyocytes was determined using the ELISA kit after treated with Ang II (10^{-6} M) with or without the Class I PI3-kinase inhibitor, LY-294002 (LY, 1 μM) for 24 hours. Bar graphs summarizing the effect on Class I PI3-kinase activity in cardiomyocytes treated with Vehicle control, LY-294002 (LY, 1 μM, an inhibitor of Class I PI3-kinase), 10^{-6} M Ang II, or Ang II + LY. Data are presented as means ± SE, which were derived from three experiments and at least triplicate wells in each experiment. $^{**}P < 0.01$ vs. cardiomyocytes treated with vehicle control. $^{\#}P < 0.05$ vs. cardiomyocytes treated with Ang II.

2.3.3. The effect of blocking different types of Ang II receptors on Ang II-induced autophagy, ROS generation, cardiac hypertrophy and Class I PI3-kinase activity

After we determined the role of mTOR in Ang II-induced cardiac remodeling, we tested which type(s) of Ang II receptor is (are) responsible for Ang II-induced cardiac remodeling. The effect of high dose of Ang II on autophagy in cardiomyocytes was examined with and without presence of Losartan or PD-123319 to block Ang II receptor type 1 or 2 respectively. The results are presented in Figure 13, and preincubation of cardiomyocytes with Ang II receptor type 1 antagonist of Losartan (Los, 1 μM, 30 min) significantly diminished Ang II-induced autophagy by 59.7 % (0.95 ± 0.07 in Losartan alone vs. 1.05± 0.09 in Losartan plus Ang II, n=3 experiments, $P < 0.05$ vs. Ang II). In contrast, pretreatment with Ang II receptor type 2 antagonist of PD-123319

(PD, 1 μM, 30 min) did not significantly alter Ang II-induced autophagy (1.02 ± 0.07 in PD-123319 alone vs. 2.57 ± 0.16 in PD-123319 plus Ang II, n=3 experiments, $P > 0.05$ vs. Ang II). In addition, treatment with Losartan or PD-123319 alone did not alter the basal autophagy in cardiomyocytes. Taken together, the results demonstrate that Ang II-induced autophagic alteration in cardiomyocytes is mainly mediated via Ang II receptor Type 1 activation.

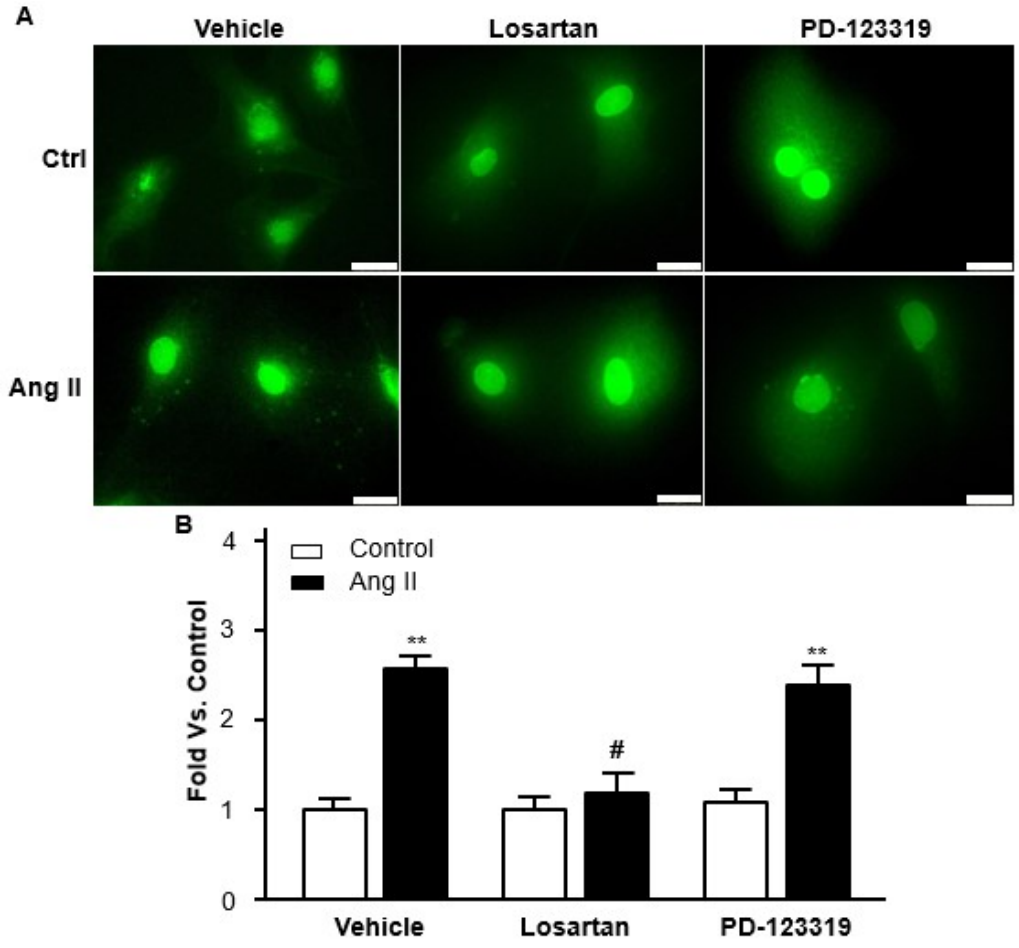

Figure 13: Effect of blockade of Ang II receptor type 1 or type 2 on Ang II-induced autophagy in cardiomyocytes. Autophagy was examined in cardiomyocytes by immunostaining fluorescence with MAP-LC3 antibody 24 hours after treated with Ang II (10^{-6} M) with or without the Ang II receptor type 1 antagonist of Losartan (Los, 1 μM), or the Ang II receptor type 2 antagonist of PD-123319 (PD, 1 μM). **A:** Representative fluorescence micrographs of cultured cardiomyocytes stained with MAP-LC3 antibody after the following treatments: vehicle control, Losartan, PD-123319, Ang II, Losartan + Ang II, or PD-123319 + Ang II. **B:** Bar graphs summarizing quantitative analysis of autophagic alterations in cardiomyocytes treated under the conditions described in the above. The scale in the images is 25 μm. Data are means ± SE and were derived from three experiments and at least triplicate wells in each experiment. $^{**}P < 0.01$ vs. cardiomyocytes that treated with vehicle control. $^{\#}P < 0.05$ vs. cardiomyocytes that treated with Ang II.

Next, we tested the effect of different Ang II receptor antagonists on ROS generation. The mitochondrial ROS production was measured using the MitoSox fluorescence in cardiomyocytes treated by control or Ang II (10^{-6} M) with or without pretreatment with the Ang II receptor type 1 antagonist of Losartan (1 μM, 30 min) or the Ang II receptor type 2 antagonist of PD-123319 (1

μM, 30 min). The results are presented in Figure 14, demonstrating treatment with Losartan dramatically attenuated Ang II-induced increases in mitochondrial ROS accumulation by 32.4 % in cardiomyocytes (97.50 ± 2.66 % in Losartan alone vs. 114.40 ± 2.71 % in Losartan plus Ang II, n=3 experiments, $P < 0.05$ vs. Ang II). In contrast, treatment with PD-123319 did not significantly alter Ang II-induced elevations in mitochondrial ROS production in cardiomyocytes (103.20 ± 3.25 % in PD-123319 alone vs. 159.2 ± 4.70 % in PD-123319 plus Ang II, n=3 experiments, $P > 0.05$ vs. Ang II). In addition, treatment with Losartan or PD-123319 alone did not alter the basal mitochondrial ROS production. The results demonstrated that Ang II-induced ROS generation in cardiomyocytes is mainly mediated via Type 1 Ang II receptor activation.

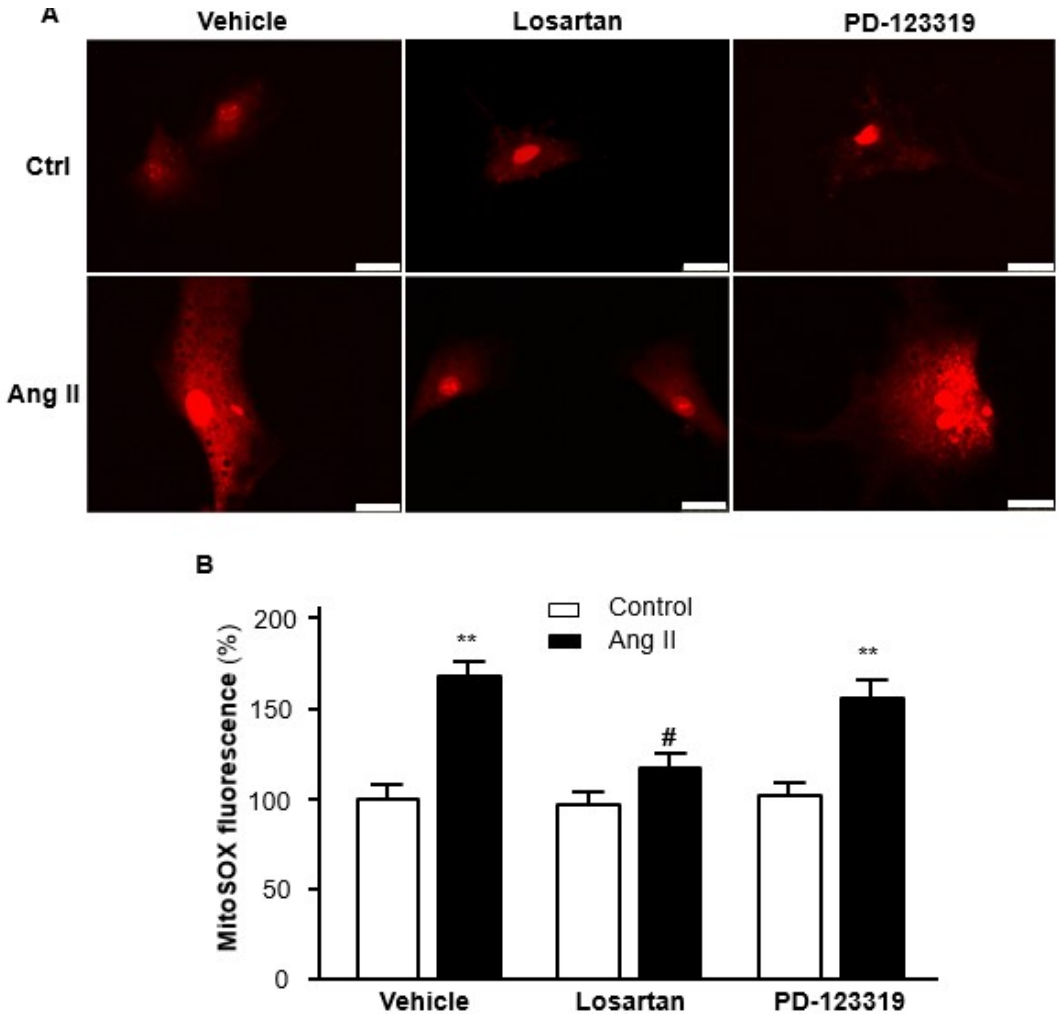

Figure 14: Effect of blockade of Ang II receptor type 1 or type 2 on Ang II-induced ROS generation in cardiomyocytes. Mitochondrial ROS levels were determined using the oxidant-sensitive fluorogenic probe MitoSOX in cardiomyocytes after treated with Ang II (10^{-6} M) with or without the Ang II receptor type 1 antagonist of Losartan (Los, 1 μM) or the Ang II receptor type 2 antagonist PD123319 (PD, 1 μM) for 24 hours. **A:** Representative fluorescence micrographs of cultured cardiomyocytes probed by MitoSOX after the following treatments: vehicle control, Losartan, PD-123319, Ang II, Losartan + Ang II, or PD-123319 + Ang II. **B:** Bar graphs summarizing the effect on mitochondrial ROS production in cardiomyocytes treated with the conditions described in the above. The scale in the images is 25 μm. Data are presented as means ± SE, which were derived from three experiments and at least triplicate wells in each experiment. $^{**}P < 0.01$ vs. cardiomyocytes treated vehicle control. $^{\#}P < 0.05$ vs. cardiomyocytes treated with Ang II.

After the determination of blockade of AT1R or AT2R on Ang II-induced ROS generation, we measured the effect of different Ang II receptor antagonists on cardiac hypertrophy. The cardiac

hypertrophy in cardiomyocytes was measured using the α-actin immunofluorescence in cardiomyocytes treated by Vehicle control or Ang II (10^{-6} M) with or without pretreatment with the Ang II receptor type 1 antagonist of Losartan (1 μM, 30 min) or Ang II receptor type 2 antagonist PD-123319 (1 μM, 30 min). The results are presented in Figure 15, demonstrating treatment with Losartan significantly attenuated Ang II-induced increases in cardiac hypertrophy by 37.8 % in cardiomyocytes (Relative cellular surface area 102.3 ± 4.12 % in Losartan alone vs. 127.2 ± 3.92 % in Losartan plus Ang II, n=3 experiments, $P < 0.05$ vs. Ang II). In contrast, treatment with PD-123319 did not significantly alter Ang II-induced elevations in cardiac hypertrophy in cardiomyocytes (103.50 ± 4.60 % in PD-123319 alone vs. 185.6 ± 8.30 % in PD-123319 plus Ang II, n=3 experiments, $P > 0.05$ vs. Ang II). In addition, treatment with Losartan or PD-123319 alone did not alter the basal cellular surface area. The results demonstrated that Ang II-induced cardiac hypertrophy in cardiomyocytes is mainly mediated via Ang II receptor Type 1.

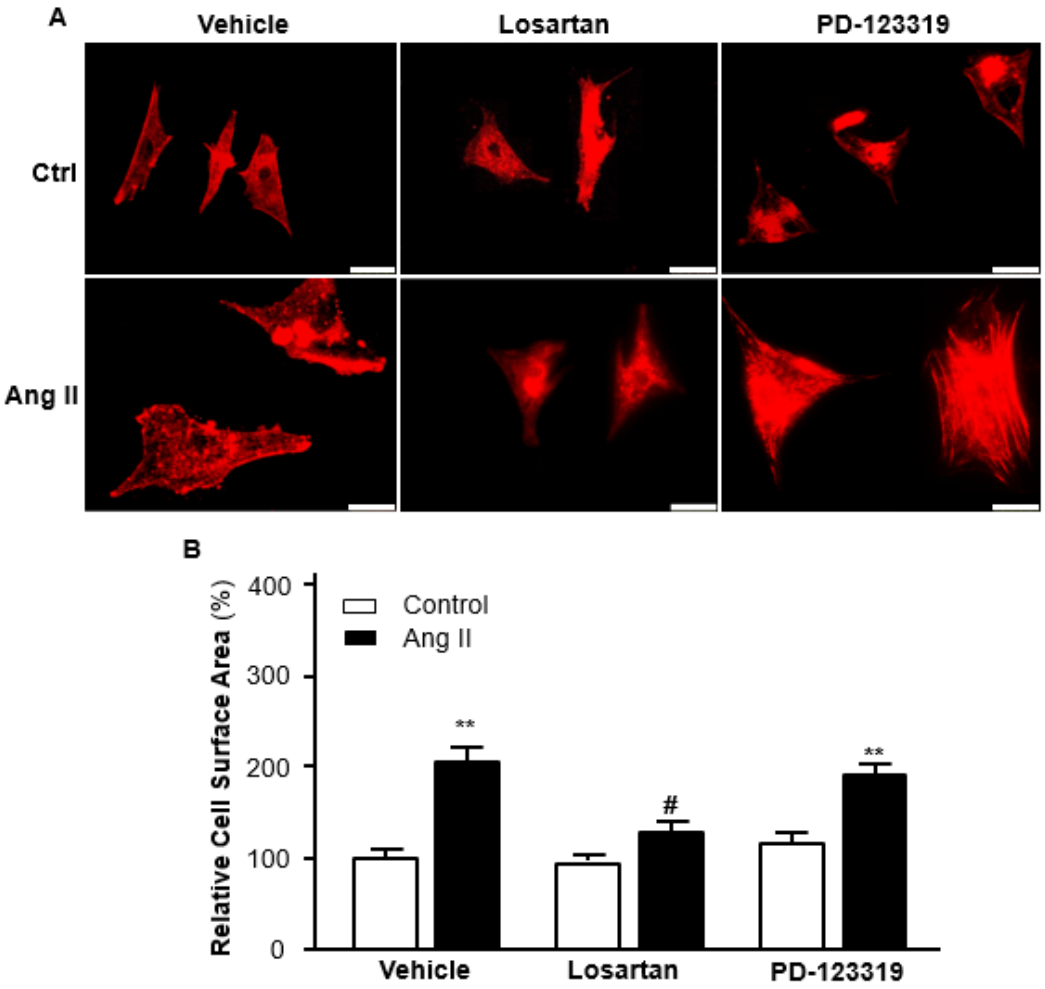

Figure 15: Effect of blockade of Ang II receptor type 1 or type 2 on Ang II-induced cardiac hypertrophy in cardiomyocytes. Cardiac hypertrophy levels were determined using the α-actin immunofluorescence staining in cardiomyocytes after treated with Ang II (10^{-6} M) with or without the Ang II receptor type 1 antagonist of Losartan (Los, 1 μM) or Ang II receptor type 2 antagonist of PD-123319 (PD, 1 μM) for 24 h. **A:** Representative fluorescence micrographs of cultured cardiomyocytes staining with α-sarcomeric actin antibody after the following treatments: Vehicle control, Losartan, PD-123319, Ang II, Ang II plus Losartan, or Ang II plus PD-123319. **B:** Bar graphs summarizing the effect on cardiac hypertrophy in cardiomyocytes treated with the conditions described in the above. The scale in the images is 25 μm. Data are presented as means ± SE, which were derived from three experiments and at least triplicate wells in each experiment. $^{**}P < 0.01$ vs. cardiomyocytes treated with vehicle control. $^{\#}P < 0.05$ vs. cardiomyocytes treated with Ang II.

After the determination of blockade of AT1R or AT2R on Ang II-induced cardiac hypertrophy, we measured the effect of different Ang II receptor antagonists on Ang II-induced elevation of Class I PI3-kinase activity. The was measured using the ELISA kit in cardiomyocytes

treated by Vehicle control or Ang II (10^{-6} M) with or without pretreatment with the Ang II receptor type 1 antagonist of Losartan (1 μM, 30 min) or Ang II receptor type 2 antagonist PD-123319 (1 μM, 30 min). The results are presented in Figure 16, demonstrating treatment with Losartan significantly attenuated Ang II-induced increases in Class I PI3-kinase activity by 41.7 % in cardiomyocytes (PIP_3 production (pmol/μg of protein) 1.42 ± 0.11 in Losartan vs. 1.76 ± 0.12 in Losartan + Ang II, n=3 experiments, $P < 0.05$ vs. Ang II). In contrast, treatment with PD-123319 did not significantly alter Ang II-induced elevations in Class I PI3-kinase in cardiomyocytes (PIP_3 production (pmol/μg of protein) 1.51 ± 0.11 in PD-123319 vs. 2.84 ± 0.14 in PD-123319+Ang II, $P > 0.05$ vs. Ang II). In addition, treatment with Losartan or PD-123319 alone did not alter the basal Class I PI3-kinase activity. The results demonstrated that Ang II-induced Class I PI3-kinase activity in cardiomyocytes is mainly mediated via Ang II receptor Type 1.

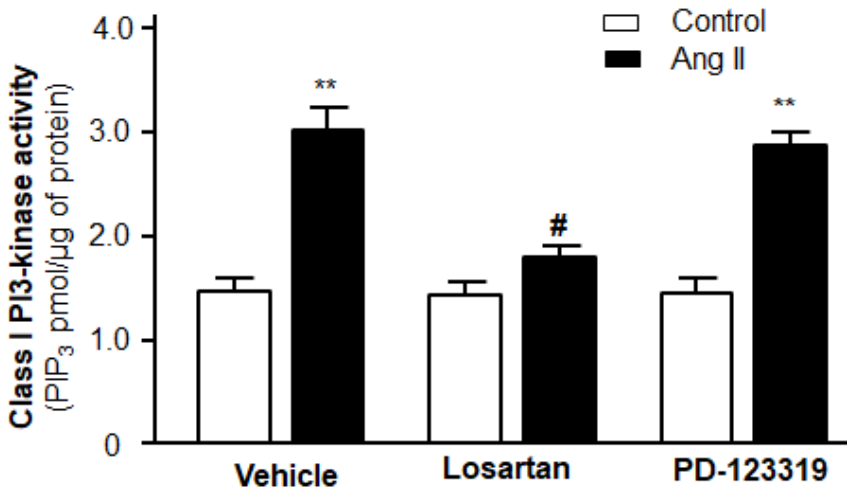

Figure 16: Effect of blockade of Ang II Receptor Type 1 or Type 2 on Ang II-induced Class I PI3-kinase activity in cardiomyocytes. Class I PI3-kinase activity in cardiomyocytes was determined using the ELISA kit after treated with Ang II (10^{-6} M) with or without the Ang II receptor type 1 antagonist of Losartan or Ang II receptor type 2 antagonist of PD-123319 for 24 h. Bar graphs summarizing the effect on Class I PI3-kinase activity in cardiomyocytes treated with the Vehicle control, Losartan (Los, 1 μM), PD-123319 (PD, 1 μM), Ang II, Ang II plus Losartan, or Ang II plus PD-123319. Data are presented as means ± SE, which were derived from three experiments and at least triplicate wells in each experiment. $^{**}P < 0.01$ vs. cardiomyocytes treated with vehicle control. $^{\#}P < 0.05$ vs. cardiomyocytes treated with Ang II.

2.3.4. The effect of rapamycin, an mTOR inhibitor and autophagic inducer on Ang II-induced ROS generation and cardiac hypertrophy

Since autophagy is an effective tool to eliminate mitochondria-derived ROS, we examined the role of mTOR as a negative regulator of autophagy in Ang II-induced mitochondrial ROS generation. The mitochondrial ROS generation was measured using the MitoSox fluorescence approach in cardiomyocytes treated by control or Ang II (10^{-6} M) with or without pretreatment with the mTOR inhibitor, Rapamycin (100 nM, 30 min). The results are presented in Figure 17, demonstrating that treatment of cardiomyocytes with Rapamycin dramatically attenuated Ang II-induced increases in mitochondrial ROS accumulation by 33.6 % in cardiomyocytes (ROS generation 98.30 ± 2.40 % in Rapamycin alone vs. 112.3 ± 3.20 % in Rapamycin plus Ang II, n=3 experiments, $P < 0.05$ vs. Ang II). In addition, treatment with rapamycin alone did not alter the basal mitochondrial ROS generation. The results demonstrated that Ang II-induced ROS generation in cardiomyocytes is alleviated after the blockade mTOR and with enhanced autophagy.

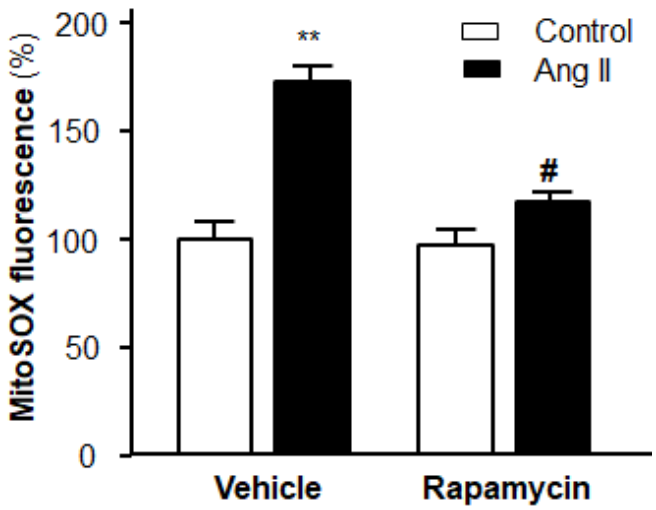

Figure 17: Effect of blockade of mTOR on Ang II induced-ROS generation in cardiomyocytes. Mitochondrial ROS levels were determined using the oxidant-sensitive fluorogenic probe MitoSOX in cardiomyocytes after treated with Ang II (10^{-6} M) with or without the mTOR inhibitor of Rapamycin (Rapa, 100 nM) for 24 hours. Bar graphs summarizing the effect on mitochondrial ROS production in cardiomyocytes treated with the conditions described in the above. Data are presented as means ± SE, which were derived from three experiments and at least triplicate wells in each experiment. $^{**}P < 0.01$ vs. cardiomyocytes treated with vehicle control. $^{\#}P < 0.05$ vs. cardiomyocytes treated with Ang II.

After the determination of blockade of mTOR on Ang II-induced ROS generation, we tested the effect of rapamycin on cardiac hypertrophy. The cardiac hypertrophy in cardiomyocytes was measured using the α-actin immunofluorescence in cardiomyocytes treated by Vehicle control or Ang II (10^{-6} M) with or without pretreatment with the mTOR inhibitor, Rapamycin (100 nM, 30 min). The results are presented in Figure 18, demonstrating treatment with rapamycin significantly attenuated Ang II-induced increases in cardiac hypertrophy by 38.7 % in cardiomyocytes (Relative cellular surface area 98.6 ± 5.4 % in Rapamycin alone vs. 125.2 ± 6.20 % in Rapamycin plus Ang II, n=3 experiments, $P < 0.05$ vs. Ang II). In addition, treatment with Rapamycin alone did not alter the basal hypertrophic state of cardiomyocytes. In summary, the results demonstrate that Ang II-induced cardiac hypertrophy in cardiomyocytes is alleviated by blockade of mTOR and promotion of autophagy in cardiomyocytes.

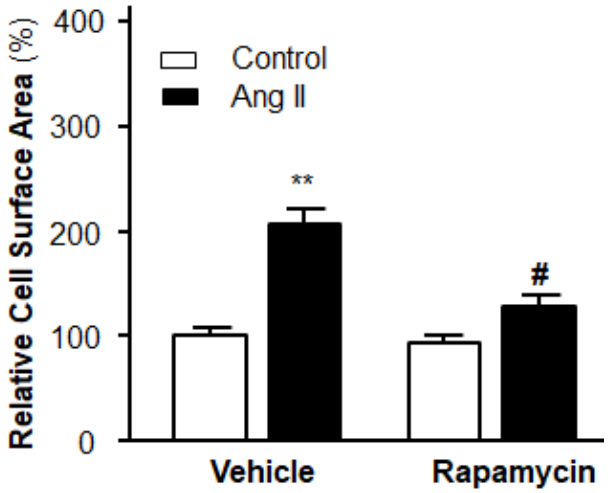

Figure 18: Effect of blockade of mTOR on Ang II induced-cardiac hypertrophy in cardiomyocytes. Cardiac hypertrophy levels were determined using the immunofluorescence staining in cardiomyocytes after treated with Ang II (10^{-6} M) with or without the mTOR inhibitor of Rapamycin (Rapa, 100 nM) for 24 hours. Bar graphs summarizing the effect on mitochondrial ROS production in cardiomyocytes treated with the conditions described in the above. Data are presented as means ± SE, which were derived from three experiments and at least triplicate wells in each experiment. $^{**}P < 0.01$ vs. cardiomyocytes treated with vehicle control. $^{\#}P < 0.05$ vs. cardiomyocytes treated with Ang II.

2.3.5. The effect of mito-TEMPO, a mitochondrial ROS scavenger on autophagy, ROS generation, and cardiac hypertrophy

After we tested the effect of blockade of two different types of Ang II receptors on Ang II-induced cardiac remodeling, scavengers targeting at ROS generation in damaged mitochondria were examined. The effect of high dose of Ang II on autophagy in cardiomyocytes was examined with and without presence of Mito-TEMPO (Mito, 1 μM, mitochondria-targeting ROS scavenger, especially for superoxide elimination) 30 minutes before exposure to 10^{-6} M Ang II. The results are presented in Figure 19, and preincubation of cardiomyocytes with mito-TEMPO significantly diminished Ang II-induced autophagy by 52.4 % (0.98 ± 0.06 in mito-TEMPO alone vs. 1.24 ± 0.11 in mito-TEMPO plus Ang II, n=3 experiments, $P < 0.05$). The results demonstrated that Ang II-induced autophagic alteration in cardiomyocytes is due to the accumulation of damaged

mitochondria. Therefore, scavenging mitochondria-derived ROS generation by mito-TEMPO helps maintain the basal state of intracellular autophagy as a self-defense mechanism.

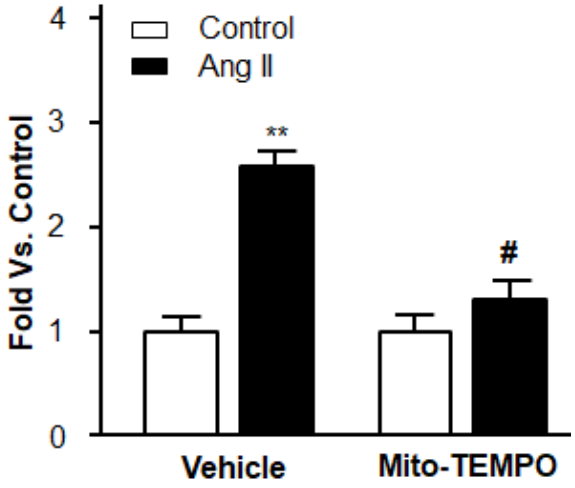

Figure 19: Effect of scavenging mitochondrial ROS on Ang II-induced autophagy in cardiomyocytes. Autophagy was examined in cardiomyocytes by immunostaining fluorescence with MAP-LC3 antibody 24 hours after treated with Ang II (10^{-6} M) with or without the mitochondria-targeting ROS scavenger of Mito-TEMPO (Mito, 1 μM) for 24 h. Bar graphs summarizing quantitative analysis of autophagic alterations in cardiomyocytes treated under the conditions described in the above. Data are means ± SE and were derived from three experiments and at least triplicate wells in each experiment. $^{**}P < 0.01$ vs. cardiomyocytes that treated with vehicle control. $^{\#}P < 0.05$ vs. cardiomyocytes that treated with Ang II.

Next, the mitochondrial ROS production was measured using the MitoSox fluorescence in cardiomyocytes treated by control or Ang II (10^{-6} M) with or without pretreatment with the mitochondria-targeting ROS scavenger of Mito-TEMPO (1 μM, 30 min). The results are presented in Figure 20, demonstrating treatment with Mito-TEMPO pretreatment largely alleviated Ang II-induced increases in mitochondrial ROS accumulation by 37.8 % in cardiomyocytes (98.20 ± 2.05 % in Mito-TEMPO alone vs. 105.5 ± 2.22 % in Mito-TEMPO plus Ang II, n=3 experiments, $P <$ 0.05 vs. Ang II). In addition, treatment with Mito-TEMPO alone did not alter the basal mitochondrial ROS production. The results demonstrated that Ang II-induced ROS generation in cardiomyocytes stems mainly from mitochondrial dysfunction.

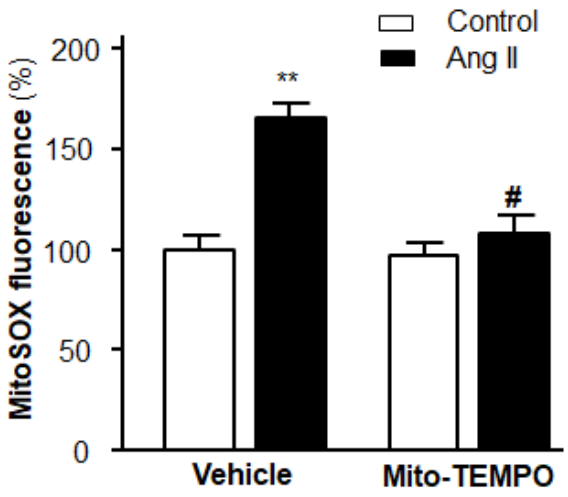

Figure 20: Effect of scavenging mitochondrial ROS on Ang II-induced ROS generation in cardiomyocytes. Mitochondrial ROS levels were determined using the oxidant-sensitive fluorogenic probe MitoSOX in cardiomyocytes after treated with Ang II (10^{-6} M) with or without the mitochondria-targeting ROS scavenger of Mito-TEMPO (Mito, 1 μM) for 24 hours. Bar graphs summarizing the effect on mitochondrial ROS production in cardiomyocytes treated with the conditions described in the above. Data are presented as means ± SE, which were derived from three experiments and at least triplicate wells in each experiment. $^{**}P < 0.01$ vs. cardiomyocytes treated vehicle control. $^{\#}P < 0.05$ vs. cardiomyocytes treated with Ang II.

Thereafter, we tested the effect of different ROS scavengers on Ang II-induced cardiac hypertrophy. The cardiac hypertrophy in cardiomyocytes was measured using the α-actin immunofluorescence in cardiomyocytes treated by Vehicle control or Ang II (10^{-6} M) with or without pretreatment with the mitochondria-targeting ROS scavenger of Mito-TEMPO (1 μM, 30 min). The results are presented in Figure 21, demonstrating treatment with Mito-TEMPO significantly attenuated Ang II-induced increases in cardiac hypertrophy by 40.2 % in cardiomyocytes (Relative cellular surface area 96.5 ± 3.97 % in Mito-TEMPO alone vs. 122.3 ± 7.10 % in Mito-TEMPO plus Ang II, n=3 experiments, $P < 0.05$ vs. Ang II). In addition, treatment with Mito-TEMPO alone did not alter the basal cellular surface area. The results demonstrated that Ang II-induced cardiac hypertrophy in cardiomyocytes is mainly due to intracellular mitochondrial dysfunction induced-ROS generation.

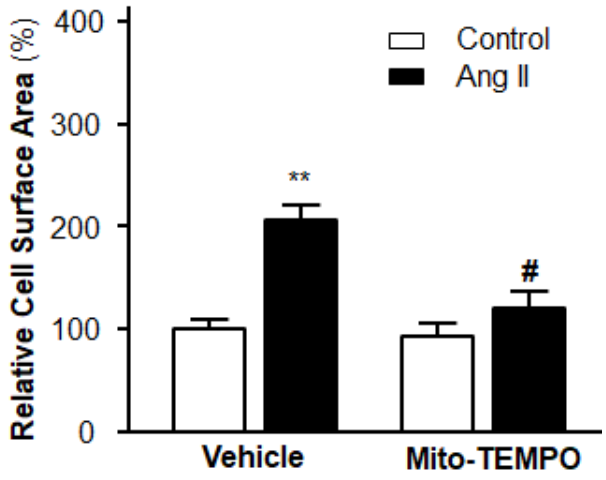

Figure 21: Effect of scavenging mitochondrial ROS on Ang II-induced cardiac hypertrophy in cardiomyocytes. Cardiac hypertrophy levels were determined using the α-actin immunofluorescence staining in cardiomyocytes after treated with Ang II (10^{-6} M) with or without the mitochondria-targeting ROS scavenger of Mito-TEMPO (Mito, 1 μM) for 24 hours. Bar graphs summarizing the effect on cardiac hypertrophy in cardiomyocytes treated with the conditions described in the above. Data are presented as means ± SE, which were derived from three experiments and at least triplicate wells in each experiment. $^{**}P < 0.01$ vs. cardiomyocytes treated with vehicle control. $^{\#}P < 0.05$ vs. cardiomyocytes treated with Ang II.

2.4. Data summary and conclusion

In the present chapter, we examined the role of Class I PI3-kinase in Ang II-induced cardiac remodeling via an autophagic-dependent pathway. The results demonstrated that Class I PI3-kinase is activated under higher dosage Ang II exposure via interaction with AT1R, and this activation impairs autophagy, damages mitochondria, causes ROS generation, and ultimately promotes cardiac hypertrophy. This conclusion is supported by the following sets of evidence: 1) Class I PI3-kinase activity and Akt phosphorylation were significantly elevated under higher Ang II exposure in a dose-dependent manner and autophagy is decreased as the elevated Class I PI3-kinase activity; 2) Pretreatment of LY-294002, a Class I PI3-kinase inhibitor diminished the activity of Class I PI3-kinase, restored autophagy, and alleviated Ang II-induced ROS generation, and cardiac hypertrophy; 3) Ang II-induced autophagic alteration, ROS generation, cardiac hypertrophy and Class I PI3-kinase activation are mainly mediated through AT1R; 4) Rapamycin,

a mTOR inhibitor and autophagic inducer, attenuated Ang II-induced ROS generation, and cardiac hypertrophy by enhancing autophagy; 5) The origin of Ang II-induced ROS generation that causes cardiac hypertrophy mainly comes from damaged mitochondria in cardiomyocytes.

Previous evidence showed that the autophagic response to Ang II infusion may be both time and dose-dependent: Early and/or low dose of Ang II exposure promotes autophagy while chronic and/or high dose of Ang II exposure impairs autophagy. It is assumed that transient Ang II with lower concentration exposure would initially exert a quick autophagic response while prolonged Ang II exposure with higher concentration may induce decreased autophagy degree and subsequent cardiac remodeling aggravation [78]. In our results, corresponding outcomes are observed that Class I PI3-kinase are activated under high dosage Ang II exposure through the interaction of AT1R in the surface of cardiomyocytes.

NADPH oxidase is thought to be the origin of ROS generation, and $gp91^{phox}$ (an essential subunit of NADPH oxidase) inactivation decelerate the speed of cardiac hypertrophy by Ang II infusion [84]. However, elimination of $gp91^{phox}$ in transgenic mice with active renin overexpression could not protect those individuals from cardiac hypertrophy [72]. Judging by this piece of information, mitochondria-derived ROS is considered as the major resource of Ang II-induced ROS generation. Our results showed that pretreatment of Mito-TEMPO, a mitochondria-derived ROS scavenger almost completely abolished the Ang II-induced ROS generation and cardiac hypertrophy, suggesting that Ang II-induced cardiac hypertrophy in primary cardiomyocytes is mainly due to the accumulation of damaged mitochondria.

Taken together, the results from this chapter indicate an important role of Class I PI3-kinase in Ang II-induced cardiac remodeling, which means activation of this kinase under higher Ang II dosage impairs autophagy, causes ROS generation and cardiac hypertrophy.

CHAPTER III. THE ROLE OF CLASS III PI3-KINASE-DEPENDENT SIGNALING PATHWAYS IN ANG II-INDUCED AUTOPHAGY, ROS GENERATION, AND HYPERTROPHY IN PRIMARY CARDIOMYOCYTES

3.1. Introduction

In the previous chapter, we discovered that under higher dosage of Ang II-induced activation of Class I PI3-kinase inhibits autophagy, exacerbates ROS generation and severe cardiac hypertrophy. This phenomenon resembles the later stage of decompensatory cardiac hypertrophy and heart failure under chronic Ang II exposure. According to the relationship between Ang II dosage and autophagy shown in Chapter II, we found lower dosage of Ang II potentiated autophagy, and it is postulated that this autophagic increment is due to the activation of another signaling pathway other than Class I PI3-kinase.

Since autophagy mainly degrades damaged intracellular components and maintains cardiac homeostasis, it is convinced that autophagy plays distinct roles at different stages of cardiac hypertrophy as a two-bladed sword and the underlining mechanism is complicated and intertwined because previous literatures reported contradictory outcomes regarding the relationship between autophagy and hypertrophy. In general, basal autophagy keeps cardiac structure and functions via energy preparation, clearance of accumulated ROS and structural misfolding protein. Also, autophagic upregulation protects cardiomyocytes from hemodynamic stress which is detrimental to cardiomyocytes [53]. Thus, it is universally recognized that elevation of autophagy under various noxious stimuli at the initial exposure prevents cardiomyocytes from further protein synthesis and resultant cardiac hypertrophy. Furthermore, it is commonly accepted that mitophagic induction helps reduce oxidative stress-induced mitochondrial damage. Failure to remove those damaged mitochondria causes their accumulation, and generates higher levels of ROS, resulting in protein, lipid, and DNA damage [85]. Increased ROS level results in a potential reduction and

leakage in mitochondrial membranes, and subsequent activation of Parkin-dependent mitophagy gets obstructed, leading to higher level of ROS generation [86]. Therefore, autophagic deterioration in mitochondria (obstruction of mitophagy) by Class III PI3-kinase blockade may exacerbate Ang II-induced ROS generation and cardiac hypertrophy. The underlining mechanism might rely on the discovery that ATG4 activity inhibition via an essential cysteine residue oxidation, blocking PE cleavage from PE-conjugated LC3 and subsequent impairment of autophagy as stated before [87].

It is reported that among those PI3-kinases, only Class I and Class III PI3-kinases are expressed in the heart [60]. Contrary to the effect of Class I PI3-kinase, Class III PI3-kinase pathway activation facilitates autophagy with sequential activations of its relevant components of Class III PI3-kinase→Beclin-I→Vps34 [88]. Activation of Class III PI3-kinase pathway is also involved in autophagic alteration in several cell-lines including H9C2 cell line which is an analog of cardiomyocytes. 3-MA, a Class III PI3-kinase inhibitor, by specifically inactivating Vps34 in Class III PI3-kinase [64], suppresses autophagosome formation in starvation-induced autophagy in rat cardiomyocyte-derived H9C2 [89]. Therefore, it is also of vital importance to examine the role of Class III PI3-kinase in Ang II-induced autophagy, ROS generation, and cardiac hypertrophy. We assume that Class III PI3-kinase is continuously activated under a very small amount of Ang II exposure and this activation, in turn, initiates the elevation of autophagy to counteract the hypertrophic effect of Ang II. Therefore, it is necessary to detect the influence of Class III PI3-kinase with its relevant blocker of 3-MA.

3.2. Materials and methods

3.2.1. Preparation of cardiomyocyte cultures

Twelve-week-old male and female SD rats were obtained from Charles River Farms (Charles River Laboratories International, Wilmington, MA). Rats were housed at 25 ± 2°C on a

12:12-h light-dark cycle and provided with food and water ad libitum. All animal protocols were approved by the North Dakota State University Institutional Animal Care and Use Committee. Primary cardiomyocytes were randomly divided into each group. Generally, dissociated neonatal rat primary cardiomyocytes were cultured for 5 days, and culture media was changed every other day. Then those cardiomyocytes were treated with relevant reagents: 10^{-10}~10^{-5} M Angiotensin II (Ang II, Alfa Aesar, J60866, Reston, VA), 1 μM 3-Methyladeninie (3-MA, BioVision, 2249-100), 1 μM Losartan (Los, Sigma Aldrich, 61188, St. Louis, MO), and 1 μM PD-123319 (PD, Sigma Aldrich, P186, St. Louis, MO). All of those reagents were administrated 30 minutes before Ang II stimulation in all experiments except dosage dependent-autophagy effect test of Ang II. 0.1% DMSO vehicle was used as negative control for other subsequent experiments. The total exposure duration of Ang II and other reagents was 24 hours for autophagy and hypertrophy determination. While for ROS generation determination, intracellular ROS levels were measured immediately after addition of Ang II or HBSS control by incubation with MitoSOX since superoxide is unstable and could be gradually neutralized by intracellular superoxide dismutase (SOD) as time elapses.

3.2.2. Treatment protocol

1~3 days old neonatal SD rats were anesthetized by sodium pentobarbital (200 mg/kg, *i.p.*, Sigma, St. Louis, MO). Ventricles of the heart were quickly excised, minced into small pieces in cold HBSS and washed for several additional times. The minced tissue was digested with 0.1% trypsin in a 37ºC water bath with shaking for 5-min rounds of tissue digestion (10-12 times). After each incubation, the supernatant was added to an equal volume of DMEM containing 10% FBS. Then, isolated cells were filtrated with 70 μm cellular sieve, centrifuged at 1,000 rpm for 10 min. Supernatants were discarded after centrifuge; and cellular pellets were suspended in DMEM composed of 10% FBS and 1% penicillin-streptomycin at 37℃ for 1.5 hr in a humidified atmosphere with 95% O_2 and 5% CO_2 to allow the most of non-myocyte cells, such as fibroblasts,

to attach on the plate bottom. Suspended cellular solution (final cellular density 5×10^5 cells/cm^2) was transduction to a 24-well plate for morphological studies and to a 96-well plate for measurement of ROS levels. In the first three days, Brdu (10^{-4} M) was added to suppress fibroblast growth. All of the manipulations were performed in culture hood to ensure an aseptic environment. After the cell cultures reached confluence (5 days on average) in an incubator filled with a humidified atmosphere of 5% CO_2 at 37 °C, cardiomyocytes were used for *in vitro* experiments.

3.2.3. Autophagy determination

Cultured cardiomyocytes were treated with relevant reagents for 24 h. Each treatment was performed in triplicate wells. In brief, after treatment, cells were fixed in 4% PFA at 4℃ for 30 min, and washed with fresh washing solution (0.1% Triton X-100 in PBS) three times. After pre-incubation with 3% of bovine serum albumin (BSA) for 20 minutes, the cells were incubated with primary antibody of MAP-LC3 (Santa Cruz Biotechnology, sc-134226, Santa Cruz, CA), which was diluted to 1:100 with PBS containing 3% BSA, for overnight at 4℃. After three washings with the PBS solution, the cells were incubated with fluorescence-conjugated Alexa Fluor 488 fluorescence-conjugated goat anti-rabbit IgG antibody (Molecular probes, A-11034, Waltham, MA) (1:1000 diluted in PBS) for 2 h at room temperature in dark. Photographic images of cardiomyocytes were taken with a fluorescence microscope (Olympus Microsystems, Waltham, MA). The MAP-LC3 antibody immunostaining positive images were analyzed, the puncta inside cardiomyocytes were counted and the average puncta number in each cell was calculated with at least 10 area of cells in each sample [77, 78]. The more average puncta in each cell indicates the larger degree of autophagy occurrence. HBSS negative control group was set as “1” and the results of each sample were expressed as “Fold *vs.* Control”.

3.2.4. ROS detection

Mitochondrial ROS generation was determined using a superoxide-sensitive (O2·-) fluorogenic probe of MitoSox (Thermo Fisher, M-36008, Rockford, IL). MitoSOX has a dihydroethidium (DHE) part linked to triphenylphosphoninum (TPP) component and yields red fluorescence when oxidized (excitation/emission wavelength: 510/580 nm). This compound is more concentrated in the mitochondria than in the cytosol since the former has more positively charged TPP [79]. Cultured cardiomyocytes were pretreated with relevant reagents except Ang II for 30 minutes. Then the cardiomyocytes were treated with Ang II (10^{-6} M) or HBSS control. Intracellular mitochondrial ROS levels were measured immediately after the addition of Ang II or HBSS control by incubation with MitoSOX (5×10^{-6} M, 15 minutes). The intracellular ROS levels were measured using a fluorometric imaging plate reader (Spectra Max Gemini EM, Molecular Devices) to detect changes in fluorescence resulting from intracellular probe oxidation. The vehicle (DMSO, 0.1%) control group was set as 100% MitoSOX fluorescence. Fluorescent images were also acquired using a fluorescence microscope (Olympus, Microsystems, Waltham, MA) to visualize the strength of MitoSOX fluorescence in primary cardiomyocytes.

3.2.5. Cardiac hypertrophy determination

Cultured cardiomyocytes were treated with relevant reagents and Ang II for 24 h. Each treatment was performed in triplicate wells. Anti-α-actin antibody was used for cardiac hypertrophy via immunofluorescence staining. In brief, cells were fixed in 4% PFA at 4℃ for 30 minutes, and washed with fresh washing solution (0.1% Triton X-100 in PBS) for three times. After pre-incubation with 3% of bovine serum albumin (BSA) for 20 minutes, the cells were incubated with primary antibody of sarcomeric α-actin (Santa Cruz Biotechnology, sc-53142, Santa Cruz, CA), which was diluted to 1:100 with PBS containing 3% BSA, overnight at 4℃. After three washings with the PBS solution, the cells were incubated with fluorescence-conjugated

Alexa Fluor 594 goat anti-mouse IgG (Molecular probes, A-11032, Waltham, MA) (1:1000 diluted in PBS) for 2 h at room temperature in dark. Photographic images of cardiomyocytes were taken with a fluorescence microscope (Olympus Microsystems, Waltham, MA). The cellular surface area of positive image for α-actin staining cardiomyocytes was measured by the image analysis software (NIH Image J) [80]. Variations of cellular size were expressed as relative cellular surface area versus the control. The 0.1% DMSO negative control group was set as 100%.

3.2.6. Class III PI3-kinase activity assay

After treatment of relevant reagents, primary cardiomyocytes from neonatal rats were rinsed with ice-cold PBS and Buffer A (20 mM Tris-HCl, pH 7.4, 137 mM NaCl, 1 mM $CaCl_2$, 1 mM $MgCl_2$, and 1 mM Na_3VO_4) three times each. Then Buffer A was removed and the cells were immediately lysed in lysis buffer Lysis Buffer (Buffer A plus 1% NP-40, 10% glycerol, and 1 mM PMSF) at 4°C for 20 minutes by rocking. The cells were scraped from dishes, transferred to 1.5 mL microcentrifuge tubes and centrifuged for 10 minutes at 13,000 g to sediment insoluble material. Thereafter, supernatant was transferred to new tubes added with 5 μL of anti-hVps34 IP antibody (Echelon Biosciences, Z-R015, Salt Lake City, UT) and the samples were immunoprecipitated as described previously [90]. to each tube and incubated for one hour at 4°C with gentle rotation. 60 μL of 50 % slurry of Protein A- Sepharose beads in PBS was added into each tube with gentle rotation for overnight, and tubes were centrifuged for 5 seconds for collection of immunoprecipitated enzymes. Sediments were washed three times with Buffer A plus 1% NP-40, three times with 0.1 M pH 7.4 Tris-HCl with 5 mM LiCl and 1 mM Na_3VO_4, twice with TNE (10 mM Tris-HCl, pH 7.4, 150 mM NaCl, 5 mM EDTA) containing 1 mM Na_3VO_4 and twice with Vps34 kinase reaction buffer (10 mM Tris pH 8, 100 mM NaCl, 1 mM EDTA, 10 mM $MnCl_2$, and 50 μM ATP). The last wash was aspirated completely. A PIP standard curve (ranging from 9.8 nM to 10 μM) was simultaneously prepared and determined at 450 nm wavelength. Each assay was

repeated at least 3 times. Then Class III PI3-kinase assay was performed using competitive enzyme-linked immunosorbent assay kit (K-3000, Echelon Biosciences, Salt Lake City, UT) by exactly following the instruction provided by the manufacturer. Each assay was repeated at least 3 times.

3.2.7. Data analysis

All data are presented as means ± SE. Statistical significance was evaluated by one- or two-way ANOVA, as appropriate, followed by either a Newman–Keuls or Bonferroni post hoc analysis when indicated. Differences will be considered significant at $P<0.05$, and individual probability values are noted in figures.

3.3. Results

3.3.1. Dose-dependent effect of Ang II on Class III PI3-kinase activity

Class III PI3-kinase activity was measured since we assume this kinase is involved in both physiological and pathological higher Ang II concentration. For this reason, a measurement of PIP production is the indirect estimation of intracellular Class III PI3-kinase levels. PIP levels were measured 24 hours after treatment of Ang II with different dosages or HBSS control. After Ang II treatment, the cardiomyocytes were lysed for determination of PIP by the ELISA kit according to the manufacturer's protocol. Results are shown in Figure 22, demonstrating that the activity of Class III PI3-kinase is enhanced under lower dosage of Ang II (PIP production (in pmol/μg of protein) 1.25 ± 0.09 in HBSS control vs. 2.93±0.09 in 10^{-7} M Ang II, increase by 134.4 %, $P<0.01$ vs. HBSS control), while the activity reaches the plateau when the Ang II concentration exceeds 10^{-7} M (PIP production (in pmol/μg of protein) 2.93 ± 0.09 in 10^{-7} M Ang II vs. 3.15 ± 0.12 in 10^{-5} M Ang II, $P > 0.05$ vs. 10^{-7} M Ang II), suggesting Class III PI3-kinase is activated under lower dosage of Ang II exposure at the initial stage. In contrast of the dose-dependent stimulatory effect of Ang II on Class I PI3-kinase, the dose-dependent stimulatory effect of Ang II on Class III PI3-

kinase started at 10^{-9} M and reached to the peak at 10^{-7} M. These results indicate that Class III PI3-kinase are more sensitive to Ang II as compared with Class I PI3-kinase in cardiomyocytes.

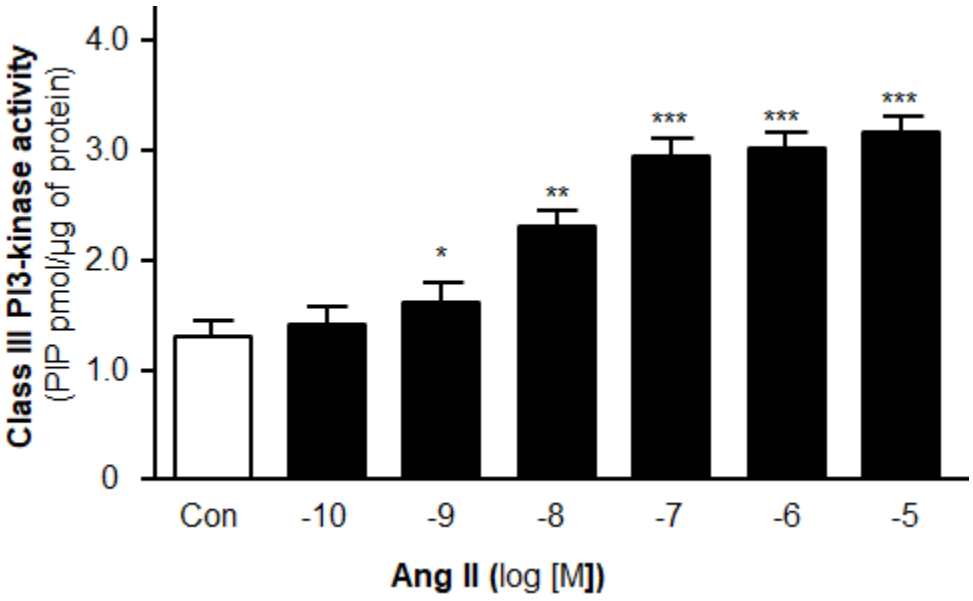

Figure 22: Dose-dependent effect of Ang II on the activities of Class III PI3-kinase in cardiomyocytes. Bar graphs summarizing the activities of Class III PI3-kinases measured using PIP ELISA kits in cardiomyocytes as described in Methods. The Class III PI3-kinase activities are presented as the concentrations of PIP in per microgram protein 24 hours after treated with HBSS control or Ang II with different dosages. Data are presented as means ± SE, which were derived from three experiments and at least triplicate wells in each experiment. $^{*}P < 0.05$, $^{**}P < 0.01$, $^{***}P < 0.001$ as compared with cardiomyocytes treated with HBSS control.

3.3.2. The effect of 3-MA, a Class III PI3-kinase inhibitor on Ang II-induced autophagy, ROS generation, cardiac hypertrophy, and Class III PI3-kinase activity

Next, we identified the involvement of Class III PI3-kinase in Ang II-induced autophagy, the effect of high dose of Ang II on cardiomyocyte autophagy was examined with and without presence of 3-MA (MA, an inhibitor of Class III PI3-kinase). The results are presented in Figure 23 and demonstrated that pretreatment with 3-MA (1 μM, 30 min) dramatically attenuated Ang II-induced autophagy by 52.1 % (0.87 ± 0.07 in 3-MA alone vs. 1.25 ± 0.08 in 3-MA plus Ang II, n=3 experiments, $P < 0.05$ vs. Ang II). In addition, treatment with 3-MA alone did not alter the basal autophagy in cardiomyocytes. Therefore, Class III PI3-kinases contribute to Ang II-induced

elevation in autophagy. Taken together, both Class I and Class III PI3-kinases contribute to Ang II-induced elevation in autophagy via a Class III PI3-kinase-mediated stimulatory mechanism and a Class I PI3-kinase-mediated inhibitory mechanism.

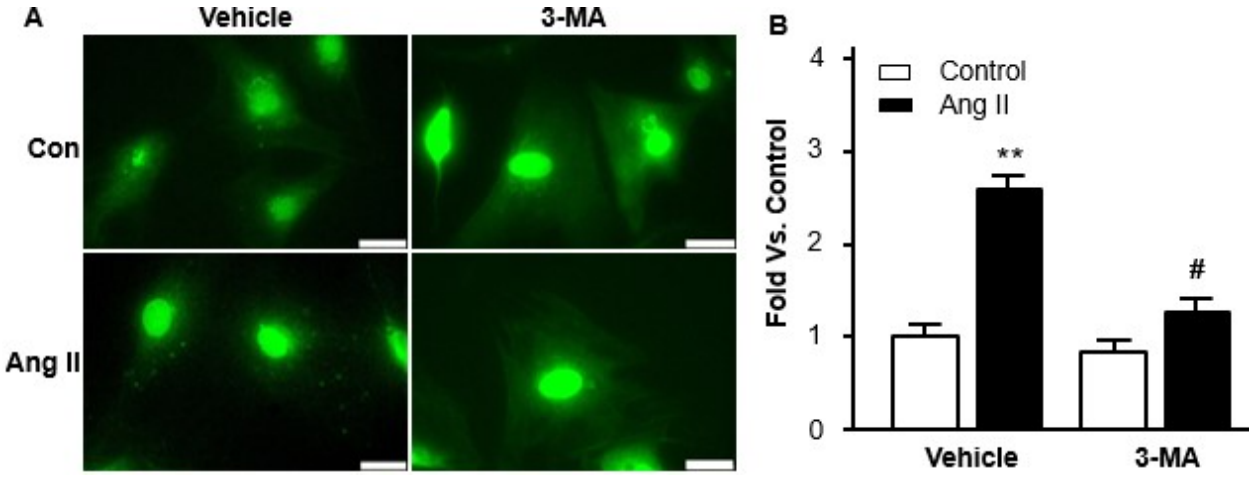

Figure 23: Effect of blockade of Class III PI3-kinase on Ang II-induced autophagy in cardiomyocytes. Autophagy was examined in cardiomyocytes by immunostaining fluorescence with MAP-LC3 antibody 24 hours after treated with Ang II (10^{-6} M) with or without the Class III PI3-kinase inhibitor, 3-MA (MA, 1 μM). **A:** Representative fluorescence micrographs of cultured cardiomyocytes stained with MAP-LC3 antibody after the following treatments: Vehicle control, 1 μM 3-MA, an inhibitor of Class III PI3-kinase, 10^{-6} M Ang II, or 3-MA + Ang II. **B:** Bar graphs demonstrating the effect of autophagy with the addition of 3-MA under 10^{-6} M Ang II exposure. The scale in the images is 25 μm. Data are means ± SE and were derived from three experiments and at least triplicate wells in each experiment. $^{**}P < 0.01$ vs. cardiomyocytes that treated with vehicle control. $^{\#}P < 0.05$ vs. cardiomyocytes that treated with Ang II.

Next, we examined the role of Class III PI3-kinase in Ang II-induced mitochondrial ROS generation. The mitochondrial ROS generation was measured using the MitoSox fluorescence approach in cardiomyocytes treated by control or Ang II (10^{-6} M) with or without pretreatment with the Class III PI3-kinase inhibitor, 3-MA (1 μM, 30 min). The results are presented in Figure 24, demonstrating that treatment with 3-MA dramatically promoted Ang II-induced elevations in mitochondrial ROS production in cardiomyocytes by 17.3 % (105.2 ± 5.32 % in 3-MA alone vs. 198.6 ± 4.52 % in 3-MA plus Ang II, n=3 experiments, $P < 0.05$ vs. Ang II). In addition, treatment with 3-MA alone did not alter the basal mitochondrial ROS production. In summary, those data

suggest that Class III PI3-kinase is involved in Ang II-induced mitochondrial ROS accumulation in cardiomyocytes through a Class III PI3-kinase-dependent stimulatory mechanism.

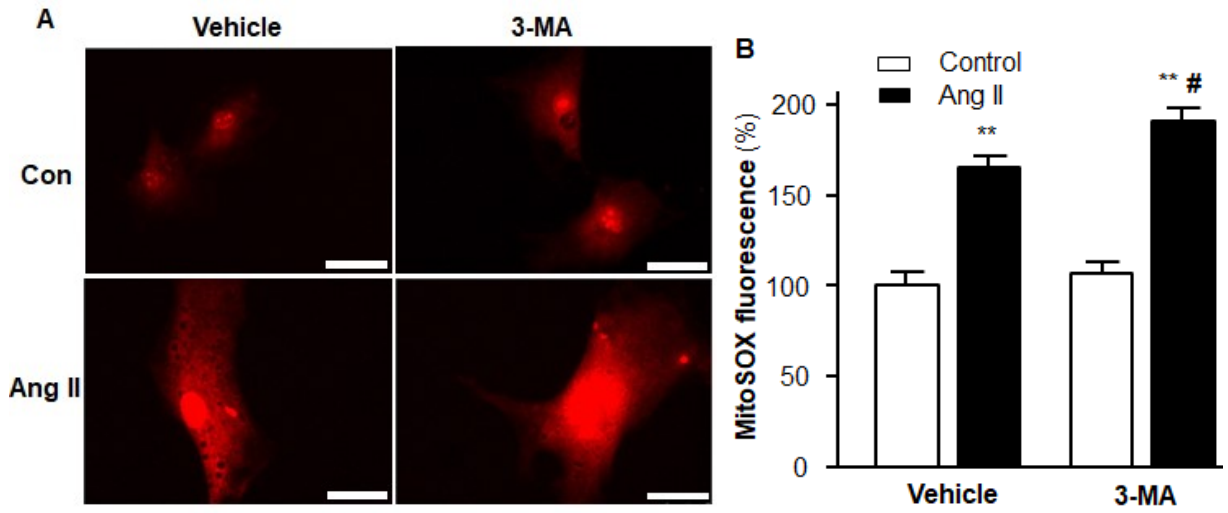

Figure 24: Effect of blockade of Class III PI3-kinase on Ang II-induced mitochondrial ROS generation in cardiomyocytes. Mitochondrial ROS levels were determined using the oxidant-sensitive fluorogenic probe MitoSOX in neonatal rat primary cardiomyocytes. Mitochondrial ROS levels were determined using the oxidant-sensitive fluorogenic probe MitoSOX in cardiomyocytes after treated with Ang II (10^{-6} M) with or without the Class III PI3-kinase inhibitor, 3-MA (MA, 1 μM) for 24 hours. **A:** Representative fluorescence micrographs of cultured cardiomyocytes loaded with MitoSOX after the following treatments: Vehicle control, 3-MA (1 μM, an inhibitor of Class III PI3-kinase), 10^{-6} M Ang II, or 3-MA + Ang II. **B:** Bar graphs summarizing the effect on mitochondrial ROS production in cardiomyocytes treated with the conditions described in the above. The scale in the images is 25 μm. Data are presented as means ± SE, which were derived from three experiments and at least triplicate wells in each experiment. $^{**}P < 0.01$ vs. cardiomyocytes treated with vehicle control. $^{\#}P < 0.05$ vs. cardiomyocytes treated with Ang II.

Thereafter, we examined the role of Class III PI3-kinase in Ang II-induced cardiac hypertrophy. The cardiac hypertrophy in cardiomyocytes was measured using the α-actin immunofluorescence in cardiomyocytes treated by Vehicle control or Ang II (10^{-6} M) with or without pretreatment with the Class III PI3-kinase inhibitor, 3-MA (1 μM, 30 min). The results are presented in Figure 25, demonstrating that treatment with 3-MA significantly attenuated Ang II-induced increases in cardiac hypertrophy by 29.9 % in cardiomyocytes (128.4 ± 6.28% in 3-MA alone vs. 265.4 ± 10.38 % in 3-MA % in 3-MA plus Ang II, n=3 experiments, $P < 0.05$ vs. Ang II). In addition, treatment with 3-MA alone slightly elevated the basal hypertrophic state of

cardiomyocytes. In summary, those data demonstrate that Class III PI3-kinases is involved in Ang II-induced cardiac hypertrophy in cardiomyocytes through a Class III PI3-kinase-dependent inhibitory mechanism.

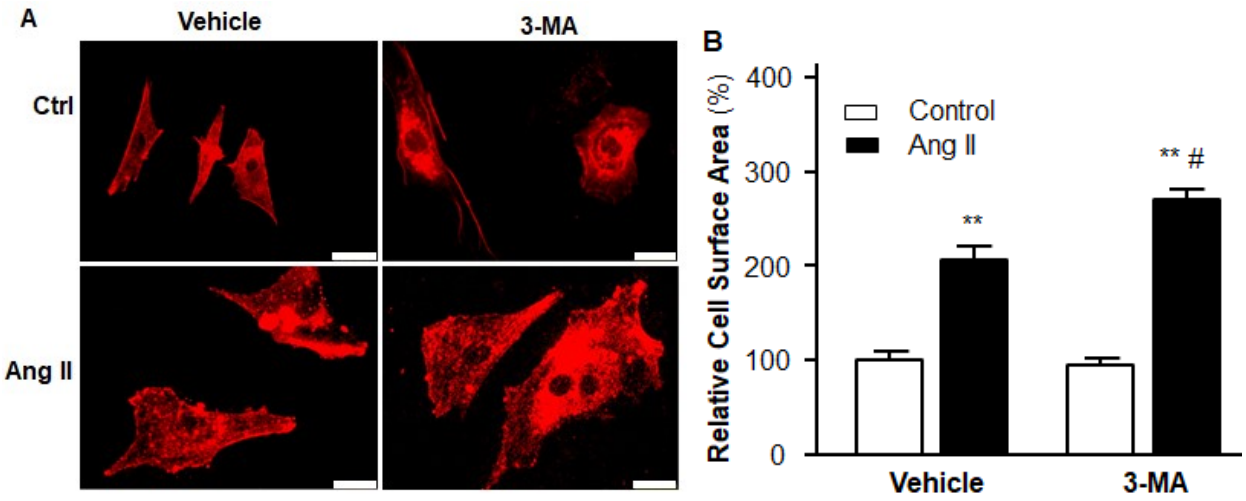

Figure 25: Effect of blockade of Class III PI3-kinase on Ang II-induced cardiac hypertrophy in cardiomyocytes. Cardiac hypertrophy in cardiomyocytes was determined using immunofluorescent staining with α-sarcomeric actin antibody after treated with Ang II (10^{-6} M) with or without the Class III PI3-kinase inhibitor, 3-MA (MA, 1 μM) for 24 hours. **A:** Representative fluorescence micrographs of cultured cardiomyocytes loaded with α-sarcomeric actin antibody after the following treatments: Vehicle control, 3-MA (1 μM, an inhibitor of Class III PI3-kinase), 10^{-6} M Ang II, or Ang II + 3-MA. **B:** Bar graphs summarizing the effect on cardiac hypertrophy in cardiomyocytes treated with the conditions described in the above. The scale in the images is 25 μm. Data are presented as means ± SE, which were derived from three experiments and at least triplicate wells in each experiment. $^{**}P < 0.01$ vs. cardiomyocytes treated with vehicle control. $^{\#}P < 0.05$ vs. cardiomyocytes treated with Ang II.

Next, we measured the effect of blockade of Class III PI3-kinase on Ang II-induced Class III PI3-kinase activity. The Class III PI3-kinase activity was measured using the ELISA kit in cardiomyocytes treated by control or Ang II (10^{-6} M) with or without treatment with the Class III PI3-kinase inhibitor, 3-MA (1 μM, 30 min). The results are presented in Figure 26, demonstrating that treatment of cardiomyocytes with Ang II significantly increased Class III PI3-kinase activity at the presence of vehicle (DMSO, 0.1%) as expected (PIP production (pmol/μg of protein) 1.25 ± 0.09 in control vs. 3.06 ± 0.12 in Ang II, n=3 experiments, P <0.01). More surprisingly, treatment

with 3-MA dramatically attenuated Ang II-induced increases in Class III PI3-kinase activity by (PIP production (pmol/μg of protein) 1.17 ± 0.10 in 3-MA vs. 1.46 ± 0.08 in 3-MA plus Ang II, n=3 experiments, $P < 0.05$ vs. Ang II). Besides, the addition of 1 μM 3-MA alone did not affect the basal activity of Class III PI3-kinase.

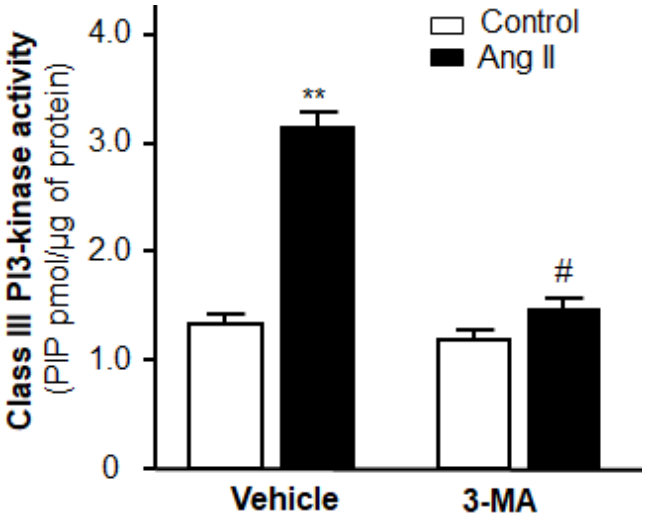

Figure 26: Effect of blockade of Class III PI3-kinase on Ang II-induced Class III PI3-kinase activity in cardiomyocytes. Class III PI3-kinase activity in cardiomyocytes was determined using the ELISA kit after treated with Ang II (10^{-6} M) with or without the Class III PI3-kinase inhibitor, 3-MA (MA, 1 μM) for 24 hours. Bar graphs summarizing the effect on Class III PI3-kinase activity in cardiomyocytes treated with Vehicle control, 3-MA (1 μM, an inhibitor of Class III PI3-kinase), 10^{-6} M Ang II, or Ang II + 3-MA. Data are presented as means ± SE, which were derived from three experiments and at least triplicate wells in each experiment. $^{**}P < 0.01$ vs. cardiomyocytes treated with vehicle control. $^{\#}P < 0.05$ vs. cardiomyocytes treated with Ang II.

3.3.3. The effect of blockade of different Ang II receptor types on Class III PI3-kinase activity

At last, we measured the effect of different Ang II receptor antagonists on Ang II-induced elevation of Class III PI3-kinase activity using the ELISA kit in cardiomyocytes treated by Vehicle control or Ang II (10^{-6} M) with or without pretreatment with the Ang II receptor type 1 antagonist of Losartan (1 μM, 30 min) or Ang II receptor type 2 antagonist PD-123319 (1 μM, 30 min). The results are presented in Figure 27, showing treatment with Losartan significantly attenuated Ang II-induced increases in Class III PI3-kinase activity by 63.3 % in cardiomyocytes (PIP production (pmol/μg of protein) 1.12 ± 0.06 in Losartan vs. 1.51 ± 0.07 in Losartan + Ang II, n=3 experiments,

$P < 0.05$ vs. Ang II). In contrast, treatment with PD-123319 did not significantly alter Ang II-induced elevations in Class III PI3-kinase in cardiomyocytes (PIP production (pmol/μg of protein) 1.35 ± 0.06 in PD-123319 vs. 2.97 ± 0.13 in PD-123319+Ang II, $P > 0.05$ vs. Ang II). In addition, treatment with Losartan or PD-123319 alone did not alter the basal Class III PI3-kinase activity. The results demonstrated that Ang II-induced Class III PI3-kinase activity in cardiomyocytes is mainly mediated via Ang II receptor Type 1.

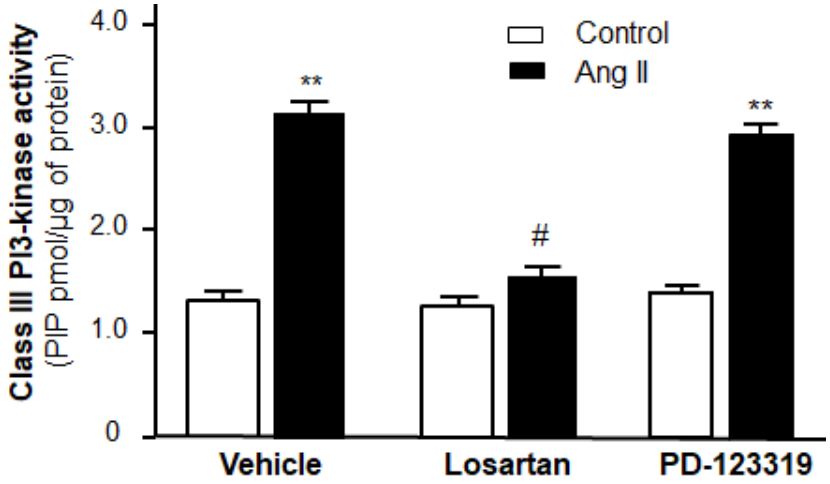

Figure 27: Effect of blockade of Ang II Receptor Type 1 or Type 2 on Ang II-induced Class III PI3-kinase activity in cardiomyocytes. Class III PI3-kinase activity in cardiomyocytes was determined using the ELISA kit after treated with Ang II (10^{-6} M) with or without the Ang II receptor type 1 antagonist of Losartan (Los, 1 μM) or Ang II receptor type 2 antagonist of PD-123319 (PD, 1 μM) for 24 h. Bar graphs summarizing the effect on Class III PI3-kinase activity in cardiomyocytes treated with the Vehicle control, Losartan (Los, 1 μM), PD-123319 (PD, 1 μM), Ang II, Ang II plus Losartan, or Ang II plus PD-123319. Data are presented as means ± SE, which were derived from three experiments and at least triplicate wells in each experiment. $^{**}P < 0.01$ vs. cardiomyocytes treated with vehicle control. $^{\#}P < 0.05$ vs. cardiomyocytes treated with Ang II.

3.4. Data summary and conclusion

The purpose of this part is to examine the role of Class III PI3-kinase in Ang II-induced cardiac remodeling via an autophagic-dependent pathway. This was achieved by observing and evaluating the effects of the relevant blocker of Class III PI3-kinase of 3-MA on autophagy, ROS generation, cardiac hypertrophy, and Class III PI3-kinase activity. The results demonstrated that Class III PI3-kinase is activated under lower Ang II dosage, facilitates autophagy, and protects

cardiomyocytes from ROS generation, and cardiac hypertrophy. This conclusion is supported by the following evidence: 1) Class III PI3-kinase activity was elevated at lower Ang II dosages with more sensitivity than that of Class I PI3-kinase, and autophagy was promoted as the elevated Class III PI3-kinase activity; 2) Pretreatment of 3-MA, a Class III PI3-kinase inhibitor lowered Class III PI3-kinase activity, diminished Ang II-induced autophagy, and exacerbated Ang II-induced ROS generation and cardiac hypertrophy; 3) Ang II-induced Class III PI3-kinase activation is also mainly mediated through AT1R instead of AT2R.

The main function of Class III PI3-kinase is to serve PI as substrate and convert it into PIP. Effector proteins consisting of FYVE or PX domains are adopted by localized PIP production, and facilitate docking and fusion process in the membrane when internal vesicles are established [91]. 3-methyladenine (3-MA) is a potent autophagic inhibitor by suppressing autophagosome formation and autophagic/lysosomal fusion in starvation-induced autophagy via glucose deprivation in rat cardiomyocyte-derived H9C2 cell lines via a Class III PI3-kinase-dependent pathway [89]. Therefore, 3-MA is widely adopted to examine the role of autophagy in various research areas such as tumorigenesis and cancer therapy, and previous studies found that this reagent might be useful to destroy cancer cells [92].

In the current study, we used 3-MA to inhibit Class III PI3-kinase, and further obstruct autophagy. Our results indicated that autophagic decrement caused elevated ROS generation and cardiac hypertrophy, suggesting autophagic induction would be an effective initiative to prevent cardiac remodeling and facilitate cardiomyocyte to survive. Vps34 is the only conserved component of PI3-kinase family in all eukaryotes, playing essential regulatory roles in physiological membrane trafficking such as endosome-lysosome formation, endocytosis, and autophagosome formation/flux, *etc* [93]. Nucleation takes place after induction within the whole process of autophagy, and Vps34 is one of those components within the Beclin1-Atg14-Vps34-

Vps15 complex which are essential for nucleation [94]. Thus, Vps34 is a vital component of Class III PI3-kinase that generates PIP, and this component is essential for the vacuolar protein delivery which is the very first step of autophagy. 3-MA is potent to inhibit the activity of Vps34 and terminate autophagy in the nucleation process Once Vps34 component is inactivated by 3-MA, the process of autophagy is totally blocked [95]. Overall, autophagic impairment by Class III PI3-kinase inhibition caused severe ROS generation and cardiac hypertrophy in primary cardiomyocytes under Ang II exposure.

CHAPTER IV. VALIDATION OF THE ROLE OF CLASS I PI3-KINASE, AUTOPHAGY, AND ROS GENERATION IN ANG II-INDUCED CARDIAC HYPERTROPHY IN CHRONIC ANG II-PERFUSED VERSUS CONTROL RATS

4.1. Introduction

In the previous chapters, we have examined the effects of both Class I and Class III PI3-kinases on autophagy, ROS generation, cardiac hypertrophy and the activities of relevant PI3-kinases in cultured primary cardiomyocytes from neonatal SD rats. Although *in vitro* studies provide a convenient, stable and reliable environment, they cannot perfectly mimic the real physiological condition in living bodies in the presence of hormone secretion and hemodynamic factors such as blood pressure, heart beat and contraction. To make up for this flaw, we performed *in vivo* study in adult rat hearts in this chapter to further identify the roles that Class I PI3-kinase play in Ang II-induced cardiac remodeling in adult rats.

It is well known that Ang II stimulates the cardiomyocytes by increasing their contractility and cardiac remodeling via stimulation of angiotensin receptor type I (AT1R). Accumulating evidences indicate that PI3-kinases are involved in the intracellular downstream signaling transduction pathways of AT1 receptors in cardiomyocytes [67, 68]. PI3-kinases are divided into three subclasses as Class I, II, III due to the specificity of substrates, varied molecular structures and diversified physiological functions, and only Class I & Class III PI3-kinases are expressed in the heart [60]. It's also reported that targeted overexpression of Class I PI3-kinase increases heart size, resulting in cardiac hypertrophy in the *in vivo* studies [62]. However, it is still unclear whether and how those PI3-kinases mediate Ang II-induced cardiac remodeling in living animals. Therefore, to elucidate the underlying mechanisms of Ang II-induced cardiac hypertrophy, it is crucial to adopt *in vivo* studies in an authentic physiological environment as a useful tool for

understanding the mechanisms of Ang II-induced cardiac remodeling via an autophagic-dependent manner.

In the previous chapters, application of ordinary chemical reagents relevant to the activity of PI3-kinases and mTOR were chosen to determine the role of PI3-kinase in Ang II-induced cardiac hypertrophy. Nevertheless, some shortcomings of the utilization of those chemical reagents in living animals should be paid attention to: 1). Their poor solubility in aqueous solvent makes it difficult to prepare a solution with desirable concentrations, while DMSO is a toxic solvent for living animals despite its higher solubility of those chemical reagents; 2). The actions of those drugs on living animals might be quite transient, while adaptations and drug resistance emerges as their prolonged exposure, losing sensitivity gradually; 3). The specificity of some reagents to their target molecules is not ideal. Thus, it is obliged for us to explore novel approaches to affect the activity of PI3-kinases without the usage of chemical reagents.

In recent years, gene delivery to overexpress or knockout of certain proteins is attractive and regarded as hot spot areas of study. The vectors that carry genes have various forms such as inorganic complex, organic polymers and bioactive viral vectors. To name a few, bioactive viral vectors are a new star for their high transfection efficiency and their ability to accomplish the process of adsorption, infusion and propagation spontaneously while the non-viral vectors don't own this privilege. Our lab has successfully delivered AAV2-apelin viral vector into the RVLM region of rat brains to enhance the apelin level and we learned its relationship with the MAP [96]. Previously, we also successfully delivered Lv-DNp85 and Lv-GFP into both primary neuron cultures and brain NTS region in WKY and SHR rats to inhibit the activity of Class I PI3-kinase [81]. Thus, we have competitive expertise to carry out this viral delivery technique in living animals.

Therefore, in the present chapter, we performed *in vivo* studies with lenti-viral vector gene transduction into adult rat hearts to consolidate our hypothesis that activated Class I PI3-kinase and impaired autophagy mediate Ang II-induced cardiac hypertrophy via a ROS-dependent mechanism. We have detected the physiological parameters such as blood pressure (BP), heart rate (HR), left ventricular contractile functions (dP/dt Max) to measure the heart functions in living adult rats by chronic blockade of Class I PI3-kinase. Further, we performed molecular biology and morphological studies to tell the effectiveness of blockade of Class I PI3-kinase with relevant lentiviral vectors.

4.2. Materials and methods

4.2.1. Animals

Twelve-week-old male SD rats were obtained from Charles River Farms (Charles River Laboratories International, Wilmington, MA). Rats were housed at 25 ± 2°C on a 12:12-h light-dark cycle and provided with food and water *ad libitum*. All animal protocols were approved by the North Dakota State University Institutional Animal Care and Use Committee.

4.2.2. Myocardial *in vivo* gene delivery

The lentiviral vectors containing dominant negative Class I PI3-kinase p85α subunit (Lv-DNp85) and negative control viral vector Lv-GFP were constructed and titered as previously described (80). The dominant negative construct of the p85α subunit of the Class I PI3-kinase (DNp85α) was delivered in vivo in a lentiviral vector driven by EF1 promoter (LV-EF1-DNp85α-IRES-eGFP). The titer was 2×10^{10} transducing units per milliliter, which was shown to be efficient in central cardiac transduction. For cardiac gene transfer, Lv-DNp85 and Lv-GFP were delivered into the heart via routine intra-aortic root injection. Briefly, adult male SD rats were anesthetized with a mixture of oxygen (1 L/min) and isoflurane (3%) delivered through their nose cones. Left anterior thoracotomy was carried out in the left second intercostal space. For arterial occlusion,

ligatures were looped around the main pulmonary arteries and the ascending aorta followed by a ligature occlusion. Then a PE-50 catheter insertion through the right carotid artery into the aortic root was made just above the aortic valve and below the occlusion ligature loop to determine blood pressure and exert injections in coronary arteria. Ice packs were used after the anesthesia to create a general hypothermia environment for the rats to cool their body temperatures below 26 ℃ and followed by injection of cardioplegic solution (2 μL/g body weight) containing (in mM): NaCl 110, KCl 20, $MgCl_2$ 16, $NaHCO_3$ 10, and $CaCl_2$ 1.2 via the arterial catheter. Substance P was also added into the cardioplegic solution with the final concentration of 25 μg/mL to enhance the permeability of coronary artery wall and let the viral vectors pass through. Thereafter, 200 μL 2×10^{10} TU/mL of Lv-GFP or Lv-DNp85 in the cardioplegic solution with Substance P was injected through the same catheter. Both occlusions were loosed 90 seconds after lenti-viral vectors injection, and dobutamine (12 μg/kg, 50 μL) was administered to make the heart beat again. and rat body temperature was heated back to normal with a heating pad. The chest was then closed by suture and the intrathoracic air was evacuated by syringe suction.

4.2.3. Ang II subcutaneous infusion and blood pressure (BP) recording

After cardiac injection of either Lv-DNp85 or Lv-GFP into the heart, Alzet osmotic pumps (Reservoir volume 200 μL) were implanted under the back skin of the rats for subcutaneous infusion of Ang II (200 ng/kg/min) or normal saline (NS). A four week-period was allowed for recovery from surgery and gene expression in the heart. The rats were then anaesthetized with 3% pentobarbital (50 mg/kg), and BP was recorded using PE-10 catheters fused to PE-50 catheters. The vascular catheters were prefilled with heparinized saline (100 IU/mL) and inserted into the right femoral artery. Left ventricular pressure (dp/dt Max) was recorded via right carotid artery catheterization. The vascular catheters were connected to a BP transducer and a bridge amplifier (AD instrument, Colorado Springs, CO, USA). The BP, heart rate (HR), and left ventricular dP/dt

Max were recorded and analyzed with PowerLab software (AD instrument). At the end of recording, hearts were harvested for subsequent morphologic measurements and protein expression investigation.

4.2.4. Measurement of cardiac hypertrophy

The hearts of each group were collected after BP and HR measurement and washed with saline. After heart weight and cardiac morphology were determined, they were transversely sectioned with a microtome (Leica). Hearts were fixed in 10% formalin/PBS and embedded in paraffin. Heart sections (10 μm) were cut using a cryo-microtome and placed on a slide. Paraffin sections were deparaffinized and rehydrated by incubating in 3 × 3 minutes in xylene, 3 × 3 minutes in 100% ethanol, 1 x 3 minutes in 95% ethanol, 1 × 3 minutes in 80% ethanol, and 1 × 5 minutes in deionized H_2O. Rehydrated tissues were stained by incubating with hematoxylin for three minutes. Excessive and unbound stain was removed by running tap water over the section. Slides were washed by dipping in Acid-ethanol followed by deionized water. Excessive water was removed by blot paper and air-dried. Air dried slides were incubated in eosin stain for 45 seconds and washed for 3 × 5 minutes in 95% ethanol, 3 × 5 minutes and 3 × 15 minutes in xylene. Slides were covered with a cover slip using a mounting medium. The cross-sectional diameter of single myocytes was measured by the cellular diameter crossing the nuclei using were evaluated by using Image Pro Plus 6.0 (Media Cybernetics, Bethesda, MD) and the outline of 100-200 cardiomyocytes were traced in each group.

4.2.5. Assessment of perivascular fibrosis

Interstitial perivascular fibrosis is a hallmark for cardiac remodeling during heart failure. Sirius Red solution known as F3B staining is the most accepted technique for studying interstitial perivascular fibrosis via evaluation of the extent of perivascular fibrosis, which was expressed as the percentage of perivascular fibrotic area in the total area of the whole artery cross-section plus

the perivascular fibrotic area. In brief, after four weeks of cardiac gene transfer, the animals were anesthetized by i.p injection of 200 mg/kg sodium pentobarbital and euthanized by decapitation. Hearts were removed. After the heart weight and cardiac morphology were examined, hearts were fixed in 10 % formalin/PBS and embedded in paraffin. Heart sections (10 μm) were cut using a cryo-microtome stained and placed on a slide. Sections were incubated in clearing agent 3 × for 5 minutes by changing the clearing agent after every 5 minutes. Slides were incubated in 100% ethanol for 3 times for 3 minutes each, in 95% ethanol for 3 times for 3 minutes each, in 80% alcohol for 3 minutes and finally wash tap water for 3 minutes. 0.1% Sirius Red was added and incubated for 60 minutes. The slide was washed with acidified water and air-dried. After drying, the slides were washed for 1 minute in 80% alcohol, 2 minutes in 95% ethanol, 2 times in 100% ethanol for 10 minutes each time, and finally 3 times for 3 minutes in clearing solution. were covered with a cover slip. The histology, morphology, and cross-sectional area of cardiomyocytes were examined and analyzed by the image analysis software (Image Pro Plus 6.0, Media Cybernetics, Bethesda, MD). The external diameter of the arteries measured was no more than 100 μm and the number of arterial cross-sections measured was more than 50, from five rats in each group.

4.2.6. Western blots analysis

Akt, p-Akt, mTOR, p-mTOR, β-actin, and LC3 (including LC3-I and LC3-II) protein levels in adult rat heart tissue were assessed by western blot analysis to determine the phosphorylation degree of those downstream components of Class I PI3-kinase. Briefly, after sacrificing those four group of rats, their heart tissues were washed with ice-cold PBS and scraped into a lysis buffer containing 20 mM Tris HCl (pH 6.8), 150 mM NaCl, 10% glycerol, 1% NP-40, and 8 μL/mL inhibitor cocktail (125 mM PMSF, 2.5 mg/mL aprotinin, 2.5 mg/mL leupeptin, 2.5 mg/mL antipain, and 2.5 mg/mL chymostatin). The samples were sonicated twice for 5 s each and

were centrifuged at 12,000 rpm for 10 min at 4°C. Supernatants were transferred into new tubes and stored in a -80°C freezer. The protein concentration was determined with a protein assay kit (Bio-Rad Laboratories, Hercules, CA). An aliquot of 30 μg of protein from each sample was separated on a 10% SDS-PAGE gel and was transferred onto nitrocellulose membranes for 2 h at 120 V. After a 10-min wash in TBST, membranes were blocked in PBST containing 10% milk for 1 h, followed by an overnight incubation in rabbit anti-Akt (Santa Cruz Biotechnology, sc-8312, Santa Cruz, CA), anti-p-Akt (Santa Cruz Biotechnology, sc-2448, Santa Cruz, CA), anti-mTOR (Santa Cruz Biotechnology, sc-1549, Santa Cruz, CA), anti-p-mTOR (Santa Cruz Biotechnology, sc-101738, Santa Cruz, CA), LC3 (Santa Cruz Biotechnology, sc-134226, Santa Cruz, CA) and mouse anti-β-actin (Santa Cruz Biotechnology, sc-47778, Santa Cruz, CA) (dilution 1:100) at 4 °C. After a 15-min wash in TBST, four 5-min washes in PBS-T will be carried out, and membranes will be then incubated for 2 h in an anti-rabbit peroxidase-conjugated antibody (dilution 1:15,000). Densitometry of p-Akt was normalized to total Akt, p-mTOR normalized to total mTOR, LC3 II to β-actin ratio and p85 protein to β-actin ratio. Immunoreactivity was detected by enhanced chemiluminescence autoradiography (ECL Western blotting detection kit, Amersham Pharmacia Biotechnology), and films were analyzed with Quantity One Software (Bio-Rad).

4.2.7. Immunofluorescence staining of heart tissue

The immunofluorescence staining of heart sections was performed to evaluate the successful cardiac gene transfer of Lv-GFP. In brief, the transverse heart sections were fixed with 4% PFA at 4℃ for 30 minutes, and cellular membranes were penetrated with 0.1% Triton X-100 in PBS for 30 minutes. After pre-incubation with 3% of bovine serum albumin (BSA) for 60 minutes, the cells were then incubated with primary antibodies of mouse sarcomeric α-actin (Santa Cruz Biotechnology, sc-53142, Santa Cruz, CA) and rabbit anti-GFP (Santa Cruz Biotechnology, sc-8334, Santa Cruz, CA), which was diluted to 1:100 with PBS containing 3% BSA, overnight at

4°C. After three washings with the PBS solution, the cells were incubated with fluorescence-conjugated Alexa Fluor 594 fluorescence-conjugated goat anti-mouse IgG antibody (Molecular probes, A-11032, Waltham, MA) and Alexa Fluor 488 fluorescence-conjugated goat anti-rabbit IgG antibody (Molecular probes, A-11034, Waltham, MA) (1:1000 diluted in PBS each) for 2 h at room temperature in dark. Photographic images of heart tissue were taken with a fluorescence microscope (Olympus Microsystems, Waltham, MA).

4.2.8. Class I PI3-kinase activity assay

After a four-week treatment, rat heart tissues from those four groups were rinsed with ice-cold PBS and Buffer A (20 mM Tris-HCl, pH 7.4, 137 mM NaCl, 1 mM $CaCl_2$, 1 mM $MgCl_2$, and 1 mM Na_3VO_4) three times each. Then Buffer A was removed and the cells were immediately lysed in lysis buffer Lysis Buffer (Buffer A plus 1% NP-40 and 1 mM PMSF) at 4°C for 20 minutes. The cells were scraped from dishes, transferred to 1.5 mL microcentrifuge tubes and centrifuged for 10 minutes to sediment insoluble material. Thereafter, supernatant was transferred to new tubes added with 5 μL of anti-PI3-Kinase antibody (Millipore Corp, 06-195, Billerica, MA) previously described [81] to each tube and incubated for one hour at 4°C with gentle rotation. 60 μL of 50% slurry of Protein A-agarose beads in PBS was added into each tube with gentle rotation for overnight, and tubes were centrifuged for 5 seconds for collection of immunoprecipitated enzymes. Sediments were washed three times with Buffer A plus 1% NP-40, three times with 0.1 M pH 7.4 Tris-HCl with 5 mM LiCl and 1 mM Na_3VO_4, twice with TNE (10 mM Tris-HCl, pH 7.4, 150 mM NaCl, 5 mM EDTA) containing 1 mM Na_3VO_4 and twice with KBZ Reaction Buffer. The last wash was aspirated completely and 30 μL of KBZ Reaction Buffer was added to cover the beads. Then the Class I PI3-kinase reactions were carried out using competitive enzyme-linked immunosorbent assay kit (Echelon Biosciences, K-1000s, Salt Lake City, UT) by exactly following the instructions provided by the manufacturer. A PIP_3 standard curve (ranging from 4.4

nM to 1.08 μM) was simultaneously prepared and determined at 450 nm wavelength. Each assay was repeated at least 3 times.

4.2.9. Reactive Oxygen Species (ROS) generation assay in heart tissues

ROS generation in heart tissue was determined using a fluorogenic probe, MitoSOX (Thermo Fisher, M-36008, Rockford, IL). MitoSOX is a superoxide-sensitive ($O_2^{\cdot-}$) fluorogenic probe, and it yields red fluorescence when oxidized in mitochondria (excitation/emission wavelength: 510/580 nm). Heart sections were embedded in a freezing medium of OTC immediately after harvest, and transverse sections (20 μm) of frozen tissue were obtained using a cryostat microtome sectioning machine, collected on glass sides, and equilibrated for 10 min in Hanks' solution. Heart sections were loaded with 5 μM MitoSOX for 30 min at 37℃ in dark room. Thereafter, the incubated heart sections were rinsed with 37℃ HBSS three times and five minutes for each time. Fluorescence images of cardiomyocytes in heart tissue were captured by a fluorescence microscope (Olympus), and the mean fluorescence intensity of cardiomyocytes was analyzed and quantified in 50 randomly selected fields in each section with Image J.

4.2.10. Data analysis

All data are presented as means ± SE. Data were statistically analyzed by GraphPad Prism 5.0 (GraphPad Software, San Diego, CA). Statistical significance was evaluated by one- or two-way ANOVA, as appropriate, followed by either a Newman–Keuls or Bonferroni's *post hoc* analysis when indicated. Differences were considered significant at $P < 0.05$, and individual probability values are noted in the figure legends.

4.3. Results

4.3.1. Identification of Lv-GFP delivery into the cardiomyocytes in adult rat hearts

We examined the efficacy of cardiac transfer of lentiviral vectors before we performed gene expression modification-induced inactivation of Class I PI3-kinase. Cardiac transfer of Lv-

GFP was adopted to investigate the successful delivery of lentiviral vectors into adult rat hearts and served as the negative control of Lv-DNp85. The results are presented in Figure 28, cardiac micro-injection of Lv-GFP (2 x 10^{10} TU/mL, 200 µL) significantly increased GFP expression in cardiomyocytes after four weeks, emitting green fluorescence and overlapped with α-actin generating red fluorescence as a cardiomyocytes marker. The results demonstrated that we have successfully transduced lentiviral vector-mediated GFP (Lv-GFP) gene into cardiomyocytes with desirable specificity for in adult rat hearts.

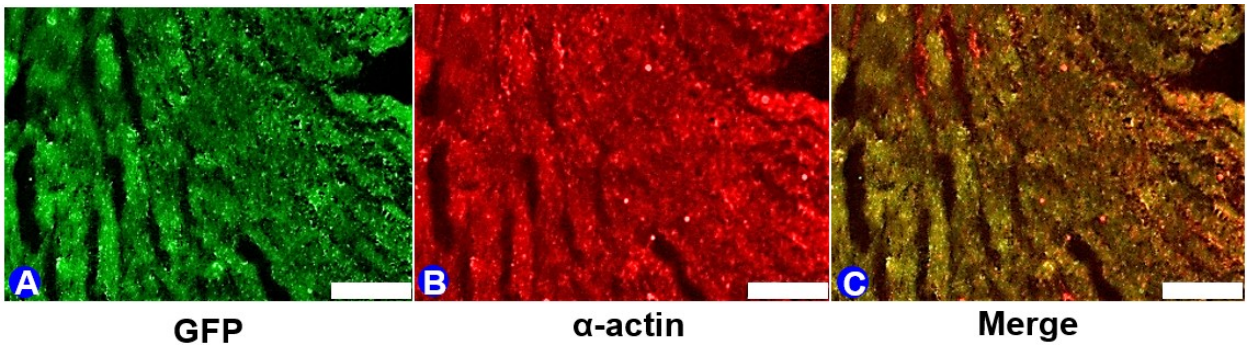

Figure 28: Effect of cardiac transfer of Lv-GFP in adult rat hearts. Immunofluorescence images showing GFP expression in cardiomyocytes in adult rat heart tissues that received Lv-GFP microinjection. **A:** Fluorescence micrograph demonstrating localization of green fluorescence protein (GFP, green). **B:** The same field of heart tissue as in A which is immunostained with anti-α-actin (red) as a cardiomyocyte marker. **C:** Merge of A and B, indicating successful lentiviral vector-mediated GFP gene transduction into cardiomyocytes. Scale bar: 250 µm.

4.3.2. Effect of cardiac transfer of Lv-DNp85 into adult rat hearts on Ang II-induced Class I PI3-kinase activity

The effects of Ang II infusion and Lv-DNp85 cardiac transduction on Class I PI3-kinase activity were evaluated to confirm lentiviral vector-mediated overexpression of a dominant negative subunit p85α of Class I PI3-kinase (Lv-DNp85) and PIP_3 production. The results are presented in Figure 29, PIP_3 production was significantly elevated by Ang II infusion by 100.21 % (PIP_3 production (in pmol/µg of protein) 1.75 ± 0.24 in the Saline+Lv-GFP group vs. 3.52 ± 0.33 in the Ang II+Lv-GFP group, n = 6, $P < 0.05$ vs. Saline+Lv-GFP) and this increase in Class I PI3-

kinase activity was mitigated by cardiac transduction of Lv-DNp85 by 41.76 % (PIP_3 production (in pmol/μg of protein) 3.52 ± 0.33 in the Ang II+Lv-GFP group vs. 2.05 ± 0.25 in the Ang II+Lv-DNp85 group, n = 6, $P < 0.05$ vs. Ang II+Lv-GFP). The results demonstrate that cardiac transfer of Lv-DNp85 increases p85α subunits expression and decreases Class I PI3-kinase activity in the heart.

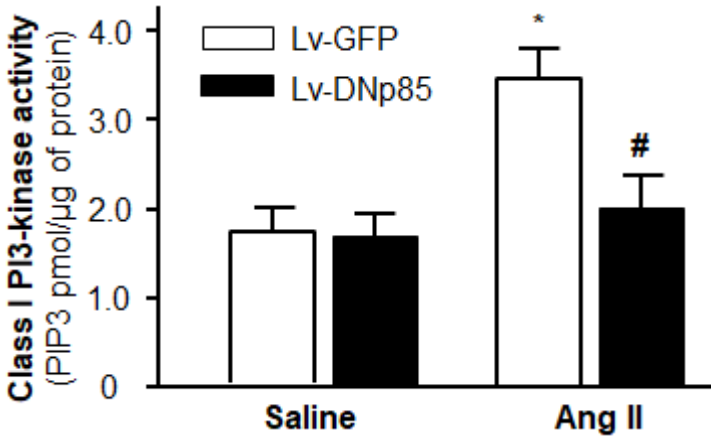

Figure 29: Effect of Ang II and cardiac transfer of Lv-DNp85 on Class I PI3-kinase activity in adult rat hearts. Production of PIP_3 were examined 4 weeks after subcutaneous infusion of Ang II or normal saline (NS) with cardiac transduction of Lv-DNp85 or Lv-GFP.**:** Bar graphs summarizing Class I PI3-kinase activity measured with PIP_3 ELISA kit in the heart tissues from these rats treated under the conditions described in the above. Data are means ± SE (n = 6 rats). $^{*}P < 0.05$ vs. rats that received Saline + Lv-GFP. $^{\#}P < 0.05$ vs. rats that received Ang II + Lv-GFP.

4.3.3. Effect of blockade of Class I PI3-kinase on Ang II-induced cardiac function changes in adult rats

Then, we determined several physiological parameters to evaluate the effect of Ang II and Class I PI3-kinase on heart function in living rats. The results are presented in Figure 30A and B, and cardiac transfer of neither Lv-GFP nor Lv-DNp85 altered the mean arterial pressure (MAP) or heart rate (HR) in rats infused with saline. While chronic subcutaneous Ang II infusion considerably elevated MAP by about 48 %, which was not attenuated by cardiac transfer of either Lv-GFP or Lv-DNp85 (132.35 ± 7.96 mmHg in Ang II + Lv-GFP and 127.83 ± 6.84 mmHg in the Ang II + Lv-DNp85 group respectively, n = 6, $P < 0.05$ vs. Rats that received Saline). Besides,

none of those four groups showed significant Heart Rate (HR) change. Thus, we conclude that neither the basal MAP nor the pressor response to subcutaneous Ang II infusion was altered by cardiac transfer of Lv-DNp85. The results demonstrated that blockade of cardiac Class I PI3-kinase has no noticeable effect on peripheral blood pressure. Taken together, those outcomes indicate that neither basal blood pressure nor Ang II-induced pressor effect is altered by cardiac transfer of Lv-DNp85.

Heart contractility was also determined by left ventricular catheterization in those four rat groups. The larger value of dP/dt Max indicates stronger cardiac contractility. The results are presented in Figure 30 C, and chronic subcutaneous infusion of Ang II significantly reduced cardiac contractility by 8.12 % (dP/dt Max 7400 ± 360 mmHg/s in the Saline+Lv-GFP group vs. 6850 ± 210 mmHg/s in the Ang II+Lv-GFP group, n = 6, $P < 0.05$ vs. Saline+Lv-GFP) due to the possible occurrence of Ang II-induced decompensated hypertrophy and perivascular fibrosis. Blockade of Class I PI3-kinase considerably attenuated Ang II-induced reduction in cardiac contractility by 13.8 % (dP/dt Max of 6850 ± 210 mmHg/s in the Ang II + Lv-GFP group vs. 7800±430 mmHg/s in the Ang II + Lv-DNp85 group, n = 6, $P < 0.05$ vs. Ang II + Lv-GFP) of left ventricle, indicating that blockade of Class I PI3-kinase remarkably restores chronic Ang II infusion-induced cardiac dysfunction.

All those results demonstrate Ang II infusion elevated blood pressure and undermined heart functions. While Lv-DNp85 overexpression in cardiomyocytes attenuated Ang II-induced contractility decline without alteration of blood pressure or hear rate.

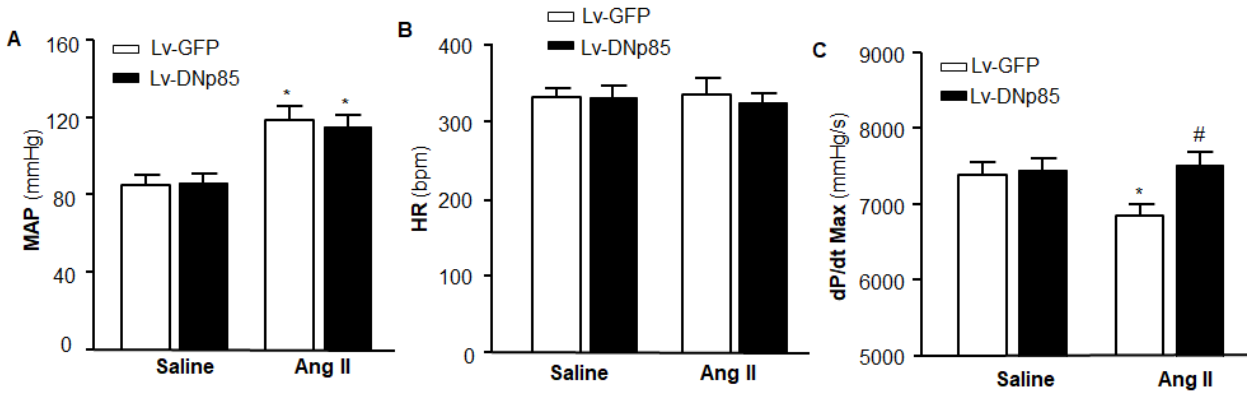

Figure 30: Effect of Ang II and cardiac transfer of Lv-DNp85 on MAP, HR and dp/dt Max in adult rats. Hemodynamic indexes were recorded to examine cardiac function in living adult rats 4 weeks after subcutaneous infusion of either Ang II or normal saline (NS) with cardiac transduction of Lv-DNp85 or Lv-GFP. Bar graphs summarizing MAP (**A**) and Heart rate (HR) (**B**) recorded via femoral arterial cannulation; and dP/dt Max (**C**) was recorded via the left ventricular catheterization through the right carotid artery. Data are means ± SE (n = 6 rats). $^{*}P < 0.05$ vs. rats that received Saline + Lv-GFP. $^{\#}P < 0.05$ vs. rats that received Ang II + Lv-GFP.

4.3.4. Effect of blockade of Class I PI3-kinase on Ang II-induced cardiac hypertrophy

Cardiac hypertrophy was identified by calculating the ratio of heart weight to body weight (HW/BW) in rats infused with normal saline or Ang II and cardiac transduction of Lv-GFP or Lv-DNp85. The results are presented in Figure 31, and no significant body weight alterations were observed in any of those four groups (BW: 344 ± 13 g in the Saline + Lv-GFP group; 339 ± 12 g in the Saline+ Lv-DNp85 group; 337 ± 14 g in the Ang II + Lv-GFP group; 342 ± 11 g in the Ang II + Lv-DNp85 group, n = 6, $P > 0.05$ vs. Saline+Lv-GFP). Whereas subcutaneous infusion of Ang II (200ng/kg/min for 4 weeks) significantly elevated HW/BW by 51.40 % (HW/BW ratio 3.05±0.15 mg/g in the Saline+Lv-GFP group vs. 4.62 ± 0.18 mg/g in the Ang II+Lv-GFP group, n = 6, $P < 0.05$ vs. Saline+Lv-GFP). Cardiac transfer of Lv-DNp85 significantly attenuated Ang II-induced elevation of HW/BW ratio by 27.05 % (HW/BW ratio of 4.62 ± 0.18 mg/g in the Ang II + Lv-GFP group vs. 3.37 ± 0.17 mg/g in the Ang II+Lv-DNp85 group, n = 6, $P < 0.05$ vs. Ang II + Lv-GFP).

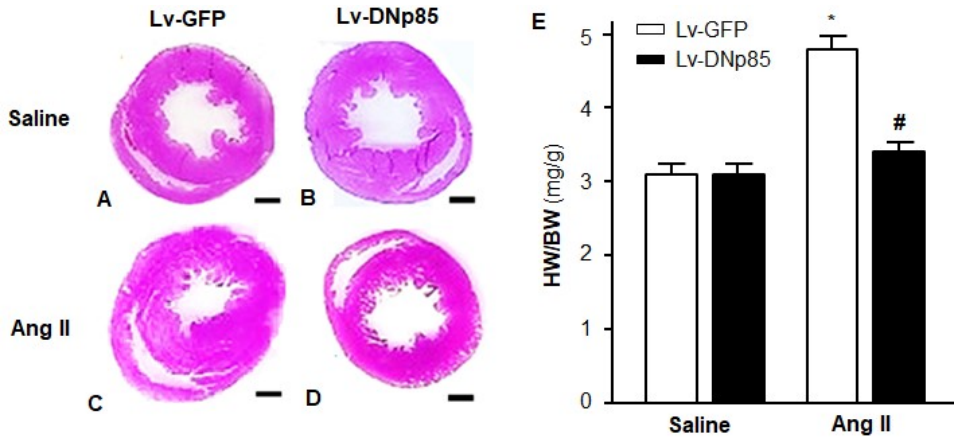

Figure 31: Effect of Ang II and Lv-DNp85 on HW/BW ratio and cardiac morphology. Cardiac morphological alterations were examined 4 weeks after subcutaneous infusion of Ang II or saline by cardiac transduction of Lv-DNp85 or Lv-GFP, as described in Methods. **A-D:** Graphs showing representative heart sections stained with hematoxylin/eosin in rats that received subcutaneous infusion of saline (**A and B**) or Ang II (**C and D**) with cardiac transduction of Lv-GFP (**A and C**) or Lv-DNp85 (**B and D**). **E:** Bar graphs summarizing heart weight/body weight ratios (HW/BW) under the conditions indicated. Scale bar: 2 mm. Data are means ± SE (n = 6 rats). $^{*}P < 0.05$ vs. rats that received Saline + Lv-GFP. $^{\#}P < 0.05$ vs. rats that received Ang II + Lv-GFP.

Cardiac morphology identification was also observed to further confirm the results of cardiac hypertrophy. The effects of Ang II infusion and Lv-DNp85 cardiac transduction on cardiac hypertrophy were evaluated in these four groups of rats by examination the dimensional size of cardiac myocytes on the heart sections using H&E staining in these four groups of rats. The results are presented in Figure 32, demonstrating that Ang II infusion greatly increased the average diameter of cardiomyocytes inducing severe cardiac hypertrophy by 45.62 % (15.5 ± 0.5 μm in the Saline + Lv-GFP group vs. 22.5 ± 1.2 μm in the Ang II + Lv-GFP group, n = 6, $P < 0.05$ vs. Saline+Lv-GFP). Ang II-induced increases in cardiomyocyte diameter were significantly attenuated by cardiac transduction of Lv-DNp85 by 21.77 % (22.5 ± 1.2 μm in the Ang II + Lv-GFP group vs. 17.6 ± 1.1 μm in the Ang II + Lv-DNp85 group, n = 6, $P < 0.05$ vs. Ang II + Lv-GFP). The results demonstrate blockade of Class I PI3-kinase attenuates chronic Ang II infusion-induced cardiac hypertrophy.

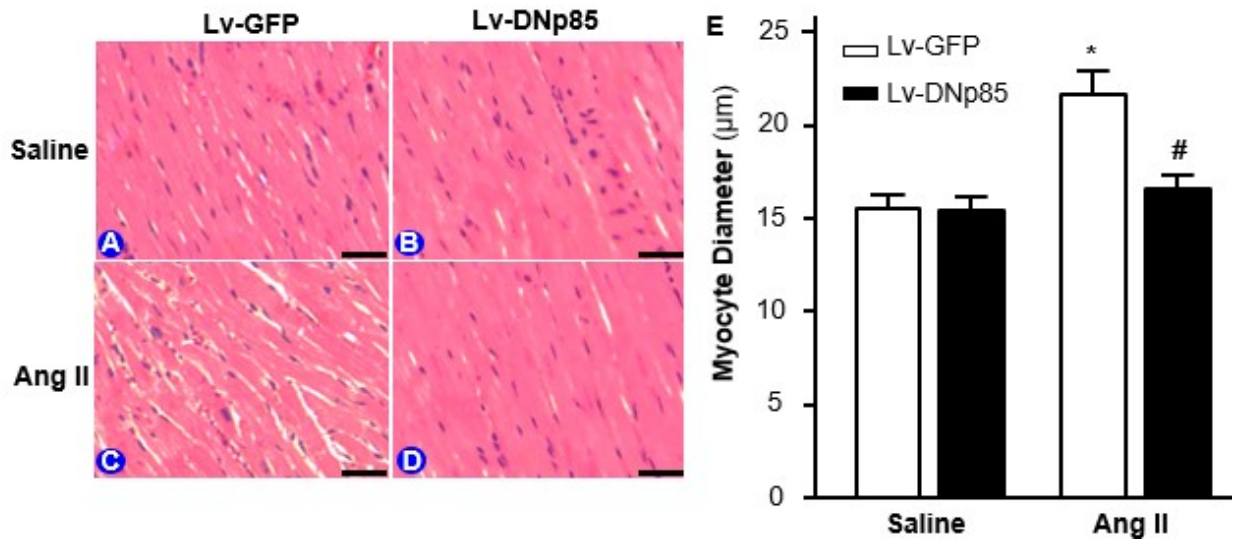

Figure 32: Effect of Ang II and Lv-DNp85 on cardiac histology. Cardiomyocyte diameters were examined 4 weeks after subcutaneous infusion of Ang II or normal saline (NS) with cardiac transduction of Lv-DNp85 or Lv-GFP. **A-D:** Micrographs showing representative heart sections stained with hematoxylin/eosin in rats that received subcutaneous infusion of NS (**A and B**) or Ang II (**C and D**) with cardiac transfer of Lv-GFP (**A and C**) or Lv-DNp85 (**B and D**). **E:** Bar graphs summarizing cross-sectional areas of cardiomyocytes from transverse cardiac sections of each group of rats. Cross-sectional areas of 100 cells per rat were observed randomly per group. Scale bar: 50 μm. Data are means ± SE (n = 6 rats). $^{*}P < 0.05$ vs. rats that received NS + Lv-GFP. $^{\#}P < 0.05$ vs. rats that received Ang II + Lv-GFP.

4.3.5. Effect of blockade of Class I PI3-kinase on Ang II-induced perivascular fibrosis

Fibroblast proliferation, perivascular fibrosis and cardiomyocyte apoptosis characterize the late stage of cardiac remodeling. Therefore, we determined the effect of Ang II infusion and Class I PI3-kinase inactivation on perivascular fibrosis in rats received cardiac transfer of Lv-GFP or Lv-DNp85 and subcutaneous infusion of Saline or Ang II for 4 weeks. The results are presented in Figure 33, perivascular collagen deposition in the heart was remarkably promoted by chronic subcutaneous infusion of Ang II by 96.4 % (Perivascular fibrosis area of 31.4 ± 3.2 % in the Saline+Lv-GFP group vs. 67.2±10.0 % in the Ang II+Lv-GFP group, n = 6, $P < 0.05$ vs. Saline+Lv-GFP), while cardiac transfer of Lv-DNp85 considerably alleviated Ang II-induced perivascular fibrosis by blockade of Class I PI3-kinase by 41.81 % (Perivascular fibrosis area of 67.2 ± 10.0 % in the Ang II+Lv-GFP group vs. 39.1 ± 3.1 % in the Ang II+Lv-DNp85 group, n =

6, $P < 0.05$ vs. Ang II + Lv-GFP). The results demonstrate that chronic blockade of Class I PI3-kinase by Lv-DNp85 may attenuate Ang II-induced perivascular fibrosis in adult rats.

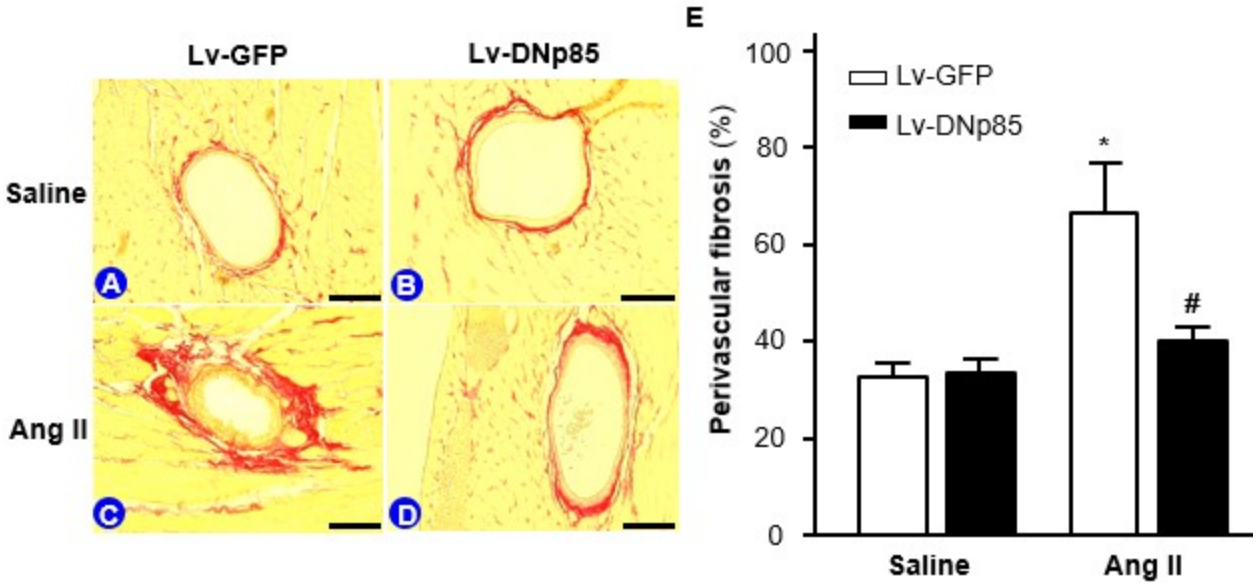

Figure 33: Effect of Ang II and Lv-DNp85 on cardiac perivascular fibrosis. Perivascular fibrosis was examined 4 weeks after subcutaneous infusion of Ang II or normal saline (NS) with cardiac transduction of Lv-DNp85 or Lv-GFP. **A-D:** Representative microscopic images showing myocardial perivascular collagen deposition (red) in rats 4 weeks after subcutaneous infusion of Saline **(A and B)** or Ang II **(C and D)** with cardiac transduction of Lv-GFP **(A and C)** or Lv-DNp85 **(B and D)**. **E:** Bar graphs summarizing the quantitative analysis of perivascular fibrosis, expressed as the ratio of perivascular collagen area to vessel cross-sectional area of the coronary arteries. Data are means ± SE (n = 6 rats). Scale bar: 100 μm. $^{*}P < 0.05$ vs. rats that received NS + Lv-GFP. $^{\#}P < 0.05$ vs. rats that received Ang II + Lv-GFP.

4.3.6. Effect of blockade of Class I PI3-kinase on Ang II-induced oxidant stress

Autophagy is a useful tool to protect cells, tissues and organs from impairment by eliminating and scavenging damaged mitochondria and other organelles & proteins producing reactive oxygen species (ROS). Thus, we measured ROS generation levels in the heart of rats receiving cardiac transfer of Lv-GFP or Lv-DNp85 along with subcutaneous infusion of saline or Ang II for 4 weeks. MitoSOX staining technique was adopted as the fluorogenic probe to measure ROS generation on heart sections. The results are presented in Figure 34, chronic Ang II infusion significantly elevated ROS generation in the heart by 91.51 % (MitoSOX Fluorescence of 100.0 ±

7.5 % in the Saline+Lv-GFP group vs. 191.5 ± 14.5 % in the Ang II+Lv-GFP group, n = 6, $P < 0.05$ vs. Saline+Lv-GFP). while cardiac transduction of Lv-DNp85 greatly attenuated ROS generation elevation (MitoSOX Fluorescence of 191.5 ± 14.5 % in the Ang II+Lv-GFP group vs. 115.3 ± 9.3 % in the Ang II+Lv-DNp85 group, n = 6, $P < 0.05$ vs. Ang II + Lv-GFP). The results demonstrate Ang II-induced elevation of ROS generation is attenuated by cardiac transfer of Lv-DNp85 to inactivate Class I PI3-kinase.

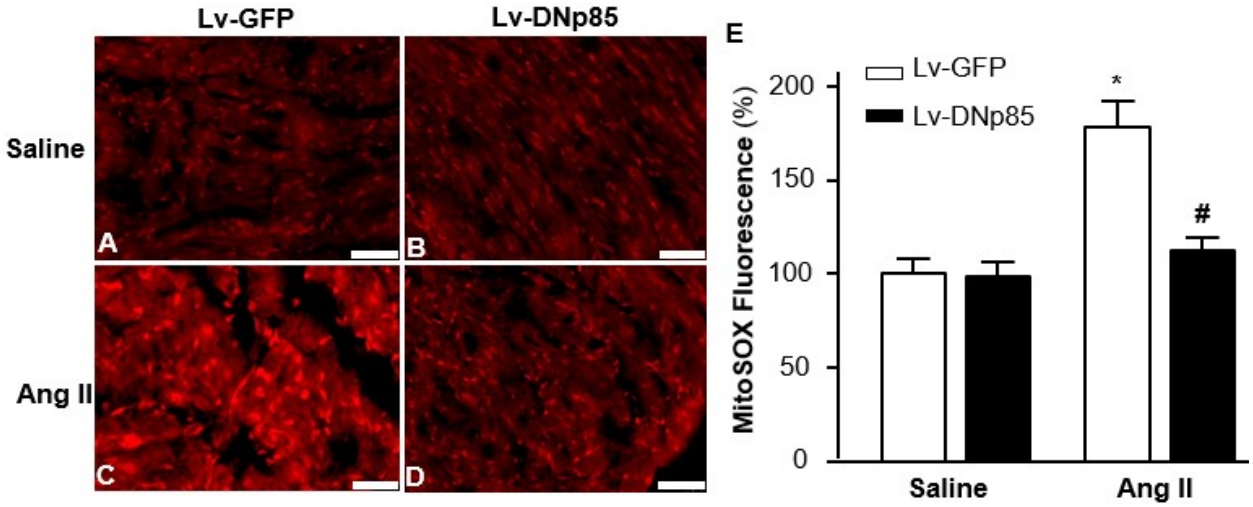

Figure 34: Effect of Ang II and Lv-DNp85 on ROS generation in adult rat hearts. ROS generation in heart tissue was examined 4 weeks after subcutaneous infusion of Ang II or normal saline (NS) with cardiac transduction of Lv-DNp85 or Lv-GFP. **A-D:** Representative microscopic images showing the ROS fluorescence (red staining) in rats 4 weeks after subcutaneous infusion of saline **(A and B)** or Ang II **(C and D)** with cardiac transduction of Lv-GFP **(A and C)** or Lv-DNp85 **(B and D)**. **E:** Bar graphs summarizing the quantitative analysis of ROS generation levels measured with the fluorescent probe of MitoSOX, expressed as the percentage of MitoSOX Fluorescence. Scale bar: 50 μm. Data are means ± SE (n = 6 rats). $^{*}P < 0.05$ vs. rats that received Saline + Lv-GFP. $^{\#}P < 0.05$ vs. rats that received Ang II + Lv-GFP.

4.3.7. Effect blockade of Class I PI3-kinase on Ang II-induced autophagic impairment

Accumulating evidence indicates the possible involvement of autophagic alteration in the pathogenesis of cardiac hypertrophy and cardiomyocyte death. Thus, it is obliged to examine the chronic effect of Ang II and blockade of Class I PI3-kinase on cardiac autophagy by examining the abundance of microtubule-associated protein light chain 3 (MAP-LC3), an autophagosome

marker with two forms known as LC3-I and LC3-II. LC3-I (18kD) is converted to LC3-II (16KD) during autophagy via Atg protein-facilitated conjugation with Phosphatidyl-ethanolamine (PE), and LC3-II is recruited by autophagosomes. Enhanced LC3-II/β-actin ratio indicates stronger occurrence of autophagy. After cardiac transfer of Lv-GFP or Lv-DNp85 along with subcutaneous infusion of Saline or Ang II for 4 weeks. The results are presented in Figure 35, chronic Ang II infusion in Lv-GFP group reduced cardiac autophagy by 40 % (LC3 II/β-actin of 0.25 ± 0.02 in the Saline+Lv-GFP group vs. 0.15 ± 0.016 in the Ang II+Lv-GFP group, n = 6, $P < 0.05$ vs. Saline+Lv-GFP), while this Ang II-induced reduction in autophagy was mitigated by cardiac transduction of Lv-DNp85 by 53.33 % (LC3 II/β-actin ratio of 0.15 ± 0.016 in the Ang II + Lv-GFP group vs. 0.23 ± 0.016 in the Ang II+Lv-DNp85 group, n = 6, $P < 0.05$ vs. Ang II + Lv-GFP). The results demonstrate that chronic blockade of PI3-kinase attenuates Ang II-induced impairment of autophagy in the heart tissue.

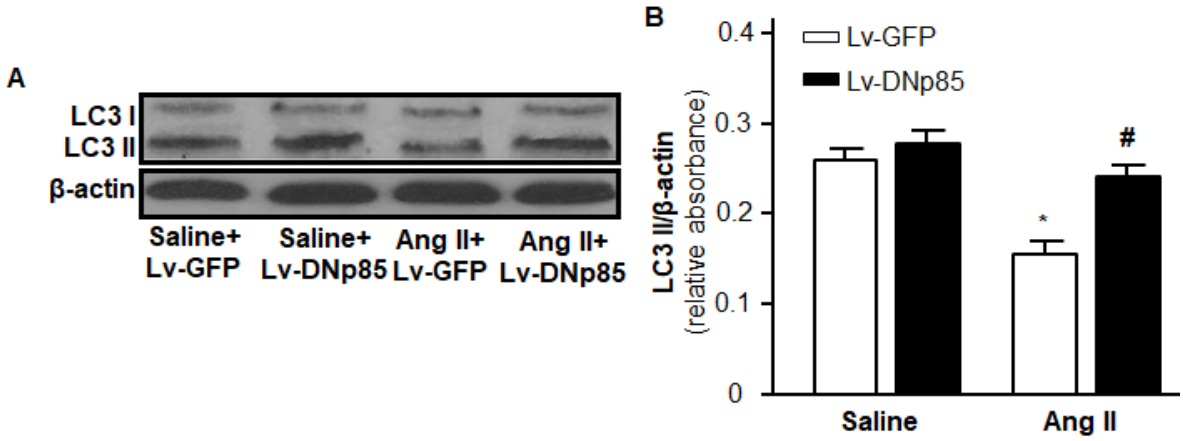

Figure 35: Effect of Ang II and Lv-DNp85 on autophagy in adult rat hearts. Autophagy in heart tissue was examined 4 weeks after subcutaneous infusion of Ang II or normal saline (NS) with cardiac transduction of Lv-DNp85 or Lv-GFP. **A:** Representative western blots of heart lysate for LC3 protein and β-actin. **B:** Bar graphs summarizing the ratio of LC3 II/β-actin in hearts of rats that received chronic subcutaneous infusion of Ang II or saline with cardiac transfer of Lv-DNp85 or Lv-GFP for four weeks. Data are means ± SE (n = 6 rats). $^{*}P < 0.05$ vs. rats that received Saline + Lv-GFP. $^{\#}P < 0.05$ vs. rats that received Ang II + Lv-GFP.

4.3.8. Effect of blockade of Class I PI3-kinase on Ang II-induced Akt and mTOR phosphorylation

Akt, the alias of protein kinase B, is one of the downstream components of Class I PI3-kinase, and mTOR is one of the downstream effectors of Akt in intracellular signal transduction pathways. Activation of mTOR impairs autophagy, and this signaling transduction pathway is via the cascade of AT1R→Class I PI3-kinase→Akt→mTOR. The cardiac tissue were collected to detect Akt and mTOR phosphorylation using conventional Western Blots with antibodies against phosphorylated Akt or mTOR and total Akt or mTOR. The results are presented in Figure 36 and Figure 37, indicating that 4-week infusion of Ang II significantly increased the ratio of phosphorylation of Akt by 55.26 % and mTOR by 145.16 % (p-Akt/Total Akt: 0.38 ± 0.07 in the in Saline+Lv-GFP group vs. 0.59 ± 0.12 in the Ang II + Lv-GFP group, p-mTOR/Total mTOR of 0.31 ± 0.06 in the Saline + Lv-GFP group vs. 0.76 ± 0.12 in the Ang II+Lv-GFP group, n = 6, $P <$ 0.05 vs. Saline+Lv-GFP), suggesting a chronic stimulatory effect of Ang II on Class I PI3-kinase. Cardiac transduction of Lv-DNp85 successfully attenuated Ang II infusion-induced phosphorylation of Akt by 63.81 % and mTOR by 68.33 % (p-Akt/Total Akt: 0.59 ± 0.12 in the Ang II + Lv-GFP group vs. 0.36 ± 0.06 in the Ang II+Lv-DNp85 group, p-mTOR/Total mTOR: 0.76 ± 0.12 in the Ang II+Lv-GFP group vs. 0.35 ± 0.05 in the Ang II+Lv-DNp85 group, n = 6, P < 0.05 vs. Ang II + Lv-GFP). The results demonstrate that cardiac transduction of Lv-DNp85 attenuates Ang II-induced activation of Class I PI3-kinase. These results demonstrate that Akt and mTOR phosphorylation are involved in the downstream signaling of Class I PI3-kinase in Ang II-induced impairment of autophagy in the heart.

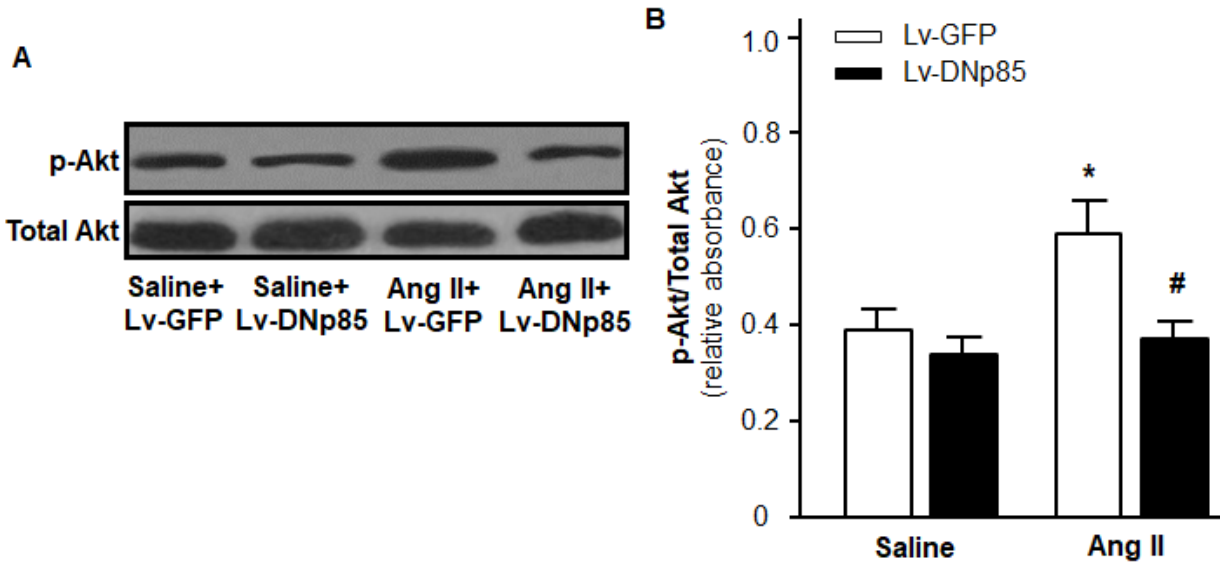

Figure 36: Effect of Ang II and Lv-DNp85 on Akt phosphorylation in adult rat hearts. Akt phosphorylation in heart tissue was examined 4 weeks after subcutaneous infusion of Ang II or normal saline (NS) with cardiac transduction of Lv-DNp85 or Lv-GFP. **A:** Representative western blots of heart lysate probed for phosphorylated Akt (p-Akt) and total Akt in each group of rats. **B:** Bar graphs summarizing the ratio of phosphorylated Akt vs. total Akt. Data are presented as means ± SE (n = 6 rats). $^{*}P < 0.05$ vs. rats that received Lv-GFP. $^{\#}P < 0.05$ vs. rats that received Ang II + Lv-GFP.

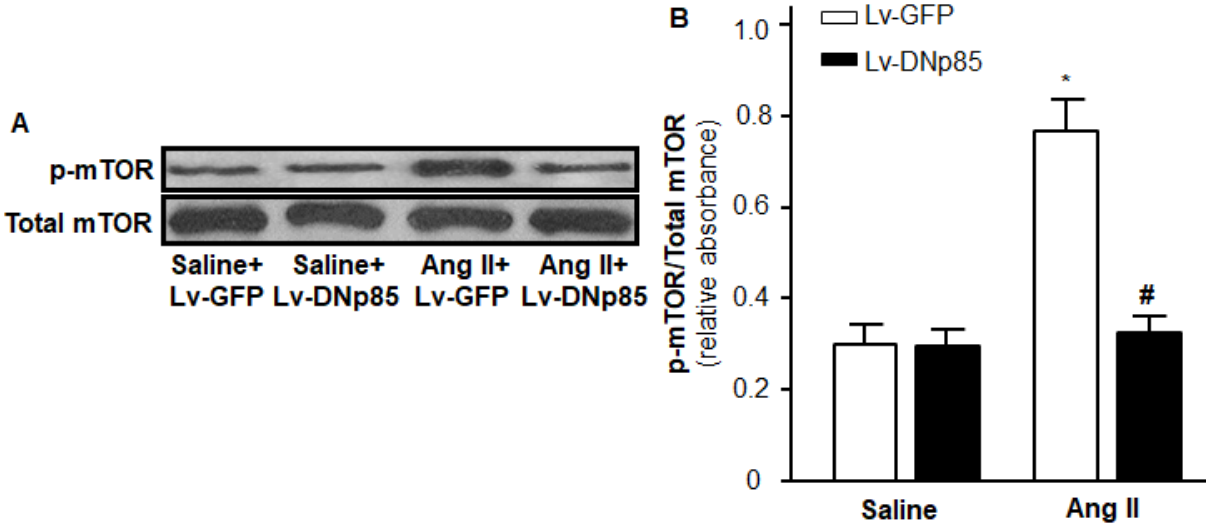

Figure 37: Effect of Ang II and Lv-DNp85 on mTOR phosphorylation in adult rat hearts. mTOR phosphorylation in heart tissue was examined 4 weeks after subcutaneous infusion of Ang II or normal saline (NS) with cardiac transduction of Lv-DNp85 or Lv-GFP. **A:** Representative western blots of heart lysate for phosphorylated mTOR (p-mTOR) and total mTOR. **B:** Bar graphs summarizing the ratio of phosphorylated mTOR vs. Total mTOR. Data are presented as means ± SE (n = 6 rats). $^{*}P < 0.05$ vs. rats that received Lv-GFP. $^{\#}P < 0.05$ vs. rats that received Ang II+Lv-GFP.

4.4. Data summary and conclusion

In this chapter, we examined the role of Class I PI3-kinase in Ang II-induced cardiac remodeling in adult rat hearts. The results verified our initial hypothesis that chronic administration of Ang II caused cardiac remodeling via an autophagic-dependent manner in living animal hearts. This conclusion is supported by those following findings: 1) Chronic subcutaneous infusion of Ang II remarkably elevated the activity of Class I PI3-kinase, generating increasing amount of PIP_3 as the final product. Chronic Ang II administration also enhanced the phosphorylation of Akt and mTOR which are two essential downstream components of Class I PI3-kinase. Activation of mTOR by phosphorylation impaired autophagy and this autophagic impairment exacerbated ROS generation accumulation, perivascular fibrosis, cardiac hypertrophy and contractile dysfunction in adult rat hearts. 2) Lentiviral vectors of Lv-GFP and Lv-DNp85 were successfully delivered into the heart of adult rats via cardiac coronary artery microinjection. Those Ang II-induced pathophysiological alterations in the adult rat hearts were greatly attenuated by blockade of Class I PI3-kinase using cardiac transfer of dominant negative PI3-kinase p85 subunit (Lv-DNp85) while administration of negative control lenti-viral vector of Lv-GFP did not alter Ang II-induced pathophysiological actions.

Lenti-viral vectors are adopted as a novel gene delivery technique. Bioactive viral vectors are mainly divided into two categories: adeno-viral vectors and lenti-viral vectors. The advantage of the adeno-viral vectors is their larger capacity of gene fragments as large as 8k while the lenti-viral vectors have a relatively smaller capacity to accommodate the gene fragments (~2k). Nevertheless, it has been proved that the lenti-viral vectors could be successfully administrated into several non-dividing cell lines like primary and stem cells which are difficult to be transfected by conventional vectors [97]. Thus, we used lenti-viral vector in this part to testify our hypothesis. Dominant negative treatment is a novel and effective method to perform gene therapy. Unlike the

conventional gene knockout or RNA silencing method, the dominant negative mutation treatment conserves the whole intact protein without losing any subunits. However, not only does the mutant protein lose the biological functions itself, but also the mutant protein inhibits or even abolishes the function of adjacent wild type protein subunits, losing the whole function [98]. Known as the adapter protein of Class Ia PI3-kinase, p85α subunit was over-expressed after cardiac transfer of Lv-DNp85. Western blot analysis showed elevated p85 subunit expression in dominant negative lenti-viral vector treatment while other approaches proved the loss of the protein function in signaling transduction. The underlying mechanism is the formation of the protein dimer or polymer which has no signal transduction function, thereafter the function of adjacent wild type protein has also been inhibited. There are reports of marketed dominant negative viral vector forms of DNp85 for Class Ia PI3-kinase [99] and DNVps34p for Class III PI3-kinase [100]. Thus, the usage of lenti-viral vectors could further prove the function of Class I PI3-kinase by disabling the relevant signaling transduction functions of this kinase.

Our initial aim is to make successful delivery of lenti-viral vectors into the cardiomyocytes of living adult rat hearts to exert certain physiological effects since chemical compounds such as LY-294002 and wortmannin neither have the desirable blockade specificity on Class I PI3-kinase nor could be used in a heart-specific manner in chronic *in vivo* studies. Therefore, it is obliged to use lenti-viral vectors in our chronic *in vivo* studies. We performed coronary artery microinjection technique, and four weeks later, the overlap of GFP and α-actin under fluorescence microscope indicates we have successfully delivered lenti-viral vectors. Also, diminished PIP_3 production in heart tissue mean successful delivery of Lv-DNp85 into cardiomyocytes.

The next objective after successful cardiac delivery of lenti-viral vectors is to compare the physiological parameters relevant to Ang II-induced cardiac remodeling. First, we determined blood pressure and heart rate, it is found that the elevation of blood pressure in Ang II group is not

altered by Lv-DNp85 administration, and the heart rate in all four groups remained identical. The plausible explanation is that Ang II constricts the blood vessels, increasing the peripheral resistance, and the blood pressure gets elevated prior to the occurrence of cardiac remodeling. For the steady heart rate in all those four groups, it is possible that the elevated blood pressure might cause the heart to beat slower so as to preserve the total cardiac output, while Ang II could direct stimulate the α_1 receptor in the heart, accelerating the heart rate. Thus, those two contradictory chronotropic factors compensate for each other, keeping the heart rate within a steady value.

Then, we determined the pathophysiological indexes relevant to cardiac remodeling such as cardiomyocyte diameter, HW/BW ratio, perivascular fibrosis and dP/dt Max. We found Lv-DNp85 administration strongly attenuated Ang II-induced cardiac remodeling by ameliorating above-mentioned pathophysiological parameters, suggesting preserved heart function under the presence of Ang II. To determine the possible route of the effect of Lv-DNp85 and Class I PI3-kinase in attenuating cardiac remodeling, we detect the phosphorylation degree of Akt and mTOR, ROS generation and the degree of autophagy since evidence showed that the specific knockout of autophagy related protein (Atg) in the heart provoked cardiac hypertrophy and dysfunction [101]. The results demonstrated that diminished degree of Akt and mTOR phosphorylation, ROS generation and restored autophagy were observed in Ang II+ Lv-DNp85 group when compared with Ang II+ Lv-GFP group, suggesting Ang II-induced cardiac remodeling might be mediated via the Class I PI3-kinase/Akt/mTOR pathway via impairing autophagy.

In summary, all of those results indicate that selective inactivation of Class I PI3-kinase by Lv-DNp85 cardiac transfection in the heart restores autophagy, ameliorates left ventricular contractility which has been deteriorated by Ang II infusion, and alleviates Ang II-induced Akt and mTOR phosphorylation, ROS generation, perivascular fibrosis and cardiac hypertrophy, which are the most ordinary pathophysiological alterations in HF. Those evidences strongly

support the hypothesis that elevated action of Class I PI3-kinase in the heart contributes to the development of Ang II-induced cardiac injury and heart failure via autophagic impairment.

CHAPTER V. OVERALL DISCUSSION

This present study examined the possible involvement of different PI3-kinases in both primary neonatal and living adult cardiomyocytes from SD rats in Ang II-induced cardiac remodeling with both *in vitro* and *in vivo* approaches. Furthermore, the fundamental goal in this ongoing project was to identify the intracellular signaling mechanisms underlying PI3-kinases using various biochemical, molecular biological, pharmacological and morphological techniques. The most notable and prominent discoveries of this study is the involvement of only Class III PI3-kinase activation under lower dosage of Ang II exposure initially, while both Class I and Class III PI3-kinases are activated under higher dosage of Ang II exposure or in a chronic manner, representing different stages of compensatory and decompensatory cardiac hypertrophy. The results demonstrate that both Class I and Class III PI3-kinases are involved at different stages in Ang II-induced cardiac remodeling via an autophagic-dependent mechanism, and impaired autophagy results in the loss of capability to scavenge the damaged mitochondria accumulation-induced ROS generation, contributing to the emergence and progression of cardiac remodeling and subsequent heart dysfunction.

5.1. Intracellular mechanisms for the heart switching from compensation to decompensation

Intense exercise was accompanied with enhanced aldosterone, renin, K^+, and vasopressin in plasma. Among those factors, Renin-Angiotensin System is an essential hormonal pathway for cellular growth via mechanical stretch in cardiomyocytes. There are two major separate sources of RAS that produce Ang II: one source is the systemic RAS converting hepatocyte-generated angiotensinogen to Ang I by kidney-released renin, while the other source is local RAS which responds to local stimuli and produces Ang II in an autocrine or paracrine manner [65]. The normal Ang II concentration in plasma ranges from 0.4 to 0.8 nM, and exercise training-produced Ang II concentration is very tiny (within nanomolar scale) [102]. During exercise training-induced

hemodynamic overload, physiological cardiac hypertrophy in the left ventricle occurs in a compensatory mechanism without perivascular fibrosis or apoptosis as an effective approach to adapt to this hemodynamic overload by elongation of cardiomyocytes in a parallel manner, enhancing the ventricular stroke volume and stimulating cardiac output with ameliorated aerobic capacity [13, 103]. Thus, exercise training is a safe and a most effective non-pharmacological therapeutic approach to combat cardiac remodeling, cardiac apoptosis, and perivascular fibrosis with normal heart structure, preserved or ameliorated heart function, and very tiny alterations of gene expression pattern in cardiomyocytes [104]. Generally speaking, aerobic exercise dilates the peripheral vessels to maintain more blood flow in the skeletal muscles. In this process, the renal blood pressure become lowered due to the rise of peripheral blood flow, resulting in the rise of circulating renin level soon after acute exercise. Meanwhile, lactic acid produced in skeletal muscle begins to accumulate and suppress angiotensinases that degrade Ang I and II, leading to vasoconstriction and cardiac hypertrophy [105] .

Exercise-induced cardiac hypertrophy are divided into two categories: concentric and eccentric hypertrophy. Concentric hypertrophy refers to the addition of cardiac sarcomeres in a parallel manner (myocyte width increase), and it is the result of static or isometric physical exercise like weight lifting with little or no movement. Nevertheless, isotonic and aerobic exercises such as swimming and running lead to eccentric hypertrophy which means the cardiac sarcomeres are added in a series pattern with the increased chamber volume (myocyte length increase), and the cardiac output are increased with elevated skeletal muscle effectiveness and decreased peripheral vascular resistance [103, 106]. Both types of exercise-induced cardiac hypertrophy are losartan preventable, suggesting the participation of AT1R [107]. It is found swimming training starting from very young age successfully prevented hypertension in spontaneous hypertensive rats (SHR) even though they are genetically programmed to develop elevated blood pressure level with

decreased plasma Ang II concentration, which is similar to the treatment of ACE inhibitors like captopril, or AT1R antagonists like losartan [108]. In this process, local Renin-Angiotensin System is activated mainly due to hemodynamic overload with elevated circulating Ang II levels, while slight elevation of local cardiac Ang II is not a direct factor that is associated with cardiac hypertrophy [109]. Under physiological conditions in the health body, rapid internalization and desensitization of Ang II receptor type 1 (AT1R) were observed in the heart in spite of the rising dosage of cardiac Ang II level to avoid pathological cardiac hypertrophy. It is also postulated AT1R might enlarge the cornary artery to maintain the cardiac blood flow [110], serving as a protective mechanism to protect heart from pathological cardiac hypertrophy. Swimming training-induced physiological hypertrophy in Wistar rats didn't show significant manifestations of pathological cardiac markers. Simultaneously, enhanced ACE2 and Ang (1-7) levels as well as decreased ACE and Ang II amounts were observed in such aerobic exercise training [111]. Thus, exercise training might have the preferential ACE2/Ang (1-7)/MAS Receptor axis over general RAS (ACE/Ang II/AT1R) axis. Ang (1-7) is generated from Ang II via ACE2 cleavage, and it is a potent vasodilator with anti-hypertrophic and anti-fibrotic effects to lower down the blood pressure and prevent the heart from cardiac hypertrophy. Our lab has already proved the cardiac protective role of Ang (1-7) both in cardiomyocytes and adult rat hearts [79, 112]. It is also reported that aerobic exercise decreased Ang II levels and increased AT2R expression in the normal heart. Convincing evidence indicates the physiological effects of AT2R are vasodilation due to the stimulation of NO and bradykinin release [113], which just counteracts AT1R as a powerful vasopressor and aldosterone secretion stimulator. Thus, regulation of the activities of AT2R expression and Ang (1-7) production within the RAS is an important method to keep cardiovascular homeostasis. Recently, microRNAs such as miR-195, miR-21, miR-133 and miR-

1 are also discovered to have contribution to regulate physiological cardiac hypertrophy through varied signaling pathways, which is a novel field worth further investigation [107].

Unlike exercise-induced physiological cardiac hypertrophy, pathological cardiac hypertrophy means the enlargement of the heart accompanied with preexisting morbid states such as heart attack, hypertension, cardiomyopathy, diabetes and unhealthy living habits. The most distinctive consequence of pathological cardiac hypertrophy is cardiac remodeling, including unbalances of extracellular matrix homeostasis, perivascular fibrosis, autophagic defect, mitochondrial dysfunction, abnormal metabolism, impaired ATP generation and gene expression modifications [114]. Cardiac remodeling makes the cardiomyocytes stiffen and reduce the elasticity and the ability to efficiently pump blood of the heart, resulting in contractile dysfunction, ventricular dilation, and heart failure [115]. Heart failure at the initial stage is compensatory since cardiomyocytes are able to beat faster and squeeze harder to compensate for both stroke volume and heart rate to restore the loss of blood supply. However, chronic hemodynamic overload with more demand of oxygen lets the cardiomyocytes die off, causing worsening heart failure with a vicious cycle, and this stage of heart failure is decompensatory [116]. During this vicious cycle, Ang II is continuously released and reaches a relatively higher level in both plasma and heart, resulting in severer symptoms of heart failure. The major difference between compensatory and decompensatory cardiac hypertrophy is that the former has no significant heart failure symptoms. However, as time goes by, the benefits of the initial compensatory cardiac hypertrophy progress into decompensatory stage, suggesting the process of cardiac remodeling either lose the effectiveness in a concerted manner or reaches the threshold that is detrimental to normal heart function [117].

The intracellular mechanisms in decompensatory cardiac hypertrophy are quite complex and intertwined besides those involved in compensatory cardiac hypertrophy. Generally speaking,

the initiation of the signaling usually occurs at the cellular membrane, and the ligand could be catecholamines, ET-1, Ang II and IGF-I, interacting with G-protein-coupled receptors (GPCR) and generates DAG and PIP_3. Meanwhile, receptors of tyrosine kinase or with Ser/Thr domains are also regarded as mediators. Internal stretch-sensitive receptors are activated when hemodynamic overload is encountered. Essential mediators of cardiac hypertrophy could stem from cytoplasmic signaling pathways such as ERK/MAPK, calcineurin-NFAT and IGF-I/PI3K/Akt/mTOR, nuclear transcription factors such as CDK7 and CDK9, or from HDACs shuttling regulated by kinase [13]. Finally, those receptors converge on a limited number of intercellular signal-transduction circuits and regulate cardiac growth via gene expression change, accelerating the translation & synthesis rate and decelerating the degradation speed of cytoplasmic protein. Those above-mentioned components are discovered in physiological cardiac hypertrophy with an adaptive manner. However, excessive extracellular stimuli like Ang II, TNF-α and catecholamines are associated with c-Jun, N-terminal kinase and p38 as essential upstream activators to induce fibrosis and apoptosis in cardiomyocytes which are only present during exercise-induced pathological hypertrophy [118]. Of note, mitochondria plays a crucial role in Ang II-induced decompensatory cardiac hypertrophy and heart failure: in physiological hypertrophy, mitochondrial biogenesis is enhanced with mitochondrial oxidative capacity, facilitating oxygen consumption, ATP generation and antioxidant defense. However, in pathological cardiac hypertrophy and decompensatory heart failure, disturbance of signaling pathways occur and lead to mitochondrial dysfunction with decreased mitochondrial biogenesis, oxidative capacity, and mitochondrial DNA transcription, resulting in impaired oxygen consumption, ATP generation, antioxidant defense and mitochondrial biogenesis, along with elevated fatty acid uptake and lipotoxicity [119]. In this process, constitutive activation of Akt

might suppress normal mitochondrial function and induce ROS accumulation due to excessive oxidative stress although Akt activation is present in physiological cardiac hypertrophy [120].

5.2. Role of Ang II in cardiac remodeling

Cardiac remodeling, including cardiac hypertrophy, perivascular fibrosis, apoptosis and changes in metabolism, is the direct source of heart failure. Ang II is one of those major effector hormones in renin-angiotensin-aldosterone-system (RAAS), interacting with various AT receptors in both central and peripheral cardio-regulatory regions. As a peptide product of RAAS, Ang II plays a crucial role in cardiovascular physiology and pathology and causes pressor effect via vasoconstriction, resulting in deleterious sequelae like cardiac and vascular hypertrophy or renal dysfunction. Nevertheless, we cannot easily distinguish the mechanisms of Ang II in cardiac hypertrophy. In general, this peptide elevates the overall cardiac workload by its vascular-constricting effect, and cardiac hypertrophy is secondary to cardiac hemodynamic overload. However, recently researchers found that Ang II also directly stimulates the growth of cardiomyocytes including the acceleration of transmission speed of sympathetic nerves, enhancement of cardiac contractility, and initiation of cardiac structural remodeling [19]. This viewpoint was verified through investigation of heart explants in heart failure patients [121]. Thus, a shortcoming in the determination of *in vivo* effects of Ang II is that this peptide exerts both growth-promoting effects to the cardiomyocytes and generalized elevations in hemodynamic workload. So it's obliged for us to figure out the possible intracellular mechanisms of cardiac remodeling induced by direct Ang II exposure.

In this project, we have overcome this shortcoming through two approaches: 1. We adopted primary cardiomyocytes culture in our *in vitro* experiment. The physiological parameters such as blood pressure, heart rate and cardiac contractility are totally absent, facilitating the investigation of direct effect of Ang II on cardiomyocytes without any generalized influence. 2. We used

selective inactivation of Class I PI3-kinase in the heart by cardiac transfer of Lv-DNp85. The application of Lv-DNp85 together with subcutaneous Ang II infusion did not attenuate the blood pressure elevation, enabling us to rule out the peripheral impacts of Ang II on cardiac remodeling since hemodynamic workload in both Ang II + Lv-DNp85 group and Ang II + Lv-GFP group remain comparable. Thus, the general systemic effect of Ang II chronic administration as hemodynamic overload still exists, meanwhile, the circulating Ang II level remains stable. Thus, our approach first manifests the *in vivo* targeting of Ang II as a biological active peptide in a heart-specific manner, and distinguishes the impact of Ang II on the heart between local (direct) and systemic (indirect). Therefore, congestive heart failure rat models were successfully established by using chronic subcutaneous Ang II infusion for four weeks. Cardiac function was determined by cannulation of cardiac catheter inserted through the left carotid artery. Results indicated the heart weight and body weight ratio was significantly elevated in Ang II vs. Saline rats in Lv-GFP group, suggesting the occurrence of cardiac hypertrophy. It is also observed dP/dt Max were dramatically diminished in Ang II+ Lv-GFP rats when compared with Saline+ Lv-GFP rats, indicating chronic infusion of Ang II induces severe left ventricular dysfunction which has a positive relationship with cardiac hypertrophy as one of those forms of cardiac remodeling.

The normal physiological concentration of plasma Ang II in mammals is about 0.5 nM, while in the pathological states such as heart failure, stroke and myocardial infarction, the scale of plasma Ang II concentration elevation would be up to ~200 fold [102, 118]. This process might take place in a chronical manner within several months or even years. To shorten the study duration and eliminate the internal physiological modulation that exists in the *in vivo* experiments, primary culture of cardiomyocytes were adopted and 24-hour Ang II treatment with different concentrations with a ten-fold gradient was carried out. These *in vitro* experiments show quick outcomes and give us a reliable vision of the dose-dependent effect of Ang II. Our dose-dependent

effect of 24-hour treatment of Ang II caused significant elevations of ROS generation and cardiac hypertrophy in cultured cardiomyocytes when the concentration of Ang II was above 10^{-7} M, and cardiomyocytes began to die with abnormal and deformed nuclei above this Ang II concentration (data not shown). Therefore, 10^{-7} M Ang II is regarded as the watershed of the higher and lower Ang II concentration in our *in vitro* experiments. Lower concentration of Ang II such as 10^{-8} M didn't present significant ROS generation and cardiac hypertrophy in primary cardiomyocytes, while higher concentration of Ang II such as 10^{-6} M prominently caused notable ROS generation and cardiac hypertrophy.

It is universally recognized that ROS generation plays an essential role in Ang II-induced cardiac remodeling. To confirm the possible involvement of elevated ROS generation in Ang II-induced cardiac remodeling, we performed both *in vitro* and *in vivo* experiments. After treatment of primary cardiomyocytes for 24 hours or adult rats for 4 weeks with Ang II, relevant pathophysiological parameters were measured to prove the effect of Ang II on cardiac remodeling. Our morphological analysis of both primary cardiomyocytes and adult rat heart slices confirmed cellular size enlargement after chronic Ang II exposure. In addition, we noticed elevated ROS generation along with enhanced degree of cardiac remodeling in both *in vitro* and *in vivo* experiments, suggesting elevated ROS generation as one of those intracellular mechanisms might contribute to cardiac remodeling.

It is universally accepted that Ang II-stimulated ROS generation majorly stems from activation of NADPH oxidase by phosphorylation via MAPK or PI3-kinase. Nevertheless, our lab has recently identified that both protection of mitochondria from injury and scavenging excessive ROS generation derived from damaged mitochondria are two effective ways to alleviate Ang II-induced cardiac remodeling [79]. Other report also excludes the involvement of NADPH oxidase in Ang II-induced ROS generation since elimination of gp91phox, an essential part inside NADPH

oxidase, did not efficiently prevent hypertension and cardiac hypertrophy in transgenic mice overexpressing active renin [72]. Thus, damaged mitochondria accumulation is proposed as another source of ROS generation in cardiomyocytes, and this hypothesis is supported as the mitochondrial ROS scavenger Mito-TEMPO remarkably attenuated Ang II-induced ROS generation and cardiac hypertrophy. Those pieces of evidence prove ROS generation derived from damaged mitochondria is the major source in chronic Ang II-induced cardiac remodeling. Despite the viewpoint that mitochondria-derived ROS generation come mainly from mitochondrial respiratory chain, we cannot completely rule out the potential contribution of ROS generation from other cytosolic sources like xanthine oxidase (XO) and NADPH oxidase (NOX).

5.3. Autophagic alterations in Ang II-induced cardiac remodeling

From the previous information, we found that Ang II-induced ROS generation in cardiomyocytes mainly comes from the accumulation of damaged mitochondria, and elimination of the ROS generation by mito-TEMPO as a mitochondria-derived ROS scavenger almost abolished the Ang II-induced ROS generation in primary cardiomyocytes. Mitochondria serve as both sources and attacking targets for ROS. Once the damaged mitochondria get accumulated and failed to be efficiently degraded, a vicious cycle takes place: the ROS generation from damaged mitochondria further do harm to healthy mitochondria, producing aggravated ROS generation as a positive feedback cascade. Gradually, the whole heart tissue are affected and continuous enhancement of ROS generation eventually causes cardiac remodeling.

To combat the accumulation of the damaged mitochondria and maintain cellular hemostasis, there should be at least one intracellular mechanism to wipe out those damaged mitochondria. Thus, autophagy has just come into our mind. Autophagy, known as the process of as self-digestion, refers to the intracellular recycling and degrading aged and damaged organelles and proteins to keep a homeostatic intracellular environment. Abnormal regulation of autophagy

in cardiovascular system results in various heart diseases. Thus, our subsequent focus is to study the alteration of autophagy in Ang II-induced cardiac remodeling in both *in vitro* and *in vivo* models. We detected autophagy in cardiomyocytes in our *in vitro* experiments with immunocytochemistry in primary cardiomyocytes and in our *in vivo* experiments with western blot in adult rat heart tissues.

In our *in vitro* study of Ang II-induced autophagy in cardiomyocytes, the initial phase of autophagic elevation (beginning from 10^{-9} M and peaking at 10^{-7} M Ang II) represents the compensatory stage of cardiac hypertrophy, where enhanced autophagy enables the degradation of redundant proteins; while the subsequent phase of autophagic impairment under higher Ang II dosage (exceeding 10^{-7} M and reached nadir at 10^{-5} M Ang II) represents the decompensatory stage of cardiac hypertrophy, where excessive protein synthesis occur due to higher dosage of Ang II stimulation and insufficient autophagy, leading to heart failure. This initial rising and subsequent falling degree of autophagy under different concentration of Ang II exposure was also reported in the HL-1 cardiomyocyte cell lines. Unfavorable condition such as hypoxia in HL-1 cardiomyocyte cell lines also showed the same autophagic alteration trend at different hypoxia durations [78]. The plausible explanation of this event is that primary cardiomyocytes swift from initial compensatory state under lower dosage of Ang II to the final decompensatory state under lower dosage of Ang II. The cardiomyocytes respond very early after exposure to tissue injury mediators, while continuous hazardous stimuli may make the primary cardiomyocyte exhaust their endogenous defense, and the continuous ROS generation simulates the protein synthesis and cellular damage, eventually manifesting cardiac hypertrophy. It's also observed that 10^{-5} M Ang II-induced autophagy is still higher than the basal level, and the plausible explanation may be that the injury caused by autophagy from cellular level extends to subsequent tissue damage [78].

Although similar autophagic degree was observed between 10^{-5} M & 10^{-9} M Ang II or between 10^{-6} M & 10^{-8} M Ang II in our *in vitro* results in cardiomyocytes, the amount of Ang II-induced accumulation of damaged mitochondria (degree of ROS generation) and the speed of Ang II-induced protein synthesis (degree of cardiac hypertrophy) in cardiomyocytes are totally different between those higher and lower Ang II concentrations (higher Ang II concentration causes elevated accumulation of damaged mitochondria and accelerates the speed of protein synthesis). Therefore, it's prudent to conclude a shift of the cardiomyocytes from compensation to decompensation when the concentration of Ang II is above 10^{-7} M according to the dose-dependent result of Ang II on ROS generation and cardiac hypertrophy in cardiomyocytes (data not shown). 10^{-8} M Ang II exposure is an example of compensation heart since no significant ROS generation and cardiac hypertrophy happen in this Ang II concentration, while 10^{-6} M Ang II is an example of decompensation heart for significant ROS generation and cardiac hypertrophy take place.

Nowadays, ROS generation are considered not only as one of potential toxic origins under various hazardous stimulations, but also as constituent components of signaling transduction pathways at physiological levels. Thus, it is believed excessive intracellular ROS might activate autophagy, and scavenging of the ROS in cardiomyocytes by antioxidants reduces overt toxicity as well as inhibit autophagy induced by chronic Ang II exposure. From our results, we observed the usage of mito-TEMPO (mitochondria-derived ROS scavenger) almost abolished autophagic increment. Furthermore, Ang II-induced ROS generation and cardiac hypertrophy were alleviated by mito-TEMPO in cardiomyocytes. All those factors prove that ROS generation from damaged mitochondria is the major source in Ang II-induced cardiac remodeling.

To further consolidate the role of autophagy in Ang II-induced cardiac remodeling, autophagic blockers of Bafilomycin A1 (Baf A1) or Chloroquine Phosphate (CQ) can be used in primary cardiomyocytes to directly block Ang II-induced autophagy. Baf A1 inhibits the fusion of

autophagosome with lysosome, obstructing the formation of autolysosome as the final step of autophagy [122]. The alkaline characteristic of CQ enables the neutralization of the acidic environment in the lysosomes and autolysosomes [123]. We then assume combined usage of autophagic inhibitors with Ang II would exacerbate Ang II-induced ROS generation and cardiac hypertrophy, suggesting impaired autophagy contributes to the cardiac remodeling under hazardous stimuli.

As for the *in vivo* experiments, we also determined autophagic alterations in the heart tissue after chronic Ang II subcutaneous infusion. Autophagic impairment was observed as decreased LC3-II/LC3-I ratio in Ang II+ Lv-GFP group when compared with Saline+ Lv-GFP group by means of western blot technique. Interpretations of the discrepancy between *in vitro* and *in vivo* studies are not definitely elucidated, but may be due to the different test sample origins as neonatal primary cardiomyocytes and adult rat heart tissues. Also, distinct PI3-kinases may be involved at different stages of Ang II-induced cardiac remodeling, and the duration of Ang II administration is also different in our *in vitro* neonatal primary cardiomyocytes (24 hours) and *in vivo* adult rat heart tissues (4 weeks) experiments. Taken together with our *in vitro* and *in vivo* results of autophagic alteration, we conclude that autophagy is enhanced in the initial exposure or lower dosage of Ang II, while prolonged exposure or higher dosage of Ang II causes autophagic impairment. Autophagic impairment severely aggravate cardiac conditions of pressure overload or ischemia-reperfusion, and targeting at the intracellular signaling pathways of Ang II-induced autophagic impairment in the heart might be an effective approach to protect heart from stress-induced damage.

5.4. PI3-kinases-dependent autophagic alterations in Ang II-induced cardiac remodeling

After determination and interpretation of Ang II-induced autophagic alteration, our next aim is to find out the underlying intracellular mechanisms that cause such autophagic alterations

in cardiomyocytes. Judging by the information illustrated above, one of those effective approaches to keep cardiomyocytes from Ang II-induced cardiac remodeling is mitochondria protection via scavenging ROS generation by enhancing mitophagy. This is a novel strategy to relief cardiac hypertrophy and relevant secondary pathological complications. In our *in vitro* study, we noticed the degree of autophagy in primary cardiomyocytes has a dose-dependent relationship with Ang II concentration. Previous studies showed the role of PI3-kinases in the enhanced chronotropic effect of Ang II in neurons [81] and targeted overexpression of Class I PI3-kinase resulted in cardiac hypertrophy in transgenic mice [62], so we hypothesize PI3-kinases might be responsible for Ang II-induced autophagic alterations in cardiomyocytes.

One of those intracellular downstream components of PI3-kinases Class I that might be activated by membrane-translocated PIP_3 formation is Protein kinase B (Akt) [124]. Akt has a central serine/threonine (Ser/Thr) catalytic domain with three isoforms as AKT1, AKT2 and AKT3 which could be stimulated by PIP_3-induced phosphorylation via conformational alterations [125]. Once phosphorylation and activation of Akt are completed, several downstream components such as GLUT (glucose transporter), GSK (glycogen synthase kinase)-3, FOXOs (the forkhead family of transcription factors) and mTOR (mammalian target of rapamycin) [126] are further activated. Among those downstream components activated by Akt, mTOR is the most worthwhile to be further elucidated. It is known mTOR is one of the direct downstream targets of Akt, and plays essential roles in cellular growth and proliferation by supervising whether nutrients are available or enough, the cell is in an environment of appropriate energy and oxygen levels in case, and whether mitogenic signals are present [127]. For mTOR, it is a 289kDa kinase with two discrete complexes named as mTORC1 (mTOR catalytic subunit, Raptor, PRAS40, and mLST8/GbL) and mTORC2 (mTOR, Rictor, mSIN1, and mLST8/GbL) [128], and this kinase has an evolutionary-conserved Ser/Thr which could be activated by multiple factors. Activation of mTOR prevents

autophagy, and rapamycin, a specific inhibitor of mTOR, is a strong autophagic inducer [129]. mTOR is a sensitive biomolecular sensor and it regulates biogenesis based on the amount of available nutrients through activation of p70S6K by enhancing mRNA translation with 5'-polypyrimidine tracts and suppressing the translational repressor of mRNAs with a 5'-cap named 4E-BP1 [130].

We sought to investigate the possible involvement of PI3-kinases in Ang II-induced cardiac remodeling via autophagic-dependent mechanisms. By measuring PIP_3 and PIP production as the respective final product of Class I and Class III PI3-kinase, we identified Ang II administration caused stronger activities of Class I and Class III PI3-kinases in primary cardiomyocytes. As for our *in vivo* study, it is also found that four weeks' chronic Ang II administration caused hyper-activity in Class I PI3-kinase, resulting in elevated PIP_3 production as the final product. Results also indicated the activity of Class III PI3-kinase reached the plateau at lower Ang II concentration (10^{-7} M) than that of Class I PI3-kinase (10^{-5} M Ang II), suggesting the Class III PI3-kinase is earlier saturated in the dosage-activity response than Class I PI3-kinase via Ang II stimulation.

As mentioned before, only Class I and Class III PI3-kinases are expressed in the heart [131] and activation of those two PI3-kinases presents contradictory effects on autophagy: activation of Class I PI3-kinase pathway with major components of Class I PI3-kinase→Akt →mTOR→GSK→S6K→FOXO3 suppresses autophagy [132], while Class III PI3-kinase pathway activation with the relevant components of PI3-K Class III→Beclin-I→Vps34 facilitates autophagy [88]. Under Ang II stimulation, autophagy initially increased and reached its peak under 10^{-7} M Ang II, suggesting the major activation of Class III PI3-kinase. However, exposure of higher concentration of Ang II diminished autophagy and autophagy achieved the nadir at 10^{-5} M Ang II, suggesting the subsequent activation of Class I PI3-kinase and the saturated activation of Class III PI3-kinase. Those results correspond with the trend of autophagic result in HL-1

cardiomyocyte cell line under 24 hours of Ang II exposure with varied concentrations [78] and support our initial hypothesis that under lower concentrations of Ang II exposure, only Class III PI3-kinase is activated and autophagy is enhanced, while under higher concentration of Ang II exposure, both Class I and Class III PI3-kinase are activated, resulting in impaired autophagy. Thus, we have enough confidence to draw the conclusion that Class I and Class III PI3-kinases are both involved in autophagic regulatory, while small amount stimulation of harmful simulations like Ang II, lectin, hypoxia, and carbon monoxide might be beneficial to initiate tissue protective mechanisms [133]. From our results, we knew that both Class III and Class I PI3-kinases in cardiomyocytes were significantly activated by 10^{-6} M Ang II. Furthermore, most of the cardiomyocytes still remain alive at this 10^{-6} M Ang II concentration while large quantities of cardiomyocytes began to die out under 10^{-5} M Ang II exposure. Therefore, 10^{-6} M Ang II is chosen in our subsequent *in vitro* experiments since it mimics the decompensatory heart while this Ang II concentration still keeps the majority of cultured cardiomyocytes alive. Furthermore, we don't need to detect the presence of Class I and Class III PI3-kinases additionally in cardiomyocytes by means of immunohistochemistry or polymerase chain reaction (PCR) since they are ubiquitously present in almost every type of eukaryotic cells.

To further confirm the involvement of Class I and Class III PI3-kinases in Ang II-induced autophagic alteration in cardiomyocytes under 10^{-6} M Ang II exposure, we used certain approaches to inhibit those two kinases respectively or jointly. Akt and mTOR are two consecutive downstream signaling kinases in Class I PI3-kinase mediated signaling pathways in the physiological system. Protein abundance determination by western blot indicated treatment of Ang II significantly increased the ratio of p-Akt/total Akt and p-mTOR/total mTOR, suggesting the activation of Akt and mTOR by phosphorylation under Ang II. Combined usage of Ang II with LY-294002, an inhibitor Class I PI3-kinase *in vitro*, or with Lv-DNp85, a lenti-viral vector to

inhibit the Class I PI3-kinase *in vivo* resulted in considerable decrease in Ang II-induced PIP_3 production as well as p-Akt/total Akt and p-mTOR/total mTOR ratio, suggesting blockade of Class I PI3-kinase attenuated the effect of Ang II-induced autophagic impairment via inhibiting phosphorylation of Akt and mTOR, two essential downstream components of Class I PI3-kinase. Then we found pretreatment of 1 μM LY-294,002 under 10^{-6} M Ang II exposure elevated autophagy, attenuated ROS generation, and cardiac hypertrophy, so we are able to draw the conclusion that the activation of Class I PI3-kinase stimulates the mTOR component and reduces autophagy [135]. For the *in vivo* study, we used cardiac transfer of Lv-DNp85 protein to inactivate the Class I PI3-kinase, and similar results were observed as restored autophagy, attenuated ROS generation, cardiac hypertrophy and fibrosis as well as ameliorated cardiac functions in Ang II+Lv-DNp85 group when compared with Ang II+ Lv-GFP group.

When it comes to the possible cross-inhibition effect of LY-294002 on Class III PI3-kinase and 3-MA on Class I PI3-kinase, preliminary experiments of the dose-dependent effect of those two reagents on Class I and Class III PI3-kinases were carried out to seek their appropriate concentrations as to minimize their cross-inhibition effect. The IC_{50} value of LY-294002 on Class I and Class III PI3-kinase is 0.51 μM and over 50 μM respectively [135]. Meanwhile, the IC_{50} value of 3-MA on Class I and Class III PI3-kinase is 0.76 μM and over 100 μM respectively [64]. Therefore, the concentration of 1 μM LY-294002 or 3-MA was chosen to inhibit Class I and Class III PI3-kinase activity with a minimal interreference of inhibition to each other. In our preliminary results, the effects of cross-inhibition of 1 μM LY-294002 on Ang II-induced Class III PI3-kinase by measuring PIP production and 1 μM 3-MA on Ang II-induced Class I PI3-kinase by measuring PIP_3 production are both less than 10 % (data not shown), indicating sufficient targeting specificity of LY-294002 on Class I PI3-kinase activity and 3-MA on Class III PI3-kinase activity at 1 μM concentration.

Moreover, straight inhibition of mTOR by rapamycin as an autophagic inducer showed remarkable attenuation of Ang II-induced ROS generation and cardiac hypertrophy in our *in vitro* study. Thus, we validated that Ang II-induced cardiac remodeling is mediated by Class I PI3-kinase/Akt/mTOR signaling transduction pathway. Subsequent usage of different angiotensin II antagonists further verified this activation of Class I PI3-kinase-Akt-mTOR signaling transduction pathway is mediated through AT1R on the surface membrane of cardiomyocytes.

On the other hand, Vps34 complex is essential for the autophagosomes formation due to its facilitation of the pre-autophagosomal structure establishment by recruiting autophagy-related (Atg) protein [136] and 3-MA, a blocker of Vps34 component in the Class III PI3-kinase pathway [137], reduces the degree of autophagy. The result that pretreatment of 1 μM 3-MA in cardiomyocytes under 10^{-6} M Ang II exposure diminished autophagy, exacerbated ROS generation, elevated cardiac hypertrophy further proves our hypothesis that activation of Class III PI3-kinase pathway facilitates the occurrence of autophagy under both lower and higher concentration of Ang II exposure.

CHAPTER VI. CONCLUSION AND FUTURE DIRECTIONS

6.1. Overall conclusions

In the present study, we determined the effects of Ang II and its impact on the Class I and Class III PI3-kinases and further elucidated the signaling mechanisms underlying those actions of Ang II-induced cardiac remodeling using *in vitro* and *in vivo* SD rat models. The overall conclusions from the *in vivo* and *in vitro* studies are summarized as Figure 38:

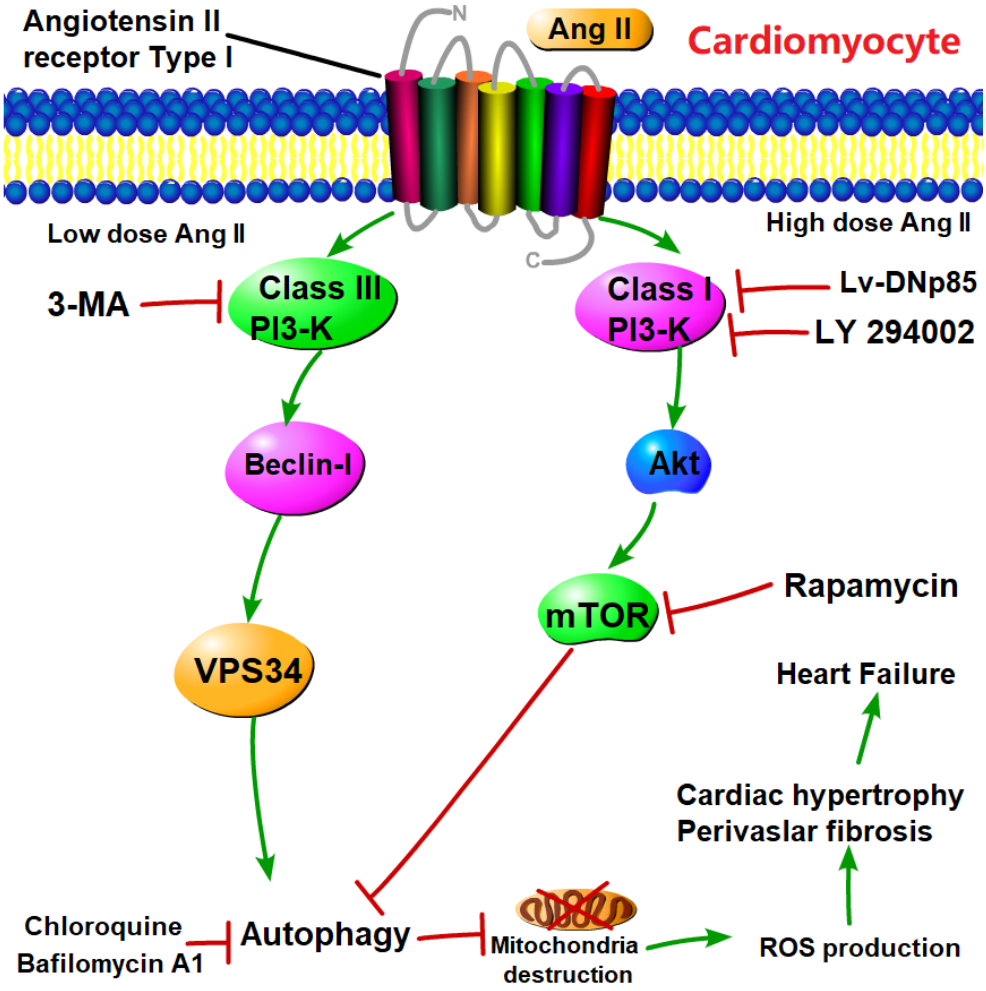

Figure 38: Diagram summarizing proposed Ang II-induced PI3-kinase-dependent pathways activation in cardiomyocytes.

Taken together, all results indicate that both Class I and Class III PI3-kinases play essential roles in Ang II-induced cardiac remodeling. Activation of Class III PI3-kinase under lower dosage

of Ang II facilitates autophagy, representing the compensatory period of cardiac hypertrophy. Nevertheless, when the dosage of Ang II goes higher and the exposure duration is longer, Class I PI3-kinase is activated and the downstream component of Akt and mTOR are stimulated. Stimulation of mTOR inhibits autophagy, causes accumulation of damaged mitochondria and generates higher level of ROS. The enhanced ROS generation triggers several intracellular kinases and transcription factors, promoting protein synthesis and cardiac remodeling, which represents the decompensatory period of cardiac remodeling.

6.1.1. *In vitro* studies on primary cardiomyocytes of neonatal SD rats

1. Lower dosage Ang II increases autophagy while higher dosage Ang II decreases autophagy with two distinctive phases, while the degree of autophagy at the highest Ang II concentration of 10^{-5} M is still higher than basal level of autophagy.

2. Ang II stimulation activates Class III PI3-kinase at lower dosage, and there is a shit activation of PI3-kinases from Class III to Class I at higher dosage Ang II. Smaller Ang II concentration saturates Class III PI3-kinase than that of Class I PI3-kinase. Detection of phosphorylation of Akt as the downstream component of Class I PI3-kinase by measuring p-Akt/total Akt ratio also verifies dose-dependent relationship between Ang II and Class I PI3-kinase.

3. Pretreatment of LY-294002 to inhibit Class I PI3-kinase greatly restores Ang II-induced autophagic impairment, and attenuates Ang II-induced Class I PI3-kinase activation, ROS generation, cardiac hypertrophy.

4. Inhibition Class III PI3-kinase by pretreatment of 3-MA remarkably impairs Ang II-induced autophagy and Class III PI3-kinase activity, and exacerbates Ang II-induced ROS generation and cardiac hypertrophy.

5. Pretreatment of AT1R antagonist Losartan greatly diminishes Ang II-induced elevation of Class I & Class III PI3-kinase activities, autophagy, ROS generation and cardiac hypertrophy, while AT2R antagonist PD123319 does not show such effects.

6. Pretreatment of mito-TEMPO as a mitochondrial-derived ROS scavenger considerably attenuates Ang II-induced autophagy, ROS generation and cardiac hypertrophy.

7. Pretreatment of mTOR inhibitor of rapamycin as an autophagic inducer considerably attenuates Ang II-induced ROS generation and cardiac hypertrophy.

6.1.2. *In vivo* study on adult SD rat hearts

1. Lv-GFP is successfully delivered into the adult rat hearts as immunofluorescence show the overlap of GFP protein and α-actin.

2. Cardiac transfer of Lv-DNp85 is successful, and this transfer greatly attenuates Ang II-induced Class I PI3-kinase activity, ROS generation, cardiac hypertrophy, perivascular fibrosis and remarkably ameliorates Ang II-induced cardiac dysfunction in spite of the presence of Ang II-induced hypertension.

3. Cardiac delivery of Lv-DNp85 remarkably diminishes Ang II-induced increment of p-Akt/total Akt and p-mTOR/total mTOR ratio, and considerably restores Ang II-induced autophagic impairment.

To summarize, all results indicate that PI3-kinases play a crucial role in the progression of Ang II-induced cardiac remodeling. Activation of distinct types of PI3-kinases might be involved depending on the concentration and duration of Ang II exposure, leading to the shift of cardiac hypertrophy from compensatory stage to decompensatory stage, resulting in congestive heart failure.

6.2. Future research directions

These studies were primarily based on the use of pharmacological reagents to regulate the activity of PI3-kinases and their relevant downstream effectors via an autophagic-dependent mechanism, and we ought to be very prudent in data interpretation. In our *in vivo* study, we used Lv-DNp85 to inactivate Class I PI3-kinase, but due to the huge expense and limited time span of lenti-viral vector construction, we haven't conducted Class III PI3-kinase inactivation in adult rat hearts. Thus, it would be more perfect to perform another cardiac transfer of Lv-DNVps34 to block the Class III PI3-kinase in the rat heart since this viral vector has already been delivered into neuroblastoma cells [100]. Also, cardiac transfer of Lv-Vps34 might also be used to exogenously activate Class III PI3-kinase via overexpression of Vps34 subunit in adult rat hearts and we can further confirm the protective roles of this kinase at the initial stage of Ang II-induced cardiac hypertrophy. Furthermore, we can seek the possible relationship between AT2R and Class III PI3-kinase since they are the cascade components of intracellular signal transduction and both of them show protective effects to prevent cardiomyocytes from cardiac hypertrophy. Further, other similar treatments of hazardous stimuli such as hypoxia and/or norepinephrine might be adopted to cardiomyocytes at different exposure durations or concentrations to learn the impact on autophagy and cardiac remodeling. Recently our lab has conducted a series of researches of mitochondrial ROS-dependent mechanism on Ang II or 20-HETE-induced cardiac remodeling and apoptosis [79, 138]. Therefore, this is a brand-new area to investigate Ang II-induced mitochondrial autophagy and morphological alterations via determination of mitochondrial membrane potential by JC1-staining and mitophagy by Parkin staining. When it comes to both *in vitro* and *in vivo* autophagic measurement, it is inevitable to draw prejudiced judgements since only MAP-LC3 antibody detection is used. In order to gain a more thorough view, alternative autophagic detection approaches such as GFP-LC3 viral vector insertion, electron microscopy (EM), acridine orange

(AO) and monodansylcadaverine (MDC) fluorescence staining might also be employed to monitor the whole process of autophagy.

Moreover, there are three major types of autophagy with varied modes of cargo delivery into lysosomes: 1) Macroautophagy: this type of autophagy is the most universal, essential and absolutely the best-investigated type with preferable competence (hereafter termed as autophagy) which is launched by membrane circling target proteins, organelles with desirable capacity to establish autophagosomes [40]. 2) Microautophagy: it is the process of straight extension and/or invagination of the limiting lysosomal/vacuole membranes to entrap the damaged proteins or organelles, and those substrates are directly segregated [61]. 3) Chaperone-mediated autophagy (CMA): the chaperone protein HSC70 is capable to identify the proteins with a unanimous sequence of KFERQ and engulf the proteins in succession to the LAMP-2A (lysosome-associated membrane protein 2A) receptor to convey those proteins into lysosomes for degradation. This type of autophagy is quite unique in mammalian cells via investigation of the protein co-incubated with isolated lysosomes or with chaperone, or lysosomal receptor with genetic modifications, while the other two types of autophagy could occur both in eukaryotes and yeasts [139]. Thus, we may further investigate which type(s) of autophagy is (are) involved in Ang II-induced cardiac remodeling by relevant approaches.

6.3. Clinical significance

This is the first study to demonstrate the possible involvement of cardiac Class I and Class III PI3-kinases that present contradictory roles in autophagic regulation at different stages of Ang II-induced cardiac remodeling and subsequent pathophysiology conditions of CHF from compensatory to decompensatory. Regarding the astonishing statistics for the worldwide prevalence for heart failure, novel targets need to be explored which could substitute or at least ameliorate the existing major therapeutic strategies of HF such as diuretics, inotropic agents, ACE

inhibitors and AT1R antagonists. This study showed targeting the cardiac PI3-kinases system by developing pharmacological agents or gene therapy in the patient with HF may attenuate the pathophysiological condition with beneficial compliance. Hence, future research should be carried out in developing targeting agents against PI3-kinases and mitochondrial ROS generation.

REFERENCES

1. Mozaffarian D, Benjamin EJ, Go AS, Arnett DK, Blaha MJ, Cushman M, et al. Heart Disease and Stroke Statistics-2016 Update: A Report From the American Heart Association. *Circulation*. 2016; 133(4): e38-360.
2. Lloyd-Jones D, Adams RJ, Brown TM, Carnethon M, Dai S, De Simone G, et al. Heart disease and stroke statistics--2010 update: a report from the American Heart Association. *Circulation*. 2010; 121(7): e46-e215.
3. Heidenreich PA, Albert NM, Allen LA. Forecasting the impact of heart failure in the United States: a policy statement from the American Heart Association. *Circ Heart Fail.* 2013; 6(3): 606-19.
4. Cook C, Cole G, Asaria P, Jabbour R, Francis DP. The annual global economic burden of heart failure. *Int. J. Cardiol.* 2014; 171(3): 368-76.
5. Zannad F, Agrinier N, Alla F. Heart failure burden and therapy. *EP Eur.* 2009; 11 (Suppl 5):1-9.
6. Jessup M, Brozena S. Heart failure. *N Engl J Med*. 2003; 348(20): 2007-18.
7. Gottdiener JS, Arnold AM, Aurigemma GP, Polak JF, Tracy RP, Kitzman DW, et al. Predictors of congestive heart failure in the elderly: the cardiovascular health study. *J Am Coll Cardiol.* 2000; 35(6): 1628-37.
8. Klabunde RE. Cardiovascular physiology concepts: (2nd ed.)Wolters Kluwer Health/Lippincott Williams & Wilkins, Philadelphia; 2012.
9. Kemp CD, Conte JV. The pathophysiology of heart failure. *Cardiovasc. Pathol.* 2012; 21(5): 365-71.

10. Iwanaga Y, Hoshijima M, Gu Y, Iwatate M, Dieterle T, Ikeda Y, et al. Chronic phospholamban inhibition prevents progressive cardiac dysfunction and pathological remodeling after infarction in rats. *J Clin Invest.* 2004; 113(5): 727-36.

11. Robert O. Bonow DLM, Douglas P. Zipes, Peter Libby. Braunwald's Heart Disease: A Textbook of Cardiovascular Medicine, 2-Volume Set, 10e. 9 ed. Phildelphia: Saunders; 2011 March 2, 2011.

12. Guyatt GH, PJ. D. A review of heart failure treatment. *Mt Sinai J Med*. 2004;71(1):47-54.

13. Heineke J, Molkentin JD. Regulation of cardiac hypertrophy by intracellular signalling pathways. *Nature Rev Mol Cell Biol.* 2006; 7(8): 589-600.

14. Malpas SC. Sympathetic nervous system overactivity and its role in the development of cardiovascular disease. *Physiol Rev*. 2010; 90(2): 513-57.

15. Brouri F, Hanoun N, Mediani O, Saurini F, Hamon M, Vanhoutte PM, et al. Blockade of β1- and desensitization of β2-adrenoceptors reduce isoprenaline-induced cardiac fibrosis. *Eur. J. Pharmacol.* 2004; 485(1-3): 227-34.

16. Neri M, Cerretani D, Fiaschi AI, Laghi PF, Lazzerini PE, Maffione AB, et al. Correlation between cardiac oxidative stress and myocardial pathology due to acute and chronic norepinephrine administration in rats. *JCMM*. 2007; 11(1): 156-70.

17. Chaggar PS, Malkin CJ, Shaw SM, Williams SG, Channer KS. Neuroendocrine effects on the heart and targets for therapeutic manipulation in heart failure. *Cardiovasc Ther*. 2009; 27(3): 187-93.

18. Loeb LA, Wallace DC, Martin GM. The mitochondrial theory of aging and its relationship to reactive oxygen species damage and somatic mtDNA mutations. *Proc Natl Acad Sci U S A.* 2005; 102(52): 18769-70.

19. Katzung BG. Basic & Clinical Pharmacology, 12e: The McGraw-Hill Companies, Inc.; 2012.

20. Harvey PA, Leinwand LA. The cell biology of disease: cellular mechanisms of cardiomyopathy. *J Cell Biol.* 2011; 194(3): 355-65.

21. Hill JA, Olson EN. Cardiac plasticity. *N Engl J Med.* 2008; 358(13): 1370-80.

22. Gunasinghe SK, Spinale FG. Myocardial basis for heart failure. In: Mann DL, editor. Role of the Cardiac Interstitium Heart Failure. Philadelphia: Saunders. 2004. p. 57-70.

23. Drazner MH, Rame JE, Marino EK, Gottdiener JS, Kitzman DW, Gardin JM, et al. Increased left ventricular mass is a risk factor for the development of a depressed left ventricular ejection fraction within five years: the Cardiovascular Health Study. *J Am Coll Cardiol.* 2004; 43(12): 2207-15.

24. Majno G, Joris I. Apoptosis, oncosis, and necrosis. An overview of cell death. *Am J Pathol.* 1995; 146(1): 3-15.

25. Giordano FJ. Oxygen, oxidative stress, hypoxia, and heart failure. *J Clin Invest.* 2005; 115(3): 500-8.

26. Burgoyne JR, Mongue-Din H, Eaton P, Shah AM. Redox signaling in cardiac physiology and pathology. *Circ Res.* 2012; 111(8): 1091-106.

27. Pacher P, Beckman JS, Liaudet L. Nitric oxide and peroxynitrite in health and disease. *Physiol Rev.* 2007; 87(1): 315-424.

28. Fridovich I. Superoxide radical: an endogenous toxicant. *Annu Rev Pharmacol Toxicol.* 1983; 23: 239-57.

29. Zhang M, Shah AM. Reactive Oxygen Species in Heart Failure. *Acute Heart Failure.* 2008. p. 118-23.

30. Brown DI, Griendling KK. Regulation of signal transduction by reactive oxygen species in the cardiovascular system. *Circ Res.* 2015; 116(3): 531-49.

31. Campomanes P, Rothlisberger U, Alfonso-Prieto M, Rovira C. The Molecular Mechanism of the Catalase-like Activity in Horseradish Peroxidase. *J. Am. Chem. Soc.* 2015; 137(34): 11170-8.

32. de Duve C. The lysosome turns fifty. *Nature Cell Biol.* 2005; 7(9): 847-9.

33. De Duve C, Wattiaux R. Functions of lysosomes. *Annu Rev Physiol.* 1966; 28: 435-92.

34. Maiuri MC, Zalckvar E, Kimchi A, Kroemer G. Self-eating and self-killing: crosstalk between autophagy and apoptosis. *Nature Rev Mol Cell Biol.* 2007; 8(9): 741-52.

35. Klionsky DJ, Cuervo AM, Dunn J, Levine B, Klei IVD, Seglen PO. How shall I eat thee? *Autophagy*. 2007; 3(5): 413-6.

36. Kroemer G, Marino G, Levine B. Autophagy and the integrated stress response. *Mol Cell.* 2010; 40(2): 280-93.

37. Nair U, Jotwani A, Geng J, Gammoh N, Richerson D, Yen WL, et al. SNARE proteins are required for macroautophagy. *Cell*. 2011; 146(2): 290-302.

38. Yang Z, Klionsky DJ. Mammalian autophagy: core molecular machinery and signaling regulation. *Curr Opin Cell Biol.* 2010; 22(2): 124-31.

39. Li L, Xu J, He L, Peng L, Zhong Q, Chen L, et al. The role of autophagy in cardiac hypertrophy. *Acta biochimica et biophysica Sinica*. 2016; 48(6): 491-500.

40. Klionsky DJ. Autophagy: from phenomenology to molecular understanding in less than a decade. *Nature Rev Mol Cell Biol*. 2007; 8(11): 931-7.

41. Dunlop EA, Tee AR. mTOR and autophagy: a dynamic relationship governed by nutrients and energy. *Sem Cell Dev Biol.* 2014; 36: 121-9.

42. Russell RC, Yuan HX, Guan KL. Autophagy regulation by nutrient signaling. *Cell Res.* 2014; 24(1): 42-57.

43. Zhang CS, Jiang B, Li M, Zhu M, Peng Y, Zhang YL, et al. The lysosomal v-ATPase-Ragulator complex is a common activator for AMPK and mTORC1, acting as a switch between catabolism and anabolism. *Cell Metab.* 2014; 20(3): 526-40.

44. Inoki K, Li Y, Zhu T, Wu J, Guan KL. TSC2 is phosphorylated and inhibited by Akt and suppresses mTOR signalling. *Nature Cell Biol.* 2002; 4(9): 648-57.

45. Gangloff YG, Mueller M, Dann SG, Svoboda P, Sticker M, Spetz JF, et al. Disruption of the mouse mTOR gene leads to early postimplantation lethality and prohibits embryonic stem cell development. *Mol Cell Biol*. 2004; 24(21): 9508-16.

46. Kang R, Zeh HJ, Lotze MT, Tang D. The Beclin 1 network regulates autophagy and apoptosis. *Cell Death Differ*. 2011; 18(4): 571-80.

47. Wirth M, Joachim J, Tooze SA. Autophagosome formation--the role of ULK1 and Beclin1-PI3KC3 complexes in setting the stage. *Sem Cancer Biol*. 2013; 23(5): 301-9.

48. Polson HE, de Lartigue J, Rigden DJ, Reedijk M, Urbe S, Clague MJ, et al. Mammalian Atg18 (WIPI2) localizes to omegasome-anchored phagophores and positively regulates LC3 lipidation. *Autophagy*. 2010; 6(4): 506-22..

49. Seglen PO, Gordon PB. 3-Methyladenine: Specific inhibitor of autophagic/lysosomal protein degradation in isolated rat hepatocytes. *Proc Natl Acad Sci U S A.* 2012;109(6):2003-8. 1982; 79(6): 1889-92.

50. Maccioni RB, Cambiazo V. Role of microtubule-associated proteins in the control of microtubule assembly. *Physiol Rev.* 1995; 75(4): 835-64.

51. Boyer-Guittaut M, Poillet L, Liang Q, Bole-Richard E, Ouyang X, Benavides GA, et al. The role of GABARAPL1/GEC1 in autophagic flux and mitochondrial quality control in MDA-MB-436 breast cancer cells. *Autophagy*. 2014; 10(6): 986-1003.

52. Chakrama FZ, Seguin-Py S, Le Grand JN, Fraichard A, Delage-Mourroux R, Despouy G, et al. GABARAPL1 (GEC1) associates with autophagic vesicles. *Autophagy*. 2010; 6(4): 495-505.

53. Lavandero S, Troncoso R, Rothermel BA, Martinet W, Sadoshima J, Hill JA. Cardiovascular autophagy: concepts, controversies, and perspectives. *Autophagy*. 2013; 9(10): 1455-66.

54. Chen Y, Azad MB, Gibson SB. Superoxide is the major reactive oxygen species regulating autophagy. *Cell Death Differ*. 2009; 16(7): 1040-52.

55. Levonen AL, Hill BG, Kansanen E, Zhang J, Darley-Usmar VM. Redox regulation of antioxidants, autophagy, and the response to stress: implications for electrophile therapeutics. *Free Radic Biol Med*. 2014; 71: 196-207.

56. Cuervo AM. Autophagy and aging: keeping that old broom working. *Trends Genet.* 2008; 24(12): 604-12.

57. Engelman JA, Luo J, Cantley LC. The evolution of phosphatidylinositol 3-kinases as regulators of growth and metabolism. *Nature Rev Genet.* 2006; 7(8): 606-19

58. Liu P, Cheng H, Roberts TM, Zhao JJ. Targeting the phosphoinositide 3-kinase pathway in cancer. *Nat. Rev. Drug Discov.* 2009; 8(8): 627-44.

59. Cully M, You H, Levine AJ, Mak TW. Beyond PTEN mutations: the PI3K pathway as an integrator of multiple inputs during tumorigenesis. *Nature Rev Cancer*. 2006; 6(3): 184-92.

60. Misawa H, Ohtsubo M, Copeland NG, Gilbert DJ, Jenkins NA, Yoshimura A. Cloning and characterization of a novel class II phosphoinositide 3-kinase containing C2 domain. *Biochem Biophys Res Commun.* 1998; 244(2): 531-9.

61. Mijaljica D, Prescott M, Devenish RJ. Microautophagy in mammalian cells: Revisiting a 40-year-old conundrum. *Autophagy*. 2014; 7(7): 673-82.

62. Shioi T, Kang PM, Douglas PS, Hampe J, Yballe CM, Lawitts J, et al. The conserved phosphoinositide 3-kinase pathway determines heart size in mice. *EMBO J*. 2000; 19(11): 2537-48.

63. Tu VC. Signals of Oxidant-Induced Cardiomyocyte Hypertrophy: Key Activation of p70 S6 Kinase-1 and Phosphoinositide 3-Kinase. *J Pharmacol Exp Ther.* 2002; 300(3): 1101-10.

64. Jaber N, Dou Z, Chen JS, Catanzaro J, Jiang YP, Ballou LM, et al. Class III PI3K Vps34 plays an essential role in autophagy and in heart and liver function. P*roc Natl Acad Sci U S A.* 2012; 109(6): 2003-8

65. Sadoshima J-i, Xu Y, Slayter HS, Izumo S. Autocrine release of angiotensin II mediates stretch-induced hypertrophy of cardiac myocytes in vitro. *Cell*. 1993; 75(5): 977-84.

66. Reid IA, Morris BJ, Ganong WF. The renin-angiotensin system. *Annu Rev Physiol.* 1978; 40: 377-410.

67. Carey RM, Siragy HM. Newly recognized components of the renin-angiotensin system: potential roles in cardiovascular and renal regulation. *Endocr Rev.* 2003; 24(3): 261-71.

68. Hunyady L, Catt KJ. Pleiotropic AT1 receptor signaling pathways mediating physiological and pathogenic actions of angiotensin II. *Mol Endocrinol.* 2006; 20(5): 953-70.

69. Ramani GV, Uber PA, Mehra MR. Chronic heart failure: contemporary diagnosis and management. *Mayo Clin Proc.* 2010; 85(2): 180-95.

70. Braunwald E. Heart failure. *JACC Heart Fail. 2*013; 1(1): 1-20.

71. Dikalov SI, Nazarewicz RR. Angiotensin II-induced production of mitochondrial reactive oxygen species: potential mechanisms and relevance for cardiovascular disease. *Antioxid. Redox Signal.* 2013; 19(10): 1085-94.

72. Touyz RM, Mercure C, He Y, Javeshghani D, Yao G, Callera GE, et al. Angiotensin II-dependent chronic hypertension and cardiac hypertrophy are unaffected by gp91phox-containing NADPH oxidase. *Hypertension*. 2005; 45(4): 530-7.

73. Ago T, Kuroda J, Pain J, Fu C, Li H, Sadoshima J. Upregulation of Nox4 by hypertrophic stimuli promotes apoptosis and mitochondrial dysfunction in cardiac myocytes. *Circ Res.* 2010; 106(7): 1253-64.

74. Gottlieb RA, Mentzer RM. Autophagy during cardiac stress: joys and frustrations of autophagy. *Annu Rev Physiol.* 2010; 72: 45-59.

75. Song M, Chen Y, Gong G, Murphy E, Rabinovitch PS, Dorn GW, 2nd. Super-suppression of mitochondrial reactive oxygen species signaling impairs compensatory autophagy in primary mitophagic cardiomyopathy. *Circ Res.* 2014; 115(3): 348-53.

76. Luo J, McMullen JR, Sobkiw CL, Zhang L, Dorfman AL, Sherwood MC, et al. Class IA phosphoinositide 3-kinase regulates heart size and physiological cardiac hypertrophy. *Mol Cell Biol.* 2005; 25(21): 9491-502.

77. Hariharan N, Maejima Y, Nakae J, Paik J, Depinho RA, Sadoshima J. Deacetylation of FoxO by Sirt1 Plays an Essential Role in Mediating Starvation-Induced Autophagy in Cardiac Myocytes. *Circ Res.* 2010; 107(12): 1470-82.

78. Wang X, Dai Y, Ding Z, Khaidakov M, Mercanti F, Mehta JL. Regulation of autophagy and apoptosis in response to angiotensin II in HL-1 cardiomyocytes. *Biochem Biophys Res Commun.* 2013; 440(4): 696-700.

79. Guo L, Yin A, Zhang Q, Zhong T, O'Rourke ST, Sun C. Angiotensin-(1-7) attenuates angiotensin II-induced cardiac hypertrophy via a Sirt3-dependent mechanism. *Am J Physiol Heart Circ Physiol.* 2017; 312(5): H980-H91.

80. Xuan C, Yao F, Guo L, Liu Q, Chang S, Liu K, et al. Comparison of extracts from cooked and raw lentil in antagonizing angiotensin II-induced hypertension and cardiac hypertrophy. *Eur Rev Med Pharmacol Sci.* 2013; 17(19): 2644-53.

81. Sun C, Zubcevic J, Polson JW, Potts JT, Diez-Freire C, Zhang Q, et al. Shift to an involvement of phosphatidylinositol 3-kinase in angiotensin II actions on nucleus tractus solitarii neurons of the spontaneously hypertensive rat. *Circ Res.* 2009; 105(12): 1248-55.

82. Zhou L, Ma B, Han X. The role of autophagy in angiotensin II-induced pathological cardiac hypertrophy. *J Mol Endocrinol.* 2016; 57(4): R143-R52.

83. Bao W, Behm DJ, Nerurkar SS, Ao Z, Bentley R, Mirabile RC, et al. Effects of p38 MAPK Inhibitor on angiotensin II-dependent hypertension, organ damage, and superoxide anion production. *J Cardiovasc Pharmacol.* 2007; 49(6): 362-8.

84. Bendall JK. Pivotal Role of a gp91phox-Containing NADPH Oxidase in Angiotensin II-Induced Cardiac Hypertrophy in Mice. *Circulation*. 2002; 105(3): 293-6.

85. Azad MB, Chen Y, Gibson SB. Regulation of autophagy by reactive oxygen species (ROS): implications for cancer progression and treatment. *Antioxid Redox Signal.* 2009; 11(4): 777-90.

86. Wang Y, Nartiss Y, Steipe B, McQuibban GA, Kim PK. ROS-induced mitochondrial depolarization initiates PARK2/PARKIN-dependent mitochondrial degradation by autophagy. *Autophagy*. 2012; 8(10): 1462-76.

87. Scherz-Shouval R, Shvets E, Fass E, Shorer H, Gil L, Elazar Z. Reactive oxygen species are essential for autophagy and specifically regulate the activity of Atg4. *EMBO J.* 2007; 26(7): 1749-60.

88. Russell RC, Tian Y, Yuan H, Park HW, Chang YY, Kim J, et al. ULK1 induces autophagy by phosphorylating Beclin-1 and activating VPS34 lipid kinase. *Nature Cell Biol.* 2013; 15(7): 741-50.

89. Aki T, Yamaguchi K, Fujimiya T, Mizukami Y. Phosphoinositide 3-kinase accelerates autophagic cell death during glucose deprivation in the rat cardiomyocyte-derived cell line H9c2. *Oncogene*. 2003; 22(52): 8529-35.

90. Mbengue A, Bhattacharjee S, Pandharkar T, Liu H, Estiu G, Stahelin RV, et al. A molecular mechanism of artemisinin resistance in Plasmodium falciparum malaria. *Nature*. 2015; 520(7549): 683-7.

91. Lindmo K, Stenmark H. Regulation of membrane traffic by phosphoinositide 3-kinases. *J Cell Sci.* 2006; 119(Pt 4): 605-14.

92. Boya P, Gonzalez-Polo RA, Casares N, Perfettini JL, Dessen P, Larochette N, et al. Inhibition of macroautophagy triggers apoptosis. *Mol Cell Biol.* 2005; 25(3): 1025-40.

93. Jean S, Kiger AA. Classes of phosphoinositide 3-kinases at a glance. *J. Cell Sci.* 2014; 127(Pt 5): 923-8.

94. Mei Y, Thompson MD, Cohen RA, Tong X. Autophagy and oxidative stress in cardiovascular diseases. *Biochimica et biophysica acta.* 2015; 1852(2): 243-51.

95. Balakumar P, Jagadeesh G. Multifarious molecular signaling cascades of cardiac hypertrophy: can the muddy waters be cleared? *Pharmacol. Res.* 2010; 62(5): 365-83.

96. Zhang Q, Yao F, Raizada MK, O'Rourke ST, Sun C. Apelin gene transfer into the rostral ventrolateral medulla induces chronic blood pressure elevation in normotensive rats. *Circ Res.* 2009; 104(12): 1421-8.

97. Wollebo HS, Woldemichaele B, White MK. Lentiviral transduction of neuronal cells. *Meth Mol Biol.* 2013; 1078: 141-6.

98. Veitia RA. Exploring the molecular etiology of dominant-negative mutations. *Plant Cell.* 2007; 19(12): 3843-51.

99. Funaki M, Katagiri H, Kanda A, Anai M, Nawano M, Ogihara T, et al. p85/p110-type Phosphatidylinositol Kinase Phosphorylates Not Only the D-3, but Also the D-4 Position of the Inositol Ring. *J Biol Chem.* 1999; 274(31): 22019-24.

100. Castino R, Bellio N, Follo C, Murphy D, Isidoro C. Inhibition of PI3k class III-dependent autophagy prevents apoptosis and necrosis by oxidative stress in dopaminergic neuroblastoma cells. *Toxicol Sci.* 2010; 117(1): 152-62.

101. Nakai A, Yamaguchi O, Takeda T, Higuchi Y, Hikoso S, Taniike M, et al. The role of autophagy in cardiomyocytes in the basal state and in response to hemodynamic stress. *Nat. Med.* 2007; 13(5): 619-24.

102. Mogi M, Kawajiri M, Tsukuda K, Matsumoto S, Yamada T, Horiuchi M. Serum levels of renin-angiotensin system components in acute stroke patients. *Geriatr Gerontol Int.* 2014; 14(4): 793-8.

103. Dorn GW, 2nd. The fuzzy logic of physiological cardiac hypertrophy. *Hypertension*. 2007; 49(5): 962-70.

104. Kaplan ML, Cheslow Y, Vikstrom K, Malhotra A, Geenen DL, Nakouzi A, et al. Cardiac adaptations to chronic exercise in mice. *Am J Physiol.* 1994; 267(3 Pt 2): H1167-73.

105. Dizon LA, Seo DY, Kim HK, Kim N, Ko KS, Rhee BD, et al. Exercise perspective on common cardiac medications. Integr Med Res. 2013; 2(2): 49-55.

106. Pluim BM, Zwinderman AH, van der Laarse A, van der Wall EE. The Athlete s Heart : A Meta-Analysis of Cardiac Structure and Function. *Circulation*. 2000; 101(3): 336-44.

107. Fernandes T, Soci UP, Oliveira EM. Eccentric and concentric cardiac hypertrophy induced by exercise training: microRNAs and molecular determinants. *Braz J Med Biol Res.* 2011; 44(9): 836-47.

108. Zamo FS, Barauna VG, Chiavegatto S, Irigoyen MC, Oliveira EM. The renin-angiotensin system is modulated by swimming training depending on the age of spontaneously hypertensive rats. *Life Sci.* 2011; 89(3-4): 93-9.

109. Xiao HD, Fuchs S, Bernstein EA, Li P, Campbell DJ, Bernstein KE. Mice expressing ACE only in the heart show that increased cardiac angiotensin II is not associated with cardiac hypertrophy. *Am J Physiol Heart Circ Physiol.* 2008; 294(2): H659-67.

110. Li X, Wang K. Effects of moderateintensity endurance exercise on angiotensin II and angiotensin II type I receptors in the rat heart. *Mol Med Rep.* 2017; 16(3): 2439-44

111. Fernandes T, Hashimoto NY, Magalhaes FC, Fernandes FB, Casarini DE, Carmona AK, et al. Aerobic exercise training-induced left ventricular hypertrophy involves regulatory MicroRNAs, decreased angiotensin-converting enzyme-angiotensin ii, and synergistic regulation of angiotensin-converting enzyme 2-angiotensin (1-7). *Hypertension*. 2011; 58(2): 182-9.

112. Modgil A, Zhang Q, Pingili A, Singh N, Yao F, Ge J, et al. Angiotensin-(1-7) attenuates the chronotropic response to angiotensin II via stimulation of PTEN in the spontaneously hypertensive rat neurons. *Am J Physiol Heart Circ Physiol.* 2012; 302(5): H1116-22.

113. Negrao CE, Middlekauff HR. Exercise training in heart failure: reduction in angiotensin II, sympathetic nerve activity, and baroreflex control. *J. Appl. Physiol.* 2008; 104(3): 577-8.

114. Schirone L, Forte M, Palmerio S, Yee D, Nocella C, Angelini F, et al. A Review of the Molecular Mechanisms Underlying the Development and Progression of Cardiac Remodeling. *Oxid Med Cell Longev*. 2017; 2017: 3920195.

115. Segura AM, Frazier OH, Buja LM. Fibrosis and heart failure. *Heart Fail Rev.* 2014; 19(2): 173-85.

116. McMullen JR, Jennings GL. Differences between pathological and physiological cardiac hypertrophy: novel therapeutic strategies to treat heart failure. *Clin. Exp. Pharmacol. Physiol.* 2007; 34(4): 255-62.

117. Bregagnollo EA, Mestrinel MA, Okoshi K, Carvalho FC, Bregagnollo IF, Padovani CR, et al. Relative role of left ventricular geometric remodeling and of morphological and functional myocardial remodeling in the transition from compensated hypertrophy to heart failure in rats with supravalvar aortic stenosis. *Arquivos Brasileiros de Cardiologia.* 2007; 88(2): 225-33.

118. Liang Q. Redefining the roles of p38 and JNK signaling in cardiac hypertrophy: dichotomy between cultured myocytes and animal models. *J. Mol. Cell. Cardiol.* 2003; 35(12): 1385-94.

119. Abel ED, Doenst T. Mitochondrial adaptations to physiological vs. pathological cardiac hypertrophy. *Cardiovasc Res.* 2011; 90(2): 234-42.

120. O'Neill BT, Abel ED. Akt1 in the cardiovascular system: friend or foe? *J. Clin. Investig.* 2005; 115(8): 2059-64.

121. Serneri GGN, Boddi M, Cecioni I, Vanni S, Coppo M, Papa ML, et al. Cardiac Angiotensin II Formation in the Clinical Course of Heart Failure and Its Relationship With Left Ventricular Function. *Circ. Res.* 2001; 88(9): 961-8.

122. Yamamoto A, Tagawa Y, Yoshimori T, Moriyama Y, Masaki R, Tashiro Y. Bafilomycin A1 Prevents Maturation of Autophagic Vacuoles by Inhibiting Fusion between Autophagosomes and Lysosomes in Rat Hepatoma Cell Line, H-4-II-E Cells. *Cell Struct. Funct.* 1998; 23(1): 33-42.

123. Solomon VR, Lee H. Chloroquine and its analogs: a new promise of an old drug for effective and safe cancer therapies. *Eur. J. Pharmacol.* 2009; 625(1-3): 220-33.

124. Vivanco I, Sawyers CL. The phosphatidylinositol 3-Kinase AKT pathway in human cancer. *Nat. Rev. Cancer.* 2002; 2(7): 489-501.

125. Stephens L. Protein Kinase B Kinases That Mediate Phosphatidylinositol 3,4,5-Trisphosphate-Dependent Activation of Protein Kinase B. *Science*. 1998; 279(5351): 710-4.

126. Matsui T, Rosenzweig A. Convergent signal transduction pathways controlling cardiomyocyte survival and function: the role of PI 3-kinase and Akt. *J. Mol. Cell. Cardiol.* 2005; 38(1): 63-71.

127. Wullschleger S, Loewith R, Hall MN. TOR signaling in growth and metabolism. *Cell*. 2006; 124(3): 471-84.

128. Sabatini DM. mTOR and cancer: insights into a complex relationship. *Nat. Rev. Cancer.* 2006; 6(9): 729-34.

129. Bodine SC, Stitt TN, Gonzalez M, Kline WO, Stover GL, Bauerlein R, et al. Akt/mTOR pathway is a crucial regulator of skeletal muscle hypertrophy and can prevent muscle atrophy *in vivo*. *Nat. Cell Biol.* 2001; 3(11): 1014-9.

130. Schmelzle T, Hall MN. TOR, a Central Controller of Cell Growth. *Cell*. 2000; 103(2): 253-62.

131. Oudit GY, Penninger JM. Cardiac regulation by phosphoinositide 3-kinases and PTEN. *Cardiovasc. Res.* 2009; 82(2): 250-60.

132. Zhai C, Cheng J, Mujahid H, Wang H, Kong J, Yin Y, et al. Selective inhibition of PI3K/Akt/mTOR signaling pathway regulates autophagy of macrophage and vulnerability of atherosclerotic plaque. *PLoS One.* 2014; 9(3): e90563.

133. Hu C, Dandapat A, Sun L, Marwali MR, Inoue N, Sugawara F, et al. Modulation of angiotensin II-mediated hypertension and cardiac remodeling by lectin-like oxidized low-density lipoprotein receptor-1 deletion. *Hypertension*. 2008; 52(3): 556-62.

134. Sun C, Du J, Sumners C, Raizada MK. PI3-kinase inhibitors abolish the enhanced chronotropic effects of angiotensin II in spontaneously hypertensive rat brain neurons. *J. Neurophysiol.* 2003; 90(5): 3155-60.

135. Hou X, Hu Z, Xu H, Xu J, Zhang S, Zhong Y, et al. Advanced glycation endproducts trigger autophagy in cadiomyocyte via RAGE/PI3K/AKT/mTOR pathway. *Cardiovasc. Diabetol.* 2014; 13: 78.

136. Suzuki K, Kubota Y, Sekito T, Ohsumi Y. Hierarchy of Atg proteins in pre-autophagosomal structure organization. *Genes Cells.* 2007; 12(2): 209-18.

137. Petiot A, Ogier-Denis E, Blommaart EFC, Meijer AJ, Codogno P. Distinct Classes of Phosphatidylinositol 3'-Kinases Are Involved in Signaling Pathways That Control Macroautophagy in HT-29 Cells. *J. Biol. Chem.* 2000; 275(2): 992-8.

138. Zhao H, Qi G, Han Y, Shen X, Yao F, Xuan C, et al. 20-Hydroxyeicosatetraenoic Acid Is a Key Mediator of Angiotensin II-induced Apoptosis in Cardiac Myocytes. *J Cardiovasc Pharmacol.* 2015; 66(1): 86-95.

139. Kaushik S, Bandyopadhyay U, Sridhar S, Kiffin R, Martinez-Vicente M, Kon M, et al. Chaperone-mediated autophagy at a glance. *J. Cell Sci.* 2011; 124(Pt 4): 495-9.